General models for the distributions of electric field gradients in disordered solids

1998 J. Phys.: Condens. Matter 10 10715

(http://iopscience.iop.org/0953-8984/10/47/020)

J. Phys.: Condens. Matter **10** (1998) 10715–10774. Printed in the UK PII: S0953-8984(98)95579-5

General models for the distributions of electric field gradients in disordered solids

G Le Caër†§ and R A Brand‡‖

† Laboratoire de Science et Génie des Matériaux Métalliques, CNRS UMR 7584, Ecole des Mines, F-54042 Nancy Cédex, France

‡ Laboratorium für Angewandte Physik, Gerhard-Mercator-Universität GH Duisburg, D-47048 Duisburg, Germany

Received 3 July 1998

Abstract. Hyperfine studies of disordered materials often yield the distribution of the electric field gradient (EFG) or related quadrupole splitting (QS). The question of the structural information that may be extracted from such distributions has been considered for more than fifteen years. Experimentally most studies have been performed using Mössbauer spectroscopy, especially on ^{57}Fe. However, NMR, NQR, EPR and PAC methods have also received some attention. The EFG distribution for a random distribution of electric charges was for instance first investigated by Czjzek *et al* [1] and a general functional form was derived for the joint (bivariate) distribution of the principal EFG tensor component V_{zz} and the asymmetry parameter η. The importance of the Gauss distribution for such rotationally invariant structural models was thus evidenced. Extensions of that model which are based on degenerate multivariate Gauss distributions for the elements of the EFG tensor were proposed by Czjzek. The latter extensions have been used since that time, more particularly in Mössbauer spectroscopy, under the name 'shell models'. The mathematical foundations of all the previous models are presented and critically discussed as they are evidenced by simple calculations in the case of the EFG tensor. The present article only focuses on those aspects of the EFG distribution in disordered solids which can be discussed without explicitly looking at particular physical mechanisms. We present studies of three different model systems. A reference model directly related to the first model of Czjzek, called the Gaussian isotropic model (GIM), is shown to be the limiting case for many different models with a large number of independent contributions to the EFG tensor and not restricted to a point-charge model. The extended validity of the marginal distribution of η in the GIM model is discussed. It is also shown that the second model based on degenerate multivariate normal distributions for the EFG components yields questionable results and has been exaggeratedly used in experimental studies. The latter models are further discussed in the light of new results. The problems raised by these extensions are due to the fact that the consequences of the statistical invariance by rotation of the EFG tensor have not been sufficiently taken into account. Further difficulties arise because the structural degrees of freedom of the disordered solid under consideration have been confused with the degrees of freedom of QS distributions. The relations which are derived and discussed are further illustrated by the case of the EFG tensor distribution created at the centre of a sphere by m charges randomly distributed on its surface. The third model, a simple extension of the GIM, considers the case of an EFG tensor which is the sum of a fixed part and of a random part with variable weights. The bivariate distribution $f(V_{zz}, \eta)$ is calculated exactly in the most symmetric case and the effect of the random part is investigated as a function of its weight. The various models are more particularly discussed in connection with short-range order in disordered solids. An ambiguity problem which arises in the evaluation of bivariate distributions of centre lineshift (isomer shift) and quadrupole splitting from $\frac{1}{2} \leftrightarrow \frac{3}{2}$ Mössbauer spectra is finally quantitatively considered.

§ E-mail address: lecaer@mines.u-nancy.fr.

‖ E-mail address: r.a.brand@unidui.uni-duisberg.de.

0953-8984/98/4710715+60$19.50

Contents

1. Introduction

The distribution of the electric field gradient (EFG) or related quadrupole splitting (QS) has been often studied by Mössbauer spectroscopy, NMR, PAC and EPR to gain information on concentrated non-magnetic crystalline and non-crystalline materials. These include non-periodic solids with for instance topological and/or chemical disorder or quasi-periodic solids (glasses, nano-structured materials, quasicrystals etc). The literature on non-magnetic amorphous materials is too extensive to cite in detail. The reader is referred for example to references [1] to [6]. One of the most basic properties of the EFG distribution is the sign of the majority EFG component. Unfortunately, for ^{57}Fe Mössbauer spectroscopy this is only obtainable from spectra taken in an external magnetic field. This has only been done for some amorphous materials (see [7–11]). Many studies on quasicrystalline materials exist as well. Although these are often well ordered materials with narrow Bragg reflections, they always display broad QS distributions similar to amorphous materials (see [15–22]). As in the case of amorphous materials, only very few studies have been made of the sign of the dominating EFG component. [13–16] are exceptions.

However, some problems need to be overcome in order to obtain significant conclusions. One problem often encountered in obtaining the experimental QS marginal distribution $P(\Delta)$ from Mössbauer spectra with $\frac{1}{2} \leftrightarrow \frac{3}{2}$ transitions is the presence of centre lineshifts (isomer shifts IS) δ. The actual distribution is thus bivariate: $f(\delta, \Delta)$. It is often simplified in the literature (for example see [17, 23–25]) where $f(\delta, \Delta)$ is replaced by $P(\Delta)\delta(\delta - F(\Delta))$, assuming some explicit and exact dependence of δ on Δ, in general $\delta = a\Delta + \delta_0$. On the other hand, Alberto *et al* [26] have presented in a recent study a two dimensional Gaussian distribution method including δ–Δ correlations. Similar results have also been presented by Lagarec and Rancourt [27] using Voigt line shapes. However some ambiguity problems arise when the bivariate distribution $f(\delta, \Delta)$ is determined from Mössbauer spectra, as discussed in subsection 7.2. Another problem is to relate experimental results, once firmly established, to theoretical models in order that realistic conclusions may be drawn on the structural characteristics. The present article only focuses on those aspects of the EFG distribution in

disordered solids which can be discussed without explicitly looking at particular physical mechanisms. Detailed studies of static quadrupole effects due to various kinds of defect have been considered in detail in various review papers to which the readers are referred [2–5]. The EFG distribution in the case of random atomic arrangements has played a seminal role in the analysis of EFG and QS distributions. Czjzek *et al* [1] have provided a model distribution for this case. The same EFG distribution was independently derived by Stöckmann [2] for a cubic system with a large concentration of vacancies randomly distributed. Both derived the joint (bivariate) distribution of the principal EFG tensor component V_{zz} and the asymmetry parameter η. Because of its central role and of its general validity, the mathematical foundations of this model will be more fully analysed as they are evidenced by simple calculations in the case of the EFG tensor.

The relevance of the η distribution derived for such models to an *a priori* large class of disordered solids will moreover be emphasized. As important is the discussion of the extensions to these distribution forms that were proposed by Czjzek [29] to model the QS distributions in materials with chemical and topological short range order. Another model has been proposed by Coey as reported by Varret and Henry [30].

The serious difficulties briefly mentioned by Le Caër *et al* [9, 28] are raised by some of the latter still widely used models [29]. Some of these difficulties are due to the fact that the consequences of the assumed statistical invariance by rotation of the EFG tensor have not been sufficiently taken into account. Further difficulties are because the structural degrees of freedom of the disordered solid under consideration have been confused with degrees of freedom of QS distributions. We will also discuss several numerical simulations for random EFG tensors, which illuminate the properties discussed above. This discussion is not limited to Mössbauer spectroscopy: the discussion applies as well to any hyperfine method capable of determining certain characteristic properties of the EFG tensor and more generally to techniques which are sensitive to physical properties represented by second rank tensors. This includes for example nuclear magnetic resonance (NMR), nuclear quadrupole resonance (NQR) as well as perturbed angular correlation (PAC) studies. Both Heubes *et al* [31] as well as Damonte *et al* [32] have presented PAC results on non-magnetic glasses. These results are in good agreement with the distribution presented by Czjzek *et al* [1] as will be discussed below (the first for ^{111}Cd in a-Ga, and the second for ^{181}Hf in a-$Hf_{1-x}Cu_x$). ^{27}Al NMR results on a single-grain Al–Pd–Mn quasicrystal have been presented by Shastri *et al* [33] for different angles between the external field and the quasicrystal axis system. No dependence on angle could be found, and the resulting distribution agrees qualitatively with the Czjzek *et al* result. Recently we have been analysing similar ^{27}Al and ^{65}Cu NMR results on Al–Cu–Fe quasicrystalline powders and have found similar results [34]. NQR results have also been presented by several authors [35, 36]. Distributions of Czjzek's type of the fine structure parameter in electron paramagnetic resonance (EPR) studies of Fe^{3+} in alkali borate and transition metal fluoride glasses have also been presented [37, 38].

The main reasons to worry about the distribution of the EFG tensor itself and not only about the distribution of its eigenvalues (through the bivariate distribution of V_{zz} and η) lie in the following three points.

(1) Additivity of the various physical contributions holds for the elements of the EFG tensor itself, but not for its eigenvalues.

(2) The possibility to gain information about eventual asymmetries of Mössbauer spectra (different from those related to IS–QS correlations) which might be extracted from EFG tensor distributions. As discussed in section 4.2, asymmetries of spectral components could possibly exist according to the physical scale at which the disordered solids are characterized.

An example discussed below involves medium-range order in an amorphous solid.

(3) Some widely used models [29] make explicit assumptions about the distribution of the EFG tensor.

2. Hyperfine Hamiltonian

The hyperfine Hamiltonian for the change in nuclear levels due to the external electric charges is derived in most standard books on Mössbauer spectroscopy. The term proportional to the quadrupole moment of the nuclear charges depends on the electric field gradient created by external charges (local atom and neighbours) at the nucleus. In terms of the angular momentum operators $\mathcal{I}^2$, $\mathcal{I}_z$ and the ladder operators $\mathcal{I}_+$ and $\mathcal{I}_-$ of the nuclear states, this Hamiltonian can be written as

$$H_Q = \frac{eQ}{4I(2I-1)}\left[V_{zz}(3\mathcal{I}_z^2 - \mathcal{I}^2) + \frac{1}{2}(V_{xx} - V_{yy})(\mathcal{I}_-^2 + \mathcal{I}_+^2)\right]. \tag{1}$$

We denote the eigenvalues of the EFG tensor as V_{xx}, V_{yy} and V_{zz}. (The elements of the EFG tensor in its general non-diagonalized form will be written in lower case, with $v_{ij} = v_{ji}$, $i, j = x, y, z$ and the trace of the EFG tensor $\tilde{V}$ is $\mathrm{tr}(\tilde{V}) = v_{xx} + v_{yy} + v_{zz} = 0$.) If the eigenvalues are sorted such that $|V_{xx}| \leqslant |V_{yy}| \leqslant |V_{zz}|$ (which we denote by upper case), then the diagonal EFG tensor can be written in terms of the two variables V_{zz} and the asymmetry parameter η given by

$$0 \leqslant \eta \equiv \frac{V_{xx} - V_{yy}}{V_{zz}} \leqslant 1. \tag{2}$$

This result should not lead us to think that there are only two independent variables for defining the EFG tensor: by diagonalizing v_{ij}, we have chosen the three Euler angles (α, β, γ). Thus there are five independent variables as expected for a symmetric second-rank tensor with a zero trace.

In some cases it is simpler to consider the distribution of *unsorted* principal values v_{ii} $(i = x, y, z)$ which we denote by lower case, rather than as in equation (2). We define the ratio $\tau \equiv (v_{xx} - v_{yy})/v_{zz}$ for the non-sorted v_{ii}. This τ, in contrast to η, can take on any real value: $-\infty \leqslant \tau \leqslant \infty$. For any physical property related to a second-rank tensor $\tilde{M}$, analogous ratios may be defined. In the case that the trace of $\tilde{M}$ is nonzero, the tensor element m_{zz} is replaced by $m_{zz} - \mathrm{tr}(\tilde{M})/3$ in the definition of τ. Therefore it is useful to express the probability density of η, $p(\eta)$, from that of τ, $f(\tau)$, where $-\infty \leqslant \tau \leqslant \infty$. It is a simple matter to derive the relationship between τ and η (an interchange of the principal axes):

$$\eta = \begin{cases} |\tau| & 0 \leqslant |\tau| \leqslant 1 \\ \dfrac{|3 - |\tau||}{1 + |\tau|} & 1 \leqslant |\tau|. \end{cases}$$

Defining further $g(\tau) = (1 + \tau^2/3)(f(\tau) + f(-\tau))$, we calculate:

$$(1 + \eta^2/3)p(\eta) = g(\eta) + g\left(\frac{3-\eta}{1+\eta}\right) + g\left(\frac{3+\eta}{1-\eta}\right).$$

For some distributions $f(\tau)$, or the symmetrized form $(f(\tau) + f(-\tau))/2$, the form remains unchanged when we transform to $p(\eta)$. A simple example of this is $f(\tau) \propto 1/(1 + \tau^2/3)$, that is for $g(\tau) = \text{constant}$. A more relevant case, which will be discussed in section 3, is:

$$f(\tau) \propto \frac{|\tau(1 - \tau^2/9)|}{(1 + \tau^2/3)^{5/2}}.$$

In some NMR studies using magic angle spinning, the non-sorted principal values v_{ii} have been assumed to be Gaussian random variables [39]. To illustrate the usefulness of the previous relations, we will assume this here, and that the distributions are identical. As $\tilde{V}$ is a zero trace tensor, $\langle v_{xx} + v_{yy} + v_{zz}\rangle = 0$. Their mean value is also zero: $m = \langle v_{ii}\rangle = 0$, and the common variance is $\sigma^2 = \langle v_{ii}^2\rangle$, for any $i = x, y, z$. We denote the Gaussian random variables as $\mathcal{N}(m, \sigma^2)$. In the case considered here, the $\mathcal{N}(0, \sigma^2)$ variables are correlated with a correlation coefficient ρ. Here, $\rho\sigma^2 = \langle v_{ii} v_{jj}\rangle$ for $i \neq j$. The sum $\langle (v_{xx} + v_{yy} + v_{zz})^2\rangle = 3\sigma^2(1 + 2\rho)$. Since $\tilde{V}$ is a zero-trace tensor, this is equal to zero. The variance σ^2 is non-zero so that this has the solution $\rho = -1/2$. By contrast, the Gaussian variables $(v_{xx} - v_{yy})$ (with $\mathcal{N}(0, 3\sigma^2)$) and v_{zz} are independent as they are uncorrelated [50]: $\langle (v_{xx} - v_{yy}) v_{zz}\rangle = \langle v_{yy}^2\rangle - \langle v_{xx}^2\rangle = 0$. The distribution of τ is thus a Lorentz distribution [40]:

$$f(\tau) = \frac{1}{\pi\sqrt{3}} \frac{1}{1 + \tau^2/3}$$

that is:

$$p(\eta) = \frac{6}{\pi\sqrt{3}} \left[\frac{1}{1 + \eta^2/3} \right] \tag{3}$$

with a mean $\langle \eta\rangle = 3\sqrt{3}\log(4/3)/\pi \approx 0.476$. The QS distribution (QS is defined in equation (4)) derived from the previous Gaussian assumptions is a χ-distribution with $n = 2$ degrees of freedom (see equation (28), subsection 4.1) as found also for the so-called Coey-model (see subsection 4.3). The latter distribution $p(\eta)$ in equation (3) is furthermore the one calculated by Varret and Henry [30] for the Coey model (after correcting an error in their $\mathrm{d}\psi/\mathrm{d}\eta$ given as $\propto (1 + \eta^2/3)$ instead of the correct $\propto (1 + \eta^2/3)^{-1}$).

The QS for $\frac{1}{2} - \frac{3}{2}$ isotopes is proportional to Δ defined in equation (3) (we set $eQ/2 = 1$ where e is the electric charge of the electron, and Q is the nuclear quadrupole moment).

$$\Delta^2 = V_{zz}^2 \left(1 + \frac{\eta^2}{3}\right) = \frac{2}{3} S^2. \tag{4}$$

Following Czjzek *et al* [1], we define five real parameters $U_1, \ldots, U_5$ which are directly deduced from the irreducible spherical tensor associated with the EFG tensor $\tilde{V}$.

$$\begin{aligned}
U_1 &= v_{zz}/2 = \frac{1}{2} \sum_n (q_n/r_n^3)(3\cos^2(\theta_n) - 1) \\
U_2 &= v_{xz}/\sqrt{3} = \sqrt{3} \sum_n (q_n/r_n^3) \sin(\theta_n)\cos(\theta_n)\cos(\phi_n) \\
U_3 &= v_{yz}/\sqrt{3} = \sqrt{3} \sum_n (q_n/r_n^3) \sin(\theta_n)\cos(\theta_n)\sin(\phi_n) \\
U_4 &= v_{xy}/\sqrt{3} = \frac{\sqrt{3}}{2} \sum_n (q_n/r_n^3) \sin^2(\theta_n)\sin(2\phi_n) \\
U_5 &= (v_{xx} - v_{yy})/(2\sqrt{3}) = \frac{\sqrt{3}}{2} \sum_n (q_n/r_n^3) \sin^2(\theta_n)\cos(2\phi_n)
\end{aligned} \tag{5}$$

where we have also given the forms valid for a sum over point charges q_n with polar coordinates (r_n, θ_n, ϕ_n). In the above, we correct printing errors in equation (3) of [1] where $\sin^2(\phi_n)$ and $\cos^2(\phi_n)$ have to be replaced by $\sin(2\phi_n)$ and $\cos(2\phi_n)$ respectively. (Note

our notation for the U differs somewhat from those of Czjzek *et al*.) The variable S^2 (note Czjzek *et al* [1] used S) from equation (3) is defined by

$$S^2 = 6\sum_{m=1}^{5} U_m^2 = \sum_{i,j=x,y,z} v_{ij}^2 = \frac{3}{2}\Delta^2. \tag{6}$$

If we now consider an amorphous solid in a fixed laboratory frame of reference, we can look for the five-dimensional distribution of the elements of the EFG tensor $P(U_1, \ldots, U_5)$. The five-dimensional vector $\boldsymbol{U} = (U_1, \ldots, U_5)$ therefore constitutes our random vector. As it is not always clearly stated in the literature, we emphasize that the frame of reference must remain fixed from site to site when the distribution of the EFG tensor is investigated just as we would do for studying the distribution of a random vector, such as the hyperfine magnetic field $\boldsymbol{B}_{hf}$. If, on the contrary, we want to study the distribution of the two parameters V_{zz} and η, it is necessary to diagonalize the EFG tensor from site to site.

3. Statistical invariance by rotation

The most general idea on the structure of amorphous solids is that they are isotropic on average [1]. Such an idea can be checked experimentally, for instance from scattering experiments, and in structural models (see section 4.2). For our present problem, this means that the distribution $P(U_1, \ldots, U_5)$ remains invariant under any rotation of the frame of reference. In the rest of the text, the simplified notation $P(\,)$ will often be used to represent a probability distribution of the set of random variables included in the brackets $(\,)$. That 'P' is used does not imply, except otherwise stated, that the various $P(\,)$ distributions are identical. It is the bracket content and the context that give the specific meaning of every $P(\,)$. For instance, the distribution $P(U_1)$ is the marginal distribution of U_1 that is obtained by integrating the distribution $P(U_1, \ldots, U_5)$ over $U_2, \ldots, U_5$. We emphasize that statistical isotropy of the EFG tensor does not imply any local structural isotropy as seems to be sometimes misleadingly believed.

Consider the example of an amorphous solid in which the EFG at a given probe can be calculated. This can be done from electronic structure calculations [41, 42] for a cluster made up of a central atom and of a certain number of surrounding atoms. The cluster may be restricted in some cases to the first nearest neighbours of the central atom defined for instance by a Voronoi or a radical Voronoi construction. In the latter solid, we consider a given cluster and all clusters that are identical to it within infinitesimal atomic displacements. (The accepted displacements may actually increase with the distance to the central atom without resulting in significant changes of the EFG tensor.) Statistical isotropy of the EFG tensor will result from the fact that the distribution of orientations of the EFG principal axis system is isotropic for any cluster type that can be defined in the amorphous solid.

Similarly, the endpoints of unit vectors of a local frame of reference associated with the considered cluster, and defined by some construction method, will span uniformly a unit sphere. The latter condition implies nothing about the isotropy of the geometric arrangement of atoms in a cluster. In actual amorphous solids, slight deviations from the previous ideal model may take place according to the scale at which they are looked at (see section 4.2).

The general conditions that must be fulfilled by the elements of a Hamiltonian matrix, invariant under linear orthogonal transformations, or by tensors for homogeneous isotropic disordered systems, have been worked out by various authors (for instance see [43–49]). Some conditions are simple to derive as explained below for the case of the EFG tensor. The physically reasonable assumption of the existence of the moments of order 1 and 2,

that is of $\langle U_i \rangle$ and $\langle U_i, U_j \rangle$, whatever i and j, is made in the following. The method consists of the following steps. First we rotate the frame of reference by the Euler angles (α, β, γ). Then the new tensor elements v'_{ij} and thus the new vector components U'_k are expressed in terms of the old ones U_k (see appendix A). Then for a given i and j, $v'_{ij} \stackrel{\mathrm{d}}{=} v_{ij}$ for $i, j = x, y, z$, or $U'_k \stackrel{\mathrm{d}}{=} U_k$. We denote two random variables a and b with identical distributions as $a \stackrel{\mathrm{d}}{=} b$. A rotation of the arbitrarily selected frame of reference around the [111] direction exchanges the Ox, Oy and Oz axes and shows thus that v_{xx}, v_{yy} and v_{zz} have identical distributions. As the trace is zero, the averages $\langle v_{xx} \rangle = \langle v_{yy} \rangle = \langle v_{zz} \rangle = 0$ and thus we deduce from equation (4) that the averages $\langle U_1 \rangle = \langle U_5 \rangle = 0$. If we rotate the frame of reference by $\pi/2$ around the Ox axis ($\alpha = 3\pi/2, \beta = \gamma = \pi/2$), we deduce from for instance appendix A ($v_{xy} = \sqrt{3}U_4$) that $v_{xy} \stackrel{\mathrm{d}}{=} v_{xz} \stackrel{\mathrm{d}}{=} -v_{xy}$ and $U_4 \stackrel{\mathrm{d}}{=} -U_4 \stackrel{\mathrm{d}}{=} U_2$. The distributions of v_{xy} and of v_{xz}, and therefore those of U_2 and U_4, are symmetric about their mean: $\langle v_{xy} \rangle = \langle v_{xz} \rangle = \langle U_2 \rangle = \langle U_4 \rangle = 0$. Identical conclusions are obviously valid for v_{yz} and U_3. If we rotate the frame of reference by $\pi/4$ around the Ox axis, we deduce, for instance from appendix A ($v_{xy} = \sqrt{3}U_4$), that $v_{xy} \stackrel{\mathrm{d}}{=} -v_{xy}$ where $a \stackrel{\mathrm{d}}{=} b$ means that the random variables a and b are identically distributed. The distribution of v_{xy} and therefore the distribution of U_4 are thus symmetric about their mean: $\langle v_{xy} \rangle = \langle U_4 \rangle = 0$. Identical conclusions are obviously valid for v_{xy} and U_2 as well as for v_{yz} and U_3. If we rotate the frame of reference by $\pi/4$ around the Oz axis ($\alpha = \pi/4$, $\beta = \gamma = 0$), we obtain the following EFG tensor in the new frame of reference:

$$\frac{1}{2}\begin{bmatrix} v_{xx} + v_{yy} + 2v_{xy} & v_{yy} - v_{xx} & v_{xz} + v_{yz} \\ v_{yy} - v_{xx} & v_{xx} + v_{yy} - 2v_{xy} & v_{yz} - v_{xz} \\ v_{xz} + v_{yz} & v_{yz} - v_{xz} & 2v_{zz} \end{bmatrix}. \tag{7}$$

This proves that the following distributions are identical, as given by

$$v_{xy} \stackrel{\mathrm{d}}{=} \tfrac{1}{2}(v_{yy} - v_{xx}) \stackrel{\mathrm{d}}{=} -v_{xy}. \tag{8}$$

This shows that U_5 and U_4 are identically distributed. Similar rotations, the effects of which on the U_i are expressed by the relations given in appendix A, allow us finally to write:

$$U_5 \stackrel{\mathrm{d}}{=} U_i \qquad i = 2, 3, 4. \tag{9}$$

As v_{xx}, v_{yy} and v_{zz} are identically distributed, we deduce that:

$$\langle v_{xx}^2 \rangle = \langle v_{yy}^2 \rangle = \langle v_{zz}^2 \rangle$$

and thus using equations (4), (5) and (9) that:

$$\langle U_1 U_5 \rangle = 0$$
$$\langle U_1^2 \rangle = \langle U_i^2 \rangle = \tfrac{1}{20}\langle \Delta^2 \rangle \qquad i = 2, \ldots, 5.$$

As U_5 and U_i, $i = 2, \ldots, 5$ are identically distributed, we also deduce that:

$$\langle U_1 U_i \rangle = 0 \qquad i = 2, \ldots, 5.$$

If similar methods are applied to products of random variables, conclusions can also be obtained about the elements of the (variance) covariance matrix $\tilde{\Lambda}$ of the random vector $\boldsymbol{U}$ the elements of which are:

$$\Lambda_{ij} = \langle U_i U_j \rangle - \langle U_i \rangle \langle U_j \rangle$$

and about higher-rank correlations. The latter correlations are less important for the present problem. Given below are the essential conditions which must be fulfilled by the five elements U_k for the case of statistical isotropy of the EFG tensor [43–49].

(1) The conditions are:

$$\begin{aligned} &\langle U_i \rangle = 0 \qquad i = 1, \ldots, 5 \\ &\langle U_i^2 \rangle = \tfrac{1}{20}\langle \Delta^2 \rangle \qquad i = 1, \ldots, 5 \\ &\langle U_i U_j \rangle = 0 \qquad i \neq j, i, j = 1, \ldots, 5. \end{aligned} \tag{10}$$

There are thus no correlations between the off-diagonal and either the diagonal or the off-diagonal tensor elements. The elements of the covariance matrix are given by:

$$\Lambda_{ij} = \langle U_i U_j \rangle - \langle U_i \rangle \langle U_j \rangle = \tfrac{1}{20}\delta_{ij}\langle \Delta^2 \rangle \qquad i, j = 1, \ldots, 5 \tag{11}$$

where δ_{ij} is the Kronecker symbol. In a more compact notation:

$$\tilde{\Lambda} = \tfrac{1}{20}\langle \Delta^2 \rangle \tilde{I}_5 \tag{12}$$

where $\tilde{I}_5$ is the unit (5×5) matrix. The U_k are therefore *uncorrelated* random variables. However in general *this does not mean that they are independent* (for example see section 5, and [50], p 278).

(2) The invariance hypothesis implies that the U_i, $i = 2, \ldots, 5$ are identically distributed and that they have a symmetrical distribution with a zero mean. As we shall see in section 5, U_1 has in general a different, *a priori* asymmetric, distribution with a zero mean. Porter and Rosenzweig [51] (see also references [47] and [52], p 52) have proven that the assumptions of statistical isotropy of random matrices and of independence of elements determine a unique ensemble, called the Gaussian orthogonal ensemble (GOE) in the case of random real symmetric matrices. Similar and also more general relations have been derived recently by Averbuch for spherical tensors of any rank [49]. Applied to the EFG tensor, these theorems prove that if statistical isotropy and independence of the U_i are assumed (see appendix B) every U_i has a normal (Gaussian) distribution $N(m, s^2)$ with a zero mean $m = 0$ and a variance $s^2 = \langle \Delta^2 \rangle / 20$.

As shown by Czjzek *et al* [1], the transformation from the U_i to the set of five variables (V_{zz}, η) including the three Euler angles (α, β, γ) introduces a Jacobian $V_{zz}^4 \eta (1 - \eta^2/9) \sin(\beta)$. The origin of this is worth being recalled here. If we first perform a transformation from U_i to principal values, we obtain a Jacobian which consists of two separate factors. The first one comes from a Vandermonde determinant [52], $|V_{xx} - V_{yy}||V_{xx} - V_{zz}||V_{yy} - V_{zz}|$, and yields $|V_{zz}^3|\eta(1 - \eta^2/9)$. A second transformation from two independent principal values to (V_{zz}, η) results in a supplementary Jacobian which is proportional to V_{zz}. Thus the first factor is finally $\propto V_{zz}^4 \eta (1 - \eta^2/9)$. The second factor, $\propto \sin(\beta)$, related to the Euler angles, is associated with the uniform measure on the three-dimensional sphere.

This discussion also emphasizes the basic similarity between the zero probability of finding an EFG with $\eta = 0$, and the level-repulsion found in random-matrix theory, as both originate from geometrical correlations due to the Jacobian. (For a recent discussion of this problem, see [53, 54].)

The previous transformation yields a general bivariate distribution of (V_{zz}, η) for statistically isotropic disordered solids (see [1], equation (11)). This is given by the following expression (where Δ^2 is given by equation (3)):

$$f(V_{zz}, \eta) = \frac{V_{zz}^4 \eta}{\sqrt{2\pi}\sigma^5} \left(1 - \frac{\eta^2}{9}\right) F(D^3, \Delta^2) \tag{13}$$

$$D^3 \equiv V_{zz}^3 (1 - \eta^2) \tag{14}$$

with associated marginal distribution for V_{zz} denoted $f_e(V_{zz})$ and for η denoted $f_a(\eta)$. f_e and f_a are given by integrating equation (13) over all η or over all V_{zz} respectively. (Note

Czjzek *et al* [1] have used D instead of D^3.) Δ^2 is the second order and D^3 the third order invariant of the EFG tensor. For non-isotropic solids, $F(D^3, \Delta^2)$ in equation (13) has to be replaced by $F(V_{zz}, \eta)$. The symmetric Czjzek *et al* model (for the case $\beta = 0$, see [1]) is obtained for:

$$F(D^3, \Delta^2) = \exp(-{V_{zz}}^2[1 + \eta^2/3]/(2\sigma^2)) = \exp(-\Delta^2/2\sigma^2).$$

This model we have named the Gaussian isotropic model (GIM) for reasons made clear in the next section. The associated $f_a(\eta)$ marginal distribution is then calculated to be:

$$f_a(\eta) = r(\eta) = \frac{3\eta(1 - \eta^2/9)}{(1 + \eta^2/3)^{5/2}}. \tag{15}$$

In the following, $r(\eta)$ will represent this *model distribution*. The average value of the asymmetry parameter and of its square can be calculated to be:

$$\langle\eta\rangle = 2\sqrt{3} - (3\sqrt{3}/2)\log(3) \approx 0.609\,82$$
$$\langle\eta^2\rangle \approx 0.430\,78.$$

The standard deviation of the asymmetry parameter is given by:

$$\sigma_\eta \equiv \langle(\eta - \langle\eta\rangle)^2\rangle^{1/2} = (42 - 24\sqrt{3} - \langle\eta\rangle^2)^{1/2} \approx 0.242\,68$$

so that the ratio is given by:

$$\rho_\eta = \frac{\sigma_\eta}{\langle\eta\rangle} \approx 0.398.$$

We could as well have expressed the Jacobian discussed above in terms of τ (see section 2), the ratio of non-sorted principal values, instead of η. Then we would have derived a distribution $f(\tau)$ identical with $r(\eta)$ (equation (15)), except for additional absolute value signs. As discussed in section 2, such an $f(\tau)$ indeed remains of the same form as $r(\eta)$ when the distribution of η is calculated from that of τ.

The marginal distribution for V_{zz} is calculated to be:

$$f_e(V_{zz}) = \frac{1}{\sigma}\sqrt{\frac{2}{\pi}}\left[\left(\frac{3V_{zz}^2}{2\sigma^2} - 1\right)\exp\left(\frac{-V_{zz}^2}{2\sigma^2}\right) + \left(1 - \frac{4V_{zz}^2}{3\sigma^2}\right)\exp\left(\frac{-2V_{zz}^2}{3\sigma^2}\right)\right] \tag{16}$$

where σ^2 is given by $\langle\Delta^2\rangle/5$. The maximum is at $V_{zz}/\sigma \approx 1.867\,1035$. This form is especially useful in cases where the experimental sensitivity to η is not very high, such as in the case of ^{57}Fe Mössbauer spectroscopy [16]. We note the following properties of this marginal distribution:

- $f_e(V_{zz})$ varies as V_{zz}^4 for $V_{zz} \to 0$.
- The square average of V_{zz} is given by:

$$\langle V_{zz}^2\rangle = \sigma^2(14 - 3\sqrt{3})/2 = \langle\Delta^2\rangle(14 - 3\sqrt{3})/10 \approx 0.8804\langle\Delta^2\rangle.$$

- This is well approximated by:

$$\langle V_{zz}^2\rangle \approx \langle\Delta^2\rangle/(1 + \langle\eta^2\rangle/3) \approx 0.8744\langle\Delta^2\rangle$$

or even:

$$\langle V_{zz}^2\rangle \approx \langle\Delta^2\rangle/(1 + \langle\eta\rangle^2/3) \approx 0.8897\langle\Delta^2\rangle.$$

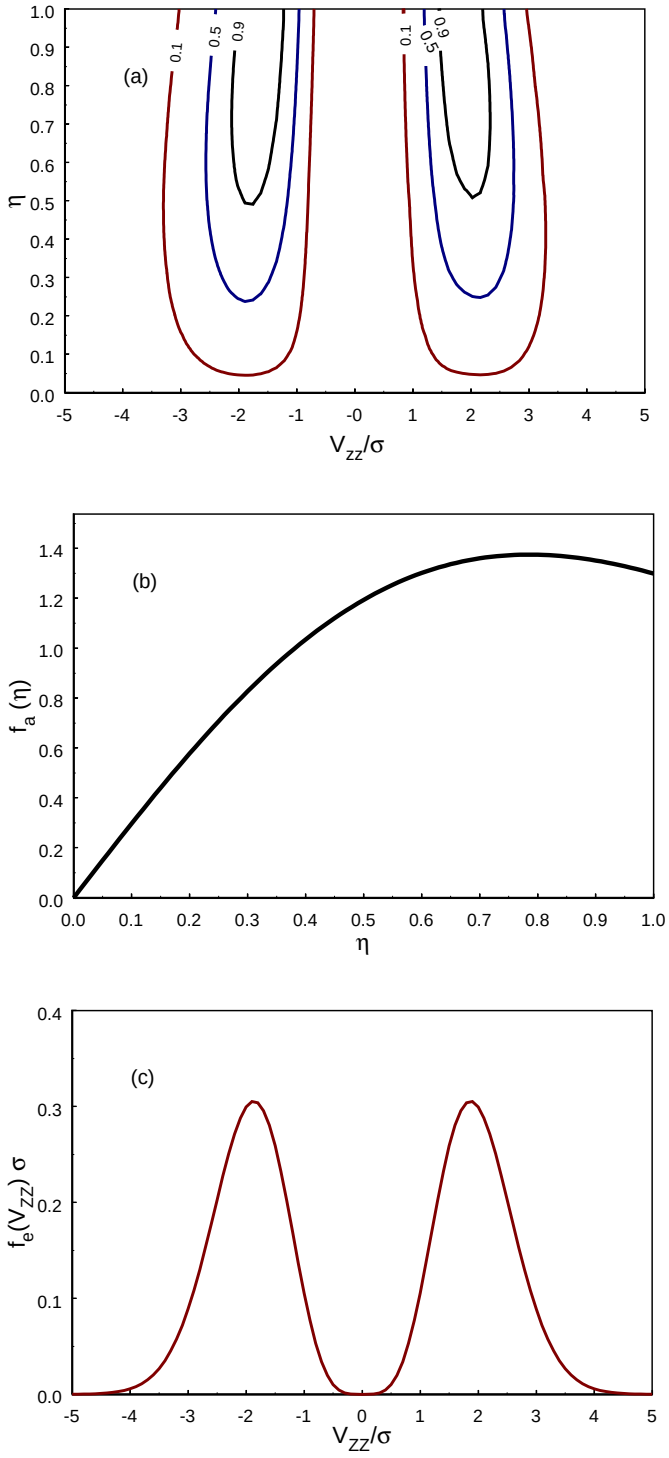

Figure 1. (a) Contour map of the Czjzek probability function, equation (13). (b) Marginal distribution $f_a(\eta)$ given by equation (15). (c) Marginal distribution $f_e(V_{zz})$ given by equation (16). V_{zz} is normalized to σ where $\sigma^2 = \langle\Delta^2\rangle/5$.

A Cartesian contour map of equation (13) is shown in figure 1(a) where V_{zz} has been normalized to σ. Figure 1(b) and (c) give the marginal distributions $f_a(\eta)$ and $f_e(V_{zz})$ respectively. As has been pointed out by Czjzek [55], a Cartesian contour map *does not* represent in an adequate way the connectivity of the parameter space. Czjzek pointed out that two symmetrical points (V_{zz}, η) and $(-V_{zz}, \eta)$ are connected both by a variation through the point $V_{zz} = 0$ and by a variation through $\eta \to 1$. When $\eta = 1$, $V_{xx} = 0$, while $V_{yy} = -V_{zz}$. Thus, the sign of V_{zz} cannot be defined for $\eta = 1$ and the two points ($V_{zz} > 0$, $\eta = 1$) and ($V_{zz} < 0$, $\eta = 1$) should be connected on the graph to represent this. In addition, the connection through $V_{zz} = 0$ but $\eta \neq 0$ is clearly unphysical. Czjzek introduced a polar plot (r, ϕ) based on the variable transformation:

$$V_{zz}^2(1 + \eta^2/3) = r^2$$
$$V_{zz}^3(1 - \eta^2) = r^3 \sin(3\phi).$$

In this representation, the segment $\phi \in (-\pi/6, \pi/6)$ contains all information. A contour map for this plot is shown in figure 2. The upper segment represents $V_{zz} > 0$, the lower $V_{zz} < 0$, and $\phi = 0$ represents $\eta = 1$. $\eta = 0$ is given by $\phi = \pi/6$ for positive V_{zz}, and by $-\pi/6$ for negative V_{zz}. The transformation from (r, ϕ) to (V_{zz}, η) is given in table 1.

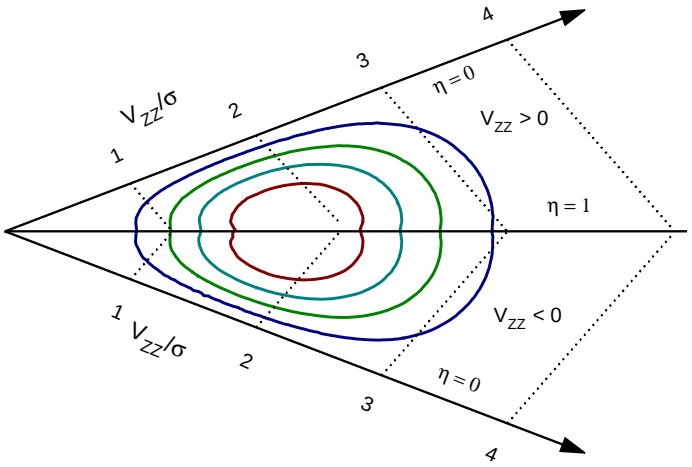

Figure 2. Contour map of the Czjzek probability function, equation (13) in polar coordinates. $\eta = 1$ is the horizontal axis. V_{zz} is normalized to σ, and the dashed lines are lines of constant V_{zz}. Radial lines are lines of constant η.

Table 1. Transformation for r, ϕ to V_{zz}, η for the EFG distribution plot of Czjzek *et al.*

Variable	$V_{zz} < 0$	$V_{zz} > 0$
$V_{zz}(r, \phi)$	$-r\cos(\pi/6 + \phi)$	$r\cos(\pi/6 + \phi)$
$V_{zz}(x, y)$	$-\frac{1}{2}(\sqrt{3}x - y)$	$\frac{1}{2}(\sqrt{3}x - y)$
$\eta(\phi)$	$\sqrt{3}\tan(\pi/6 + \phi)$	$\sqrt{3}\tan(\pi/6 + \phi)$
$\eta(x, y)$	$\sqrt{3}(x + \sqrt{3}y)/(\sqrt{3}x - y)$	$\sqrt{3}(x - \sqrt{3}y)/(\sqrt{3}x + y)$

An interesting conclusion about 'universal' features of the distribution $r(\eta)$ of the asymmetry parameter η which does not seem to have been emphasized up to now can

be deduced from equation (13). The marginal distribution $f_a(\eta)$ will indeed be identical with the model $r(\eta)$ in the following cases among others:

(A) We assume that the function:

$$F(D^3, \Delta^2) = G(\Delta^2)$$

only depends on:

$$\Delta = |V_{zz}|\sqrt{1 + \eta^2/3}$$

that is, only on the modulus of the EFG tensor. Then equation (13) may be rewritten as follows:

$$f(V_{zz}, \eta) \propto \Delta^4 G(\Delta^2) \frac{\eta(1 - \eta^2/9)}{(1 + \eta^2/3)^2}. \tag{17}$$

By making the change in variables from (V_{zz}, η) to (Δ, η), we obtain the equivalent bivariate distribution function:

$$h(\Delta, \eta) \propto \Delta^4 G(\Delta^2) \frac{\eta(1 - \eta^2/9)}{(1 + \eta^2/3)^{5/2}}. \tag{18}$$

If the following condition is fulfilled the distribution of η is $r(\eta)$ as given by equation (15). This condition is that the integration over Δ which has to be performed in equation (18) to calculate the marginal distribution of η must not contribute to an extra η-dependent term. The integration over Δ must therefore be performed in a rectangular domain given by $0 \leqslant \eta \leqslant 1$, and $\Delta_1 \leqslant \Delta \leqslant \Delta_2$. From this, conditions about V_{zz} may be derived. The universal $r(\eta)$ distribution (equation (15)) will be found in particular in disordered solids verifying equation (18) and in which $\Delta^4 G(\Delta^2)$ is defined for Δ ranging from 0 to ∞ whatever η. In practice it is sufficient that the upper bound be large as compared to the standard deviation of Δ, given by:

$$\sigma_\Delta \equiv \langle(\Delta - \langle\Delta\rangle)^2\rangle^{1/2}.$$

It is deduced from equation (17) that:

$$\text{prob}(V_{zz} > 0) = \text{prob}(V_{zz} < 0) = 1/2.$$

(B) Keeping the latter hypothesis about the range of definition of $\Delta^4 G(\Delta^2)$, we assume now that there is a hole in the V_{zz} distribution at the origin: $f_e(V_{zz} \approx 0) \approx 0$, as observed in many models and in many actual disordered solids [1]. It is thus possible to relax the symmetry condition by supposing that $f(V_{zz}, \eta)$ (equation (13)) is such that for $V_{zz} > 0$ (where $-1/2 \leqslant \alpha \leqslant 1/2$):

$$f^+(V_{zz}, \eta) = (\tfrac{1}{2} + \alpha) f_t(\Delta^2) \tag{19}$$

and for $V_{zz} < 0$:

$$f^-(V_{zz}, \eta) = (\tfrac{1}{2} - \alpha) f_t(\Delta^2). \tag{20}$$

The 'shapes' of $f^\pm(|V_{zz}|)$ are thus identical for $V_{zz} > 0$ and $V_{zz} < 0$ but their respective weights differ. To obtain equations (19) and (20), we write $F(D^3, \Delta^2)$ as:

$$F(D^3, \Delta^2) = G(\Delta^2)(\tfrac{1}{2} + \alpha s(D^3)) \tag{21}$$

where $s(x)$ is a function which mimics the behaviour of the sign(x) function. In practice an approximate sign(x) behaviour is only needed in a range in which $f_t(\Delta^2)$ is significant, $s(x)$ being equal to -1 for $x < 0$ and to $+1$ for $x > 0$. Such a function must vary very rapidly from -1 to $+1$, typically in a short interval $\mathrm{d}V_{zz}$ centred on zero in which $f_e(V_{zz} \approx 0)\,\mathrm{d}V_{zz}$ is small. Examples are for instance erf(x) or tanh(x). Further examples include a piecewise

linear function y, where $y = ax$ (with $a > 0$) for $x \in (-1/a, 1/a)$, and outside this interval, $y = -1$ for $x \leqslant -1/a$, and $y = 1$ for $x \geqslant 1/a$. Such hypotheses, although they may seem rather artificial, still lead to equation (18) being valid for $h(\Delta, \eta)$.

The distribution $r(\eta)$ given in equation (15) may conceivably be valid in more complicated cases than those dealt with here. A model which is described in section 6 (equation (52)), yields for instance distributions $f_a(\eta)$ depending parametrically on x, where $(1 - x)$ measures the deviation from GIM. These deviate little from $r(\eta)$ for $x \geqslant 0.5$ (as will be shown later in figure 16). The marginal distributions $f_e^{\pm}(|V_{zz}|)$ have rather similar although not identical 'shapes', in particular for when the parameter x is larger than $\approx$0.6. (Figure 15 presented later compares $f_e^{+}(|V_{zz}|)$ with $f_e^{-}(|V_{zz}|)$.) The extended models of Czjzek [29] for $n = 3$ and 4 also yield distributions $f_a(\eta)$ which are very well approximated by $r(\eta)$ (see subsection 4.2.2). In cases (A) and (B), the integration of $h(\Delta, \eta)$ over η yields the QS distribution. Reciprocally the distribution of $(|V_{zz}|, \eta)$ is simply given by the product of the QS distribution by $r(\eta)$ and by $(1 + \eta^2/3)^{1/2}$.

Supplementary experiments, for instance using applied magnetic fields, allow determination of the distribution of (V_{zz}, η) from the distribution of $(|V_{zz}|, \eta)$ and from the respective weights of the positive $V_{zz} > 0$ and negative $V_{zz} < 0$ parts. Such models may thus have a practical importance. Experimental average asymmetry parameters close to $\langle\eta\rangle \approx 0.6$ are very often quoted in the literature for disordered solids ([7, 32, 56, 57 58] among others). The previous assumptions may possibly be approximately verified in various amorphous alloys but experimental and simulation studies remain to be performed to establish their actual range of validity. Conditions which yield the aforementioned EFG and $r(\eta)$ distributions (such as (A), (B) or further conditions to be established) may be checked more convincingly with physically sound calculations [41, 42] in structural models. Moreover, recent methods allow constructing quite realistic models of amorphous solids (see [59–61]).

Model (A) is found for instance when the concentration of point defects in cubic solids is small and when the electric field gradients result from randomly distributed unscreened point charges as investigated by Stöckmann [2]. More generally model (A) is found when the contributions of the individual defects linearly superpose to give the total field gradient as shown for instance by Cohen and Reif [3]. In the latter case, the distribution $P(U_1, \ldots, U_5)$ is then *approximately* a multivariate ($n = 5$) Cauchy distribution. That is, as shown by Stöckmann (equations (40) and (41) of [2]), it is proportional to $(\Delta(0)^2 + \Delta^2)^{-3}$. The actual distribution must indeed be truncated as compared to the Cauchy distribution as it cannot have diverging moments. Such a Cauchy distribution is clearly rotationally invariant and further yields an example of a statistically isotropic distribution of a vector $\boldsymbol{U}$ whose components U_i are not independent as is required by the Porter–Rosenzweig theorem (see appendix B).

Grenèche *et al* [6, 57] have studied continuous random networks of corner-sharing octahedra (simulating amorphous FeF_3). They have found prob$(V_{zz} > 0) \approx$ prob$(V_{zz} < 0)$ and a distribution of η very close to the distribution of equation (15) (see [57], figure 6). Such models may possibly verify the assumptions of case (A). It is important to emphasize that their results differ from the GIM predictions because the QS distribution is not given by equation (28) with $n = 5$ (section 4.1) but is well approximated by the same equation with $n = 2.9$ ([57], figure 5). An example which may perhaps illustrate case (B) is amorphous $Fe_{24}Zr_{76}$ as a mean $\langle\eta\rangle \approx 0.67 \pm 0.07$ and prob$(V_{zz} > 0) = 1$ were reported from Mössbauer spectra recorded in applied fields [7]. A mean $\langle\eta\rangle \approx 0.5$ and prob$(V_{zz} > 0) = 1$ were reported from Mössbauer spectra of iron-based oxide glasses Fe_2O_3–BaO–B_2O_3 recorded in applied fields [58]. The models discussed above may also be useful in other fields as shown

for instance by recent EPR studies of glasses [37, 62]. It is likely that the $r(\eta)$ distribution is not very rapidly distorted when deviations occur from the ideal models described above as already shown by the early computer simulations of Czjzek *et al* [1] for amorphous solids with random ionic coordination. To conclude, the distribution $r(\eta)$, equation (15), appears to be rather robust, being an excellent approximation of many $f_a(\eta)$. As discussed above, its general validity is basically related to correlations between principal values of the EFG tensor induced by the Jacobian of the transformation from the U_k to $(V_{zz}, \eta, \alpha, \beta, \gamma)$ [53, 54]. The $r(\eta)$ distribution is therefore the most *a priori* reasonable guess for an *unknown* marginal distribution of η in an amorphous solid.

4. The multivariate normal distribution: Gaussian isotropic model and degenerate Gaussian models

As the multivariate normal distribution plays an important role in the EFG distribution models, we recall here its definition. We first define the characteristic function $\Phi(t)$ of a random variable x characterized by a repartition function given by:

$$F(x) = \text{prob}(X \leqslant x) = \int_{-\infty}^{x} \mathrm{d}F(x')$$

is given as usual by the following integral:

$$\Phi(t) = \langle \exp(\mathrm{i}tX) \rangle = \int_{-\infty}^{+\infty} \exp(\mathrm{i}tx)\, \mathrm{d}F(x). \tag{22}$$

For an n-dimensional random variable $\boldsymbol{X}$, the scalar variables t and X are replaced by the n-dimensional vectors $\boldsymbol{t}$ and $\boldsymbol{X}$ respectively and the product tX by a scalar product $\boldsymbol{t} \cdot \boldsymbol{X}$ in an n-dimensional Fourier integral. The characteristic function of an $\mathcal{N}(m, \sigma^2)$ Gaussian random variable X (where $m = \langle X \rangle$ and $\sigma^2 = \langle (X - m)^2 \rangle$) is $\Phi(t) = \langle \exp(\mathrm{i}tX) \rangle = \exp(\mathrm{i}mt - \sigma^2 t^2/2)$ [50, 63, 64], whose value at $t = 1$ is $\exp(\mathrm{i}m - \sigma^2/2)$. The multivariate normal distribution of an n-dimensional random vector $\boldsymbol{X}$, $\mathcal{N}(\boldsymbol{m}, \tilde{\Lambda})$ is defined in the most general case by its characteristic function and not by its distribution function as $\tilde{\Lambda}$ may be singular [32, 50, 56, 57]. $\boldsymbol{m} = \langle \boldsymbol{X} \rangle$ is the n-dimensional vector of the means and $\tilde{\Lambda}$ the symmetric non-negative definite $(n \times n)$ covariance matrix whose elements are $\Lambda_{ij} = \langle X_i X_j \rangle - m_i m_j$. The random variable $Z = \boldsymbol{t} \cdot \boldsymbol{X}$ [64], where $\boldsymbol{t}$ is the vector with elements $(t_1, \ldots, t_n)$, is a linear combination of Gaussian variables. It is thus a Gaussian random variable $\mathcal{N}(\boldsymbol{t} \cdot \boldsymbol{m}, {}^t\boldsymbol{t}\tilde{\Lambda}\boldsymbol{t})$ where ${}^t\boldsymbol{t}$ is the transpose of $\boldsymbol{t}$. Therefore $\langle \exp(\mathrm{i}Z) \rangle = \langle \exp(\mathrm{i}\boldsymbol{t} \cdot \boldsymbol{X}) \rangle = \exp(\mathrm{i}\boldsymbol{t} \cdot \boldsymbol{m} - {}^t\boldsymbol{t}\tilde{\Lambda}\boldsymbol{t}/2)$. This latter function of $\boldsymbol{t}$ is the characteristic function of $\boldsymbol{X}$:

$$\Phi(\boldsymbol{t}) = \exp(\mathrm{i}\boldsymbol{t} \cdot \boldsymbol{m} - \tfrac{1}{2}{}^t\boldsymbol{t}\tilde{\Lambda}\boldsymbol{t}). \tag{23}$$

A random vector $\boldsymbol{U}$ having the distribution $N(\boldsymbol{m}, \tilde{\Lambda})$ is said to be a normal vector. Its distribution is thus entirely defined by giving the vector of means and the matrix of variances and covariances. If $\tilde{\Lambda}$ is non-singular, the probability density function $P(U_1, \ldots, U_n)$ can be obtained by an inversion of the characteristic function:

$$P(U_1, \ldots, U_n) = \frac{1}{\sqrt{(2\pi)^n \det(\tilde{\Lambda})}} \exp\left[-\frac{1}{2}{}^t(\boldsymbol{U} - \boldsymbol{m})\tilde{\Lambda}^{-1}(\boldsymbol{U} - \boldsymbol{m}) \right]. \tag{24}$$

If $n = 5$ and if the five random variables U_k are linearly dependent on p Gaussian independent variables (where $p < 5$), the normal distribution is degenerate and the matrix $\tilde{\Lambda}$ is singular, with rank $p < 5$ [50, 63–65]. In this case, the probability density function is no longer given by equation (24) with $n = 5$.

4.1. Five degrees of freedom

If the EFG tensor is statistically invariant by rotation and if $P(U_1, \ldots, U_5)$ is multivariate normal, equations (12) and (24) yield for $n = 5$:

$$P(U_1, \ldots, U_5) = \prod_{i=1}^{5} P(U_i). \tag{25}$$

The U_i are independent and normally distributed:

$$P(U_i) = \frac{1}{s\sqrt{2\pi}} \exp\left(-\frac{U_i^2}{2s^2}\right) \tag{26}$$

with $s^2 = \langle\Delta^2\rangle/20$ (equation (12)). Conversely, if the U_i are independent ($n = 5$), the covariance matrix is diagonal and non-singular and the U_i are Gaussian random variables, as proven in appendix B. For $n = 5$, we recover [8, 9, 16, 28] the model of Czjzek *et al* [1] for random atomic packings but without the small asymmetric contribution found in such models. That is we find $\beta = 0$ [1] in the joint distribution function $f(V_{zz}, \eta)$ derived by the latter authors from their numerical simulations (see [1], equation (22)):

$$f(V_{zz}, \eta) = \frac{{V_{zz}}^4 \eta}{\sqrt{2\pi}\sigma^5}\left(1 - \frac{\eta^2}{9}\right)\exp\left[-\frac{V_{zz}^2}{2\sigma^2}\left(1 + \frac{\eta^2}{3}\right)\right]. \tag{27}$$

It is worthwhile recalling that the latter distribution has been derived not only for random amorphous solids [1], but also for large concentrations of defects in cubic systems [2]. Our derivation proves that it is also valid in all cases where the physics that determines the EFG distribution fulfils the conditions of applicability of the central limit theorem (see for instance [50] and section 5). The components of the EFG tensor are then sums over a large number of random terms, each of which if considered individually has a reduced importance [8, 9]. This strongly contradicts the still-used claim [66] that the previous functional form (as given by equation (27)) is only valid for the case of an EFG tensor based on a point-charge model. It will also be true for long-ranged oscillating potentials, for instance in aluminum-based Al–transition metal (TM) disordered or amorphous solids [9] where strong and long-range interactions between Al and TM play an important role [67]. The QS distribution is readily deduced from equations (3), (5), (25) and (26), which lead to a χ^2 distribution for Δ^2 with five degrees of freedom, that is a χ distribution for Δ:

$$P_n(\Delta) = \frac{1}{2^{(n-2)/2}\sigma^n\Gamma(n/2)}\Delta^{n-1}\exp\left(-\frac{\Delta^2}{2\sigma^2}\right) \tag{28}$$

with $n = 5$ and $\sigma^2 = 4s^2 = \langle\Delta^2\rangle/5$. $\Gamma(n/2)$ is the usual gamma function. The model given by equations (25) to (28) we call the Gaussian isotropic model (GIM) for reasons now obvious [8, 9, 16, 28]. It is a universal reference model, but devoid of structural information, that is made possible in some systems by the physics of the EFG. The GIM allows calculating all kinds of distributions related to the EFG tensor (equations (15) and (16), [16] and Le Caër, unpublished). By symmetry, the probabilities of finding $V_{zz} > 0$ or $V_{zz} < 0$ are equal to $1/2$. The ratio defined by Levy Yeyati *et al* [56] given by:

$$\rho_z = \frac{\sqrt{\langle V_{zz}^2\rangle - \langle|V_{zz}|\rangle^2}}{\langle|V_{zz}|\rangle} = \frac{\sigma_{|V_{zz}|}}{\langle|V_{zz}|\rangle}$$

is calculated to be equal to:

$$\tfrac{1}{5}\sqrt{14\pi - 3\sqrt{3}\pi - 25} \approx 0.326\,07$$

for the GIM [16]. The latter authors [56] quote values close to the GIM values with $\langle\eta\rangle = 0.67$ and with $\rho_z = 0.36$ from experiments in a-$Zr_{70}Cu_{30}$. From rather involved calculations in a structural model with 100 atoms they find $\langle\eta\rangle = (0.64, 0.63)$ and $\rho_z = (0.30, 0.26)$. A value $\rho_\eta = \sigma_\eta/\langle\eta\rangle \approx 0.42$ (see section 3) is further quoted for the same model in [32]. As the GIM is in the end dominated either by the universal character of the central limit theorem or by a trend towards independent U_k, it is not in a one to one correspondence with a given disordered structure. For $n = 5$, it is worth emphasizing again [8, 9, 28] that the observation of the distribution of Czjzek *et al* [1], equation (27), does not imply that a given amorphous structure can actually be described as a dense random packing of atoms. A good experimental counterexample seems to be amorphous gallium. The EFG distribution for a dense random packing model agrees with the PAC results but this model is known to fail to account for the structure factor observed in diffraction experiments [85–87]. The power of the central limit theorem that works for additive random variables must not be neglected when dealing with such experimental results. Supplementary arguments on this point will be presented in section 6.

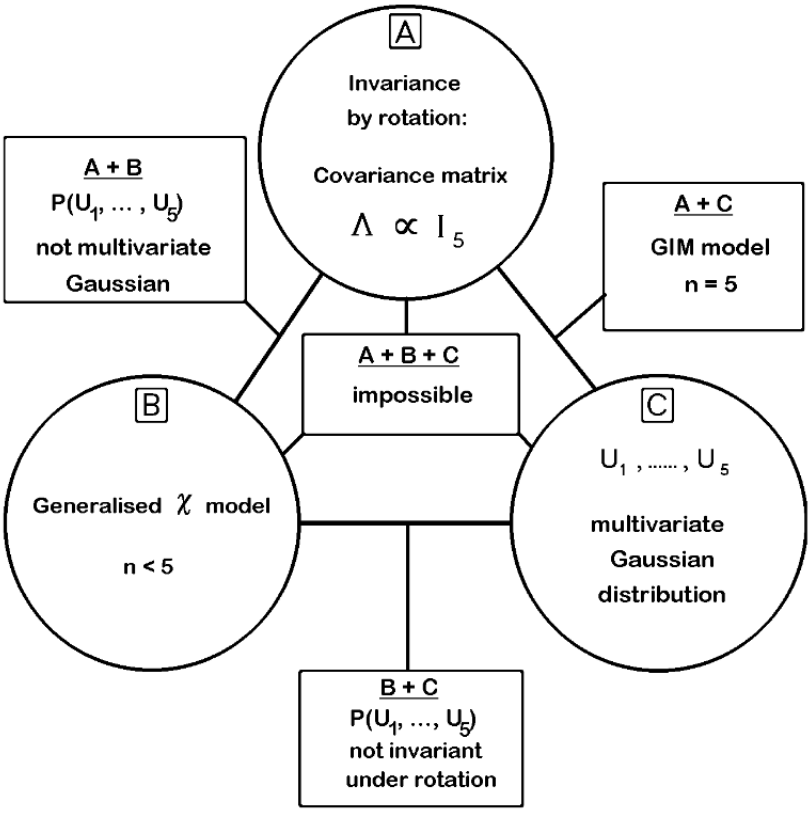

Figure 3. Relationships between three possible conditions for the EFG tensor. The GIM model corresponds to A + C. We denote a model with conditions B + C as 'degenerate Gaussian'. The Coey model would correspond to an example of A + B.

4.2. Fewer than five degrees of freedom

Quite curiously, the models that lead to a QS distribution given by equation (28) with $n = 1, \ldots, 4$ (often even extended to non-integer values less than five) are called 'shell models' in the literature. The latter name is *totally unjustified* as it suggests that the EFG tensor still possesses statistical invariance by rotation. This is in contradiction with the assumptions needed to derive such models as will be proven below (see also section 5). Czjzek has assumed in a later publication [29] that the U_k are not independent variables and that they are linear functions of n other variables ε_j with $n < 5$, where 'the parameters ε_j are Gaussian centred at the origin' [29]. This is equivalent to assuming that the five-dimensional random vector $\boldsymbol{U}$ has a degenerate multivariate normal (Gaussian) distribution since it is linearly related to an n-dimensional normal vector $\boldsymbol{\varepsilon}$ with $n < 5$. The multivariate normal distribution is entirely determined by an expectation vector (here zero) and a covariance matrix (section 4 and equation (23)). Thus the immediate consequence of the previous assumptions is indeed [50, 64, 65] that the covariance matrix of $\boldsymbol{U}$, denoted $\tilde{\Lambda}$, is singular with a rank $n < 5$. As $\tilde{\Lambda}$ cannot be simultaneously singular and proportional to $\tilde{I}_5$ (equation (12)), the EFG tensor cannot therefore be statistically invariant by rotation. The different mathematical relationships which are discussed are given schematically in figure 3. The GIM model would correspond in this figure to conditions A + C. The conditions A + B + C are impossible, but any of the combinations A + B, A + C or B + C are possible. For the reasons discussed above, it would be desirable to abandon the confusing and erroneous name of 'shell models' (see also section 5 and more particularly for $m = 3$) and to replace it by one of the following two possibilities given below.

(1) It could be termed a 'degenerate Gaussian model' if Czjzek's assumptions about the EFG tensor distribution [29] are explicitly taken into consideration (condition C), n is thus an integer $n < 5$ (condition B). The EFG tensor cannot be statistically invariant by rotation. We will denote this model as Cz(n). It is discussed below in section 4.2.2.

(2) It could also be termed a 'generalized χ model' if we only assume equation (28) to be valid with integer or non-integer values of n. This can be used for the sole purpose of fitting a QS distribution without any implication for the EFG tensor distribution. Distribution (28) is a particular subfamily of what are called in [68] the generalized gamma distributions. As it is moreover a generalization of a χ distribution to non-integer values of n, we propose to use here the name 'generalized χ models'.

Whatever $n \geqslant 1$, the average $\langle\Delta\rangle$ is equal to $\sqrt{2}\sigma\Gamma((n+1)/2)/\Gamma(n/2)$, and the maximum of the probability distribution is located at $\Delta_{\max} = \sigma\sqrt{n-1}$. The variance $\sigma_\Delta^2 = \langle(\Delta - \langle\Delta\rangle)^2\rangle$ is such that $\sigma_\Delta^2 + \langle\Delta\rangle^2 = n\sigma^2$. An empirical relationship, which may be useful in practice, holds approximately between the three latter characteristics:

$$\langle\Delta\rangle = 0.8541\Delta_{\max} + 0.5956\sigma_\Delta$$

with a relative error less than 9×10^{-3} for $n \leqslant 5$. Only the 'generalized χ models' and not the 'degenerate Gaussian models' have been actually checked in Mössbauer spectroscopy as experimental evidence of anisotropic effects has never been looked for or reported up to now. As given by figure 3, a model including condition B must be checked for condition A ($P(U_1, \ldots, U_5)$ not multinormal) or condition C ($P(U_1, \ldots, U_5)$ not invariant by rotation).

The proposed model names will be used in the rest of the text. We stress that one must not confuse the obvious rotational invariance of the quadrupole splitting (the modulus of the EFG tensor, equation (6)) with the statistical rotational invariance of the EFG tensor itself. Consequently QS measurements cannot test the validity of the assumptions made by Czjzek [29]. Such assumptions may however be checked with structural models (section 3)

by studying the distribution of the EFG tensor itself, as done for instance in section 5, and not only the QS distribution. It would be possible using random rotations to produce models which have the same QS and $f(V_{zz}, \eta)$ distributions as the 'degenerate Gaussian models' ($n < 5$) and which are simultaneously statistically isotropic. In such models, the distributions of $\boldsymbol{U}$, which depend on n, cannot be multivariate normal.

4.2.1. Structural considerations. To show the problem raised by the ($n < 5$) 'degenerate Gaussian models', we must go back to the structural models. Consider a single crystal of some ordered compound with various sites. There are strong correlations between the orientations of the EFG principal axes from site to site. $P(U_1, \ldots, U_5)$ is not invariant by rotation. If we consider now a polycrystal, built up of a collection of the latter single crystals, in which all crystallographic orientations occur in the sample with equal probability, the previous invariance will be recovered, but this invariance has an artificial character. We are not led to consider (for example for such a sample) that the significant model of the atomic structure is that at the scale of the polycrystal (sample), but that at the level of the single crystal. For an amorphous solid, a typical scale L is given by the distance at which the value of the pair correlation functions deduced from x-ray or (and) neutron diffraction measurements cannot be distinguished from an uncorrelated distribution, that is one to several nanometres (see for instance [69, 70]).

If the validity of the Czjzek model extension ($n < 5$) is established, it would mean that the disordered solid under consideration possesses some order in the orientations of the EFG principal axes in a volume of order L^3 and for instance at all nuclei of the probed atomic species surrounded by similar clusters as defined in section 3. Such an orientational order, which depends on n, would not just be of short-range character, but medium- or long-range character, that is it would extend to distances of the order of L. An orientational order on distances much smaller than L would be averaged and would produce only negligible deviations from the expected statistically isotropic model. In the case $n = 1$, it can be shown that the principal axes of the EFG tensor have the same directions at all probed nuclei. This is a consequence of the fact that $\boldsymbol{U} = x\boldsymbol{U}_0 + \boldsymbol{U}_c$ where $\boldsymbol{U}_0$ and $\boldsymbol{U}_c$ are fixed vectors and x has a Gaussian distribution with zero mean according to the assumption of Czjzek for $n = 1$. As the average of every component of $\boldsymbol{U}$ must be zero to ensure that the QS distribution is given by equation (28) with $n = 1$, $\boldsymbol{U}_c = 0$. The principal axes of the EFG tensor $\tilde{V} = x\tilde{V}_0$ are thus those of the fixed part $\tilde{V}_0$ and the eigenvalues of $\tilde{V}$ are x times the eigenvalues of $\tilde{V}_0$. The asymmetry parameter is consequently constant $\eta = \eta_0$ and $V_{zz} = xV_{zz,0}$ has a Gaussian distribution with zero mean. (Note that η is only defined for $x \neq 0$ but the probability of $x = 0$ is zero.) This anisotropy is reminiscent of an organization of structural elements either in a crystal or in a quenched analogue of an anisotropic fluid depending on the appropriate range of translational order [71]. New results on degenerate Gaussian models Cz(n) are reported in the next subsection for $2 \leqslant n \leqslant 4$.

Such questions have already been raised by Alben *et al* [72] to explain correlations responsible for anisotropic electron scattering properties from small areas of amorphous films. Using structural models, dense random packings and tetrahedrally bonded continuous random networks, they concluded [72] that the scattering anisotropy is not very different from that which occurs for random scattering but quite different from that expected for a crystal. Dense random packing models such as the Finney model have been shown to be macroscopically equivalent to isotropic liquids [71]. It is however important to look for anisotropic effects at the correct scale in order to avoid averaging effects analogous to those performed in a polycrystal in the case of crystals as furthermore such effects will generally

be small. Very recently, Gaskell and Wallis [69] have shown from the interpretation of the first diffraction peaks of a–SiO_2 that anisotropic scattering is directly related to the presence of periodic fluctuations in atomic density—with 'quasi-Bragg planes' defining a medium-range structure at a scale of $\approx$1 nm. Such characteristics would also hold for several types of glass. Bond-orientational anisotropy has been recently observed by x-ray diffraction in thin amorphous Tb–Fe–Co films [73]. Tomida and Egami [74] have also performed computer simulations to analyse the structural anisotropy induced by thermomechanical treatments of amorphous solids below the glass transition temperature. In a more recent work [75], the latter authors have analysed orientational order between local clusters, extending the study of orientational order between bonds defined by Steinhardt *et al* [71].

Although cluster orientational correlations may exist in amorphous solids, their effect on the distributions of EFG tensors at nuclei of selected chemical elements is expected to be negligible as moreover averaging is performed at the scales at which experiments are usually performed to probe such distributions. Unfortunately, Mössbauer spectroscopy gives no information on the site-to-site correlations of the EFG principal axis systems. Therefore it is not possible to know for a solid whose EFG properties show rotational invariance whether this originates from a lack of orientational correlations, or from the latter sample averaging effect. If the assumptions of the 'degenerate Gaussian models' of Czjzek [29] or extensions of them are taken as working hypotheses, the previous discussion means that at best only such experiments which are spatially sensitive may reveal some anisotropy in the orientations of EFG principal axes. Examples are depth-selective conversion electron Mössbauer spectroscopy (DCEMS) experiments or reflectivity measurements using nuclear-resonant (forward) scattering of synchrotron radiation. Appropriate systems would include thin amorphous films (possibly subjected to prior thermomechanical treatments such as creep to orient the correlated regions [74]). Certainly high signal to noise ratios would be necessary for such experiments. Such amorphous films would have to be selected in systems whose QS distributions agrees at least approximately with the generalized χ distribution (equation (28) for $n < 5$) and better with the smallest observed value of n. The latter condition would be necessary for evidencing possible differences in peak intensity ratios between DCEMS or reflectivity spectra, and bulk measurements. Amorphous $Fe_{24}Zr_{76}$ with $\text{prob}(V_{zz} > 0) = 1$ and with $n = 1$ in an extension of the χ models to non-central χ models [7] may also be a valuable system. One supplementary experimental problem is that it is very difficult to prove that the quadrupole splitting distribution belongs in fact to the latter family since IS distributions may easily perturb the determination of n, and these distributions are generally unknown [76] (see also subsection 7.2).

In summary, the previous analysis means that the only conclusion which is consistent with the 'degenerate Gaussian models' [29] but not necessarily with the 'generalized χ models' (discussion of next section) is the existence of medium-range order with strong orientational order among clusters surrounding the probe atoms. That order would be stronger for smaller values of n. Experimental validations of the 'degenerate Gaussian models' are lacking. We finally suggest using structural models to simulate DCEMS Mössbauer spectra and not only QS or EFG distributions.

4.2.2. Degenerate Gaussian models $\text{Cz}(n) : 2 \leqslant n \leqslant 4$. As discussed above, the two basic assumptions of the $\text{Cz}(n)$ models are [29]:

(a) The U_m ($m = 1, \ldots, 5$) are not independent. They are linear functions of n variables Y_i ($i = 1, \ldots, n$) which are Gaussian random variables centred at the origin. We stress again that such assumptions about the EFG distribution in the solid considered implies that

all EFG tensors must be calculated in a unique frame of reference for all sites.

(b) The QS distribution is given by equation (28) for the corresponding value of n.

We describe below general results obtained for Cz(n) models in which all Y_i are first assumed to have the same variance s^2. The more general case of different variances s_i^2 is also considered.

We define standard Gaussian random variables Z_i with zero mean and unit variance. The covariance matrix $\tilde{\Lambda}_Y$ with $\langle Y_i Y_j \rangle = s^2 \delta_{ij}$ is given by:

$$\tilde{\Lambda}_Y = s^2 \tilde{I}_n = s^2 \tilde{\Lambda}_Z. \tag{29}$$

$\tilde{I}_n$ is the unit $(n \times n)$ matrix, which is also the covariance matrix of the n-dimensional random vector $\boldsymbol{Z}$ with components Z_i. Assumption (a) for Cz(n) can be written compactly as:

$$\boldsymbol{U} = s\tilde{H}_n \boldsymbol{Z} \tag{30}$$

where the vector $\boldsymbol{U}$ is written as a (5×1) matrix, the vector $\boldsymbol{Z}$ as a $(n \times 1)$ matrix, and $\tilde{H}_n$ is a $(5 \times n)$ matrix whose properties must be determined. Designating the transpose of any matrix $\tilde{B}$ by $\tilde{B}^T$, we calculate:

$$\boldsymbol{U}^T \boldsymbol{U} = s^2 \boldsymbol{Z}^T (\tilde{H}_n^T \tilde{H}_n) \boldsymbol{Z} = s^2 \boldsymbol{Z}^T \tilde{A} \boldsymbol{Z}. \tag{31}$$

The matrix $\tilde{A} = \tilde{H}_n^T \tilde{H}_n$ is thus a symmetric $(n \times n)$ matrix. The distribution of Δ^2 (equal to $4\boldsymbol{U}^T\boldsymbol{U}$: see equation (6)) is a χ_n^2 distribution with n degrees of freedom if and only if $\tilde{A}$ is idempotent with rank n (see theorem 5.1.1 given in [77], p 196). This means that:

$$\tilde{A}^2 = \tilde{A} = \tilde{I}_n \tag{32}$$

as the only non-singular idempotent matrices are the unit matrices $\tilde{I}_n$. (In a strict sense, the distribution of Δ^2 is thus actually only proportional to such a χ_n^2 distribution but we will ignore such subtleties here.) It is indeed a simple matter using equations (32) and (31) to prove that Δ^2 and $\boldsymbol{Z}^T\boldsymbol{Z}$ have a χ_n^2 type distribution. The previous discussion also proves that $\tilde{H}_n$ is an orthogonal (5×5) matrix for $n = 5$ while it has orthonormal columns for $n < 5$. To obtain general expressions for the distributions $P_n(V_{zz}, \eta, \alpha, \beta, \gamma)$ (where $2 \leqslant n \leqslant 4$) which include the constraints of the problem, we consider the following:

$$\boldsymbol{U} = s\tilde{H}\boldsymbol{X} \tag{33}$$

where $\tilde{H}$ is an orthonormal (5×5) matrix. We set n elements of $\boldsymbol{X}$ (5×1) equal to the n elements of $\vec{Z}$, and the remaining $5 - n$ elements equal to zero. The covariance matrix of $\boldsymbol{U}$ is thus $\tilde{\Lambda} = s^2 \tilde{H} \tilde{\Lambda}_X \tilde{H}^T$ where $\tilde{\Lambda}_X$ is the covariance matrix of X, that is a diagonal matrix with n diagonal elements equal to unity and $5 - n$ equal to zero. The model given by equation (33) is thus quite general, and fulfils the conditions required by Cz(n).

From equation (33) we deduce:

$$\boldsymbol{X} = \frac{1}{s} \tilde{H}^T \boldsymbol{U}. \tag{34}$$

The distribution of $\boldsymbol{X}$ is:

$$P(X_1, \ldots, X_5) \propto \exp\left[-\frac{1}{2} \sum_{i=1}^{5} X_i^2 \right] \prod_{k=1}^{5-n} \delta(X_{j(k)}). \tag{35}$$

We denote by $j(k)$, $k = 1, \ldots, 5 - n$ the set of indices of those components of $\boldsymbol{X}$ which are equal to zero. Using equation (34), the distribution of the components of $\boldsymbol{U}$ can be derived:

$$P(U_1, \ldots, U_5) \propto \exp\left[-\frac{1}{2s^2} \sum_{i=1}^{5} U_i^2 \right] \prod_{k=1}^{5-n} \delta\left(\frac{1}{s} \sum_{l=1}^{5} H_{j(k)l}^T U_l \right). \tag{36}$$

A way of explaining the need for the $5-n$ linear constraints in equation (36) would be to express the n variables Z_i in equation (30) in terms of the n variables U_i: the remaining $5-n$ equations in (30) provide the linear constraints sought after. To derive the distribution $P_n(V_{zz}, \eta, \alpha, \beta, \gamma)$ we need to express the U_i in terms of the variables V_{zz}, η, α, β and γ using the relations given in appendix A. $(U_1, \ldots, U_5)$ represents the transformed vector derived from a vector expressed in the principal axis frame, and whose components are thus zero except for the first and the fifth (see equation (4)). Equation (36) can thus be written as:

$$P_n(V_{zz}, \eta, \alpha, \beta, \gamma) \propto V_{zz}^4 \exp\left[\frac{-V_{zz}^2(1+\eta^2/3)}{2\sigma^2}\right]\eta(1-\eta^2/9)\sin\beta \times \prod_{k=1}^{5-n}\delta\left(V_{zz}\sum_{l=1}^{5}[B_{j(k)l}(\alpha,\beta,\gamma)+\eta C_{j(k)l}(\alpha,\beta,\gamma)]\right) \tag{37}$$

where the Jacobian of the transformation from $(U_1, \ldots, U_5)$ to $(V_{zz}, \eta, \alpha, \beta, \gamma)$ is given by $2V_{zz}^4\eta(1-\eta^2/9)\sin\beta$ as has been shown by Czjzek *et al* [1] (see also section 3). The sum $\sum_{i=1}^{5} U_i^2$ has been calculated using equations (4) and (6). The Dirac delta functions are obtained by replacing the U_l in terms of the variables V_{zz}, η, α, β, and γ. The resulting expressions depend explicitly on the elements of the matrix $\tilde{H}$ and will thus differ from matrix to matrix. Some general features may nevertheless be extracted from equation (37). To obtain the distribution $f_e(V_{zz})$, one must integrate over the remaining variables $(\eta, \alpha, \beta, \gamma)$. In the integration process, the delta factors yield a factor of $|V_{zz}|^{n-5}$ (because $\delta(ax) = \delta(x)/|a|$). Thus the distribution $f_e(V_{zz})$ varies as $|V_{zz}|^{n-1}$ for small V_{zz}. The bivariate distribution $f(V_{zz}, \eta)$, and consequently $f_e(V_{zz})$, which depends on the matrix $\tilde{H}$, are thus not universal for a given n (except for the case $n = 5$). However this dependence is weak, and to a good approximation, we can replace the actual distribution by:

$$f'_e(V_{zz}) \propto |V_{zz}|^{n-1}\exp\left[\frac{-V_{zz}^2(1+\langle\eta^2\rangle/3)}{2\sigma^2}\right] \tag{38}$$

where for simplicity η^2 has been replaced by $\langle\eta^2\rangle$ ($\langle\eta\rangle^2$ might be used as well). As discussed in subsection 4.2.1, equation (38) is exact for $n = 1$ since $f_a(\eta) = \delta(\eta-\eta_0)$. The distribution given in equation (37) yields furthermore $\langle\Delta^2\rangle = 4ns^2$, with (equation (38)) $\sigma = 2s$. The following empirical distribution:

$$f(V_{zz}, \eta) \propto |V_{zz}|^{n-1}\eta(1-\eta^2/9)\exp\left[\frac{-V_{zz}^2(1+\eta^2/3)}{2\sigma^2}\right] \tag{39}$$

has been considered by Legein *et al* [62] and adapted to EPR studies of local order in glasses.

The distribution given in equation (39) coincides with the Cz(n) models for $n = 5$ only as it ignores the $5-n$ constraints on η and the angles. The associated distribution of η is $f_a(\eta) \propto \eta(1-\eta^2/9)/(1+\eta^2/3)^{n/2}$, and is approximately an $r(\eta)$ distribution (equation (15)) for $n \leqslant 4$, with an increased mean $\langle\eta\rangle_n \simeq 0.6098 + 0.0098(n-5)$, in contrast to the η distributions calculated numerically or derived for Cz(1) (subsection 4.2.1). These numerical calculations for various values of n, which also depend on the particular matrix $\tilde{H}_n$ considered, are shown in figures 4 to 6 for $n = 2$ to 4 respectively. The previous distribution (equation (39)) may however give results similar to those given by equation (37) for techniques which are not very sensitive to details of the η distribution but mainly to the average value $\langle\eta\rangle$. As described below, these average values are generally greater than

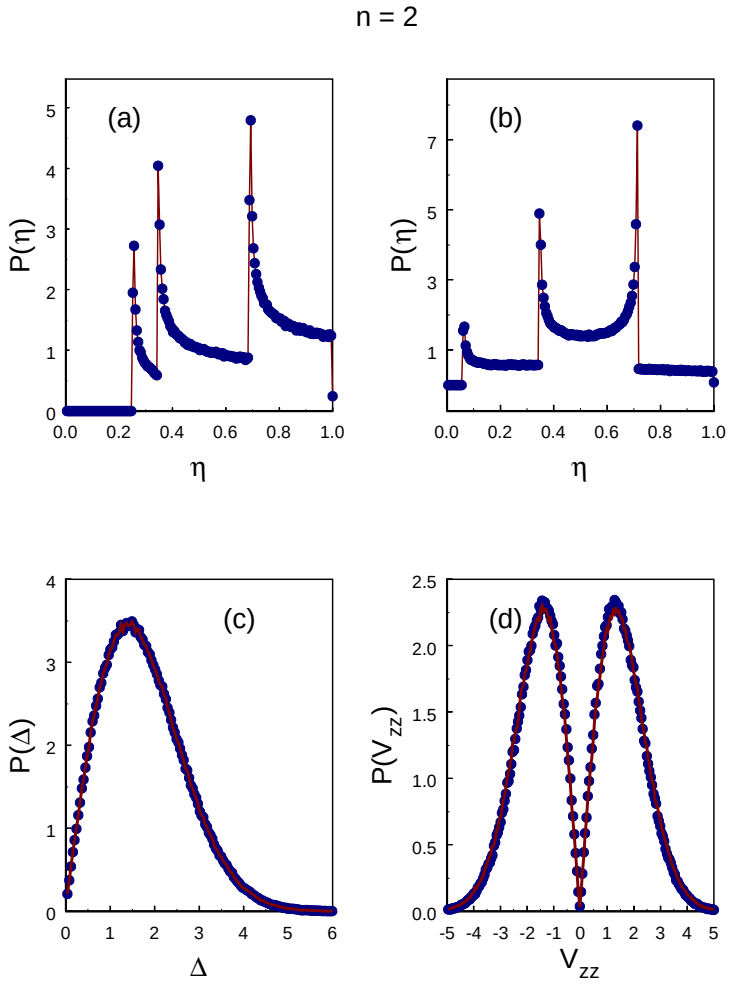

Figure 4. Simulation results for Cz(n) model for $n = 2$ for two choices of $\tilde{H}$. Shown are the simulated distributions for (a), (b) η, (c) Δ and (d) V_{zz}. In (a), 10^6 tensors for $\tilde{H}_1$: $\langle\eta\rangle = 0.6356$, $\langle\eta^2\rangle = 0.4505$; in (b), 10^6 tensors for $\tilde{H}_2$: $\langle\eta\rangle = 0.5119$, $\langle\eta^2\rangle = 0.3088$. In (c) and (d), the two choices for $\tilde{H}$ are shown as points (first) and lines (second).

0.5. The Gram–Schmidt method, described in appendix D, allows generation of random orthogonal matrices $\tilde{H}$ (5×5) which are representative of general matrices of that type. The latter matrices depend on 10 parameters. We have also considered orthogonal matrices $\tilde{O}(\alpha, \beta, \gamma)$ (see appendix A) which depend only on three parameters and thus form an ensemble of measure zero as compared to the previous general case. The latter simulations are however not necessarily useless since the physically relevant matrices (if there are any) are not known for the moment. We will therefore just describe some general features of the simulation results. Once a matrix $\tilde{H}$ is chosen, equation (33) and the Monte Carlo method can be used to generate a large ensemble of EFG tensors from which the distributions of interest may be derived numerically. As expected, the $p_n(\Delta)$ distributions are obtained in all cases. The results $f_a(\eta)$, $p_n(\Delta)$ and $f_e(V_{zz})$ for $n = 2$ to 4 are shown in figures 4 to 6.

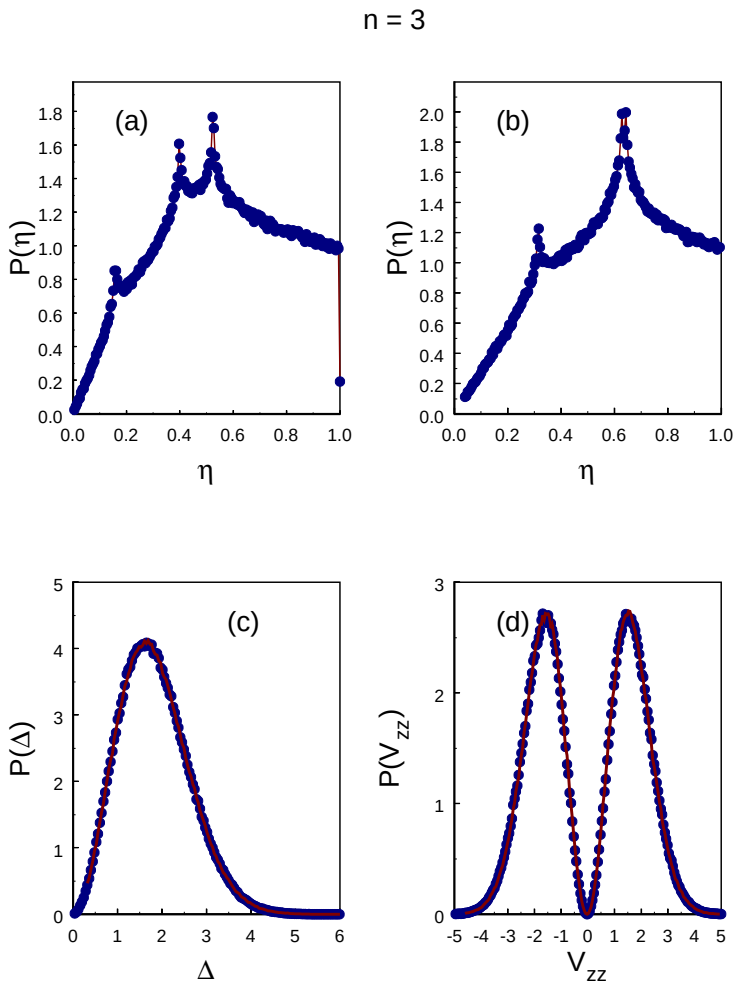

Figure 5. Simulation results for Cz(n) model for $n = 3$ for two choices of $\tilde{H}$. Shown are the simulated distributions for (a), (b) η, (b) Δ and (c) V_{zz}. In (a), 10^6 tensors for $\tilde{H}_1$: $\langle\eta\rangle = 0.5593$, $\langle\eta^2\rangle = 0.3726$; in (b), 10^6 tensors for $\tilde{H}_2$: $\langle\eta\rangle = 0.5980$, $\langle\eta^2\rangle = 0.4126$. In (c) and (d), the two choices for $\tilde{H}$ are shown as points (first) and lines (second).

The $f_e(V_{zz})$ distributions are almost independent of the choice of $\tilde{H}$ whatever n. They are very well approximated by equation (38), where we have used:

$$\langle\eta^2\rangle \to \langle\eta^2\rangle_{eff} = 3\left[\frac{\langle\Delta^2\rangle}{\langle V_{zz}^2\rangle} - 1\right].$$

The exact distributions $f_a(\eta)$ depend sensitively on the choice of $\tilde{H}$. For $n = 2$ and 3, they show clear discontinuities. Figures 4 and 5 show two different results in (a) and (b) respectively for different choices of $\tilde{H}$. The distributions for Δ and for V_{zz}, shown in the same figures as (c) and (d), cannot be distinguished for the same two choices of $\tilde{H}$ (given as points and lines for the same choices shown in (a) and (b) respectively). Whatever $\tilde{H}$, $f_a(\eta)$ for $n = 4$ differs little from $r(\eta)$, given in equation (15) and obtained for $n = 5$. The first

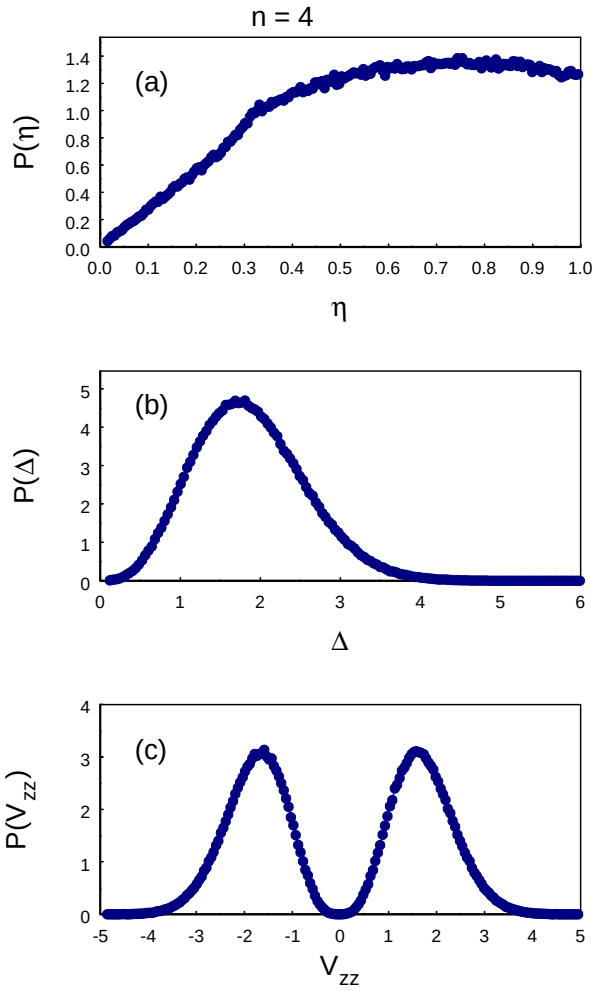

Figure 6. Simulation results for Cz(n) model for $n = 4$. Shown are the simulated distributions for (a) η, (b) Δ and (c) V_{zz}. $\langle\eta\rangle = 0.6054$, $\langle\eta^2\rangle = 0.4243$.

and second moments $\langle\eta\rangle$ and $\langle\eta^2\rangle$ are consequently very close to the corresponding values for $r(\eta)$. As a representative example, we have obtained $\langle\eta\rangle \doteq 0.6054$ and $\langle\eta^2\rangle \doteq 0.4243$ which are very close to the $n = 5$ values of 0.6098 and 0.4308 respectively. Equation (39) is thus a very good approximation of the bivariate distribution $f(V_{zz}, \eta)$, derived from equation (37) for $n = 4$.

Despite larger differences, the general shape of $f_a(\eta)$ for the case $n = 3$ still is similar to that of $r(\eta)$ for typical matrices $\tilde{H}$: we obtain typically the moments $\langle\eta\rangle \doteq 0.5593$ and $\langle\eta^2\rangle \doteq 0.3505$. The distribution $f_a(\eta)$ for $n = 2$ shows three discontinuities of density with infinite slopes for typical random matrices $\tilde{H}$. Other cases of distributions showing only one discontinuity close to the origin were however obtained for particular matrices $\tilde{H}$. To conclude, equation (28) is exact by construction for Cz(n) models; $f'_e(V_{zz})$, equation (38), may provide an excellent approximation of $f_e(V_{zz})$ whatever n. (In equation (38), $\langle\eta\rangle^2$

may be used if $\langle\eta^2\rangle$ is unknown; if both are unknown, $\langle\eta^2\rangle \doteq 0.4243$ found for $r(\eta)$ is still acceptable.) The detailed shapes of $f_a(\eta)$ are more sensitive to n and to the choice of $\tilde{H}$. The average η ranges however between $\approx$0.5 and $\approx$0.7 for typical matrices $\tilde{H}$ and $2 \leqslant n \leqslant 4$. The distribution $r(\eta)$ is a fair approximation for $f_a(\eta)$ for $n = 3, 4$. This reinforces the role played by such a distribution in disordered systems, as emphasized in section 3.

If the variances of the Y_i differ, it can be shown that the distribution given in equation (37) is still valid, but $\langle\Delta^2\rangle$ is now given by $4\sum_{i=1}^{n} s_i^2$ and thus that $\sigma = 2(1/n\sum_{i=1}^{n} s_i^2)^{1/2}$. In all cases, the distribution in equation (37) yields:

$$\text{prob}\{V_{zz} > 0\} = \text{prob}\{V_{zz} < 0\} = 0.5. \tag{40}$$

The explicit dependence on α, β and γ in equation (37) confirms the anisotropic character of the orientations of the principal axis frames which has been discussed above.

It is possible to extend the Cz(n) models as done in section 6 for the GIM to allow relaxation of the condition given in equation (40):

$$\text{Cz}'(n) = (1 - x)\tilde{V}_0 + x\text{Cz}(n) \tag{41}$$

where $\tilde{V}_0$ is a fixed EFG contribution. The covariance matrix for the latter is $x^2\tilde{\Lambda}$, still proportional to $\tilde{\Lambda}$. The resulting QS distributions have been discussed in [7, 9]. If in the future, the Cz(n) models receive experimental confirmation, extensions as given in equation (41) could also be worth being further investigated.

4.3. Coey model

A model given by Coey [30] predicts the same QS distribution as the Czjzek model, equation (28) with $n = 2$. Before discussing that particular model, we will first show that the observation of a given QS distribution $P_q(\Delta)$ does not allow conclusions on the validity of a particular set of assumptions about the EFG tensor used to derive $P_q(\Delta)$. The role of the number of degrees of freedom n will be discussed in the next section. A given QS distribution $P_q(\Delta)$ associated with a statistically anisotropic tensor distribution $P(\boldsymbol{U})$ (for instance the 'degenerate Gaussian models' [29]) can be obtained from an infinite number of distributions of EFG tensors derived from $P(\boldsymbol{U})$ by the following method. Let us consider a particular EFG tensor U (where $U_0 \leqslant U \leqslant U_0 + \mathrm{d}U$). If the frame of reference is rotated (Euler angles α, β, γ), the elements U_k' of the 'new' tensor are related to the elements U_k of the 'old' one by linear relations, the coefficients of which depend on (α, β, γ) and form an orthogonal (5×5) matrix $\mathcal{O}(\alpha, \beta, \gamma)$ (appendix A). We now select arbitrarily a probability distribution $R(\alpha, \beta, \gamma)$ which gives the weight of the random rotations performed on $\boldsymbol{U}$. A set of 'new' tensors $\boldsymbol{U}'$ whose probability distribution depends on $R(\alpha, \beta, \gamma)$ is thus associated with $\boldsymbol{U}$. The modulus of any $\boldsymbol{U}'$ (and thus QS) remains unchanged and equal to the modulus of $\boldsymbol{U}$ because $\mathcal{O}(\alpha, \beta, \gamma)$ is orthogonal. If this operation is performed identically, that is with the same $R(\alpha, \beta, \gamma)$, on all elements of the starting ensemble (in which $\text{prob}(U_0 \leqslant U \leqslant U_0 + \mathrm{d}U) = \text{prob}(U_0)\,\mathrm{d}U$), a new probability distribution of EFG tensors $P'(\boldsymbol{U})$ is derived which is a mixture of distributions. The QS distribution associated with $P'(\boldsymbol{U})$ is still $P_q(\Delta)$. Furthermore the joint distributions $f(V_{zz}, \eta)$ associated with $P'(\boldsymbol{U})$ or with $P(\boldsymbol{U})$ are identical. The arbitrariness of the tensor distribution reflects that of the choice of the probability distribution $R(\alpha, \beta, \gamma)$. It is therefore not surprising to observe that models derived from different assumptions on the EFG tensor may yield the same QS distribution.

Coey [30] has considered the plane defined by $V_{xx} + V_{yy} + V_{zz} = 0$ containing the eigenvalues V_{xx}, V_{yy} and V_{zz} of the EFG tensor introduced previously and has assumed

that the probability density in that plane only depends on the distance r from the origin, and is normally distributed (see also section 2). This leads to a QS distribution $P_2(\Delta)$ (equation (28), $n = 2$). As no assumption has been explicitly made about the distribution of the elements of the EFG tensor, this model may or may not be consistent with rotational invariance. The EFG tensor distribution will in any case differ from the one of Czjzek's extension for $n = 2$ if statistical isotropy is assumed (section 4.2). As discussed above, the rotationally invariant EFG tensor distribution can be derived from the Czjzek tensor distribution ($n = 2$) from some distributions of rotations (α, β, γ). The main, as yet unresolved problem raised by the latter model is to determine what kind of structure can give rise to $\boldsymbol{U}$ distributions which are not normally distributed, but which are consistent with the rotational invariance, and with $n = 2$ in equation (28).

4.4. Structural and statistical degrees of freedom

Two different types of degree of freedom have been dealt with and often confused in the literature:

(1) First there are the 'structural' degrees of freedom which are associated with the independent random variables which must be considered to define the arrangement of atoms around the probe atoms apart from an 'irrelevant' rigid body rotation defined by the three Euler angles (α, β, γ) [1, 29]. An example is given by Czjzek for amorphous FeF_3 [29] as the number of random distortions of the $(F^-)_6$ octahedra around Fe^{3+} ions.

(2) The term degrees of freedom, which was introduced in statistics by Fisher by analogy with dynamical systems, has different senses [79]. For the problem of the EFG in disordered systems, the latter degrees of freedom, in number n, were first considered in connection with QS distributions of the χ type [1, 29] as is usual in statistics [79]. In this case, n is the number of independent Gaussian variables to which the components of the random vector $\boldsymbol{U}$ are linearly related. This is the rank of the covariance matrix $\tilde{\Lambda}$ which is at most equal to 5. It is the basic importance of linear transformations which makes the definition of n efficient and practical for normal variables. As in statistics [79], we may extend the definition of n to be here the number of independent random variables on which the experimentally available QS distribution is based. That definition is not obviously useful and convenient in the case where the random vector $\boldsymbol{U}$ has a general probability distribution as the determination of n is far from being straightforward when the distribution of $\boldsymbol{U}$ is not multivariate normal. For rotationally invariant systems, the rank of the covariance matrix is always 5 (equation (12)). The five U_k are indeed Gaussian random variables only if they are independent as proved in appendix B (see also [47, 51] as well as [52], p 52). Consequently there is no *a priori* general transformation of non-Gaussian U_k which would allow us to express them in terms of n independent variables W_k which could be used to obtain a possible fit of the QS distribution, thus yielding n.

The next section describes the probability distribution of the EFG created at the centre of a sphere by a random repartition of m point charges on the surface of the sphere. In particular, this simplest example of a 'shell model' sheds light on the problem of the degrees of freedom and tries to answer the question of whether there is a one-to-one correspondence between the numbers of statistical and of structural degrees of freedom.

5. EFG tensor distribution for a random distribution of m point charges on the surface of a sphere

Assume that we have defined some method to place m identical point charges at points given from a random distribution on the surface of a sphere. We now want to derive the EFG tensor distribution and the QS distribution at the sphere centre. This problem, which can be solved by computer simulations, has the advantage of allowing us to check that the various conditions and conclusions discussed in sections 3 and 4 are indeed verified. The EFG distributions resulting from such repartitions of points have been calculated by Czjzek *et al* [1] for $m = 2, 3$. Czjzek [29] has moreover used the case $m = 3$ as illustrating the validity of his extended models (section 4.2) for $n = 3$ (equation (28)) since in this case, $f(V_{zz}, \eta)$ is proportional to V_{zz}^2 for small V_{zz} (figure 7(b) shows a similar behaviour for $P(\Delta)$). We will not reproduce these calculations here (see appendix of [1]). We do want to look at the distributions $P(U_i)$ of the components of the random five-dimensional vector $\boldsymbol{U}$ (equation (5)) and to discuss the number of degrees of freedom. We want to show that the observation of a quadratic V_{zz} variation at the origin for $m = 3$ charges *does not imply* that it corresponds to the extended model Cz(3) with $n = 3$ degrees of freedom (section 4.2). For m charges (described by the polar angles θ_i, ϕ_i, $i = 1, \ldots, m$) the components of the EFG tensor can be calculated from the expressions in equation (5) with $r_n = 1$ and $q_n = 1$ [1]. The U_i (equation (5)) have ranges of:

$$\begin{aligned} -\frac{m}{2} &\leqslant U_1 \leqslant m \\ -\frac{m\sqrt{3}}{2} &\leqslant U_i \leqslant \frac{m\sqrt{3}}{2} \qquad i = 2, \ldots, 5. \end{aligned} \tag{42}$$

The joint probability for θ_i to be found in the range of Θ_i and $\Theta_i + \mathrm{d}\Theta_i$ and ϕ_i to be found in the range of Φ_i and $\Phi_i + \mathrm{d}\Phi_i$ is given by:

$$\mathrm{prob}(\Theta_i \leqslant \theta_i \leqslant \Theta_i + \mathrm{d}\Theta_i, \Phi_i \leqslant \phi_i \leqslant \Phi_i + \mathrm{d}\Phi_i) = \frac{1}{4\pi} \sin(\Theta_i)\, \mathrm{d}\Theta_i\, \mathrm{d}\Phi_i.$$

By introducing the function of Θ_i:

$$Z_i = \tfrac{1}{2}(3\cos^2(\Theta_i) - 1)$$

the function U_1 may be rewritten as:

$$U_1 = \sum_{i=1}^{m} Z_i \tag{43}$$

where each $-1/2 \leqslant Z_i \leqslant 1$. The variable Z_i is distributed according to:

$$P(Z_i) = \frac{1}{\sqrt{3(1 + 2Z_i)}}.$$

From this it can be shown that the following average values hold:

$$\begin{aligned} \langle Z_i \rangle &= 0 \\ \langle Z_i^2 \rangle &= \tfrac{1}{5}. \end{aligned}$$

As the Z_i are independent, we have:

$$\begin{aligned} \langle U_1 \rangle &= 0 \\ \langle U_1^2 \rangle &= \frac{m}{5}. \end{aligned} \tag{44}$$

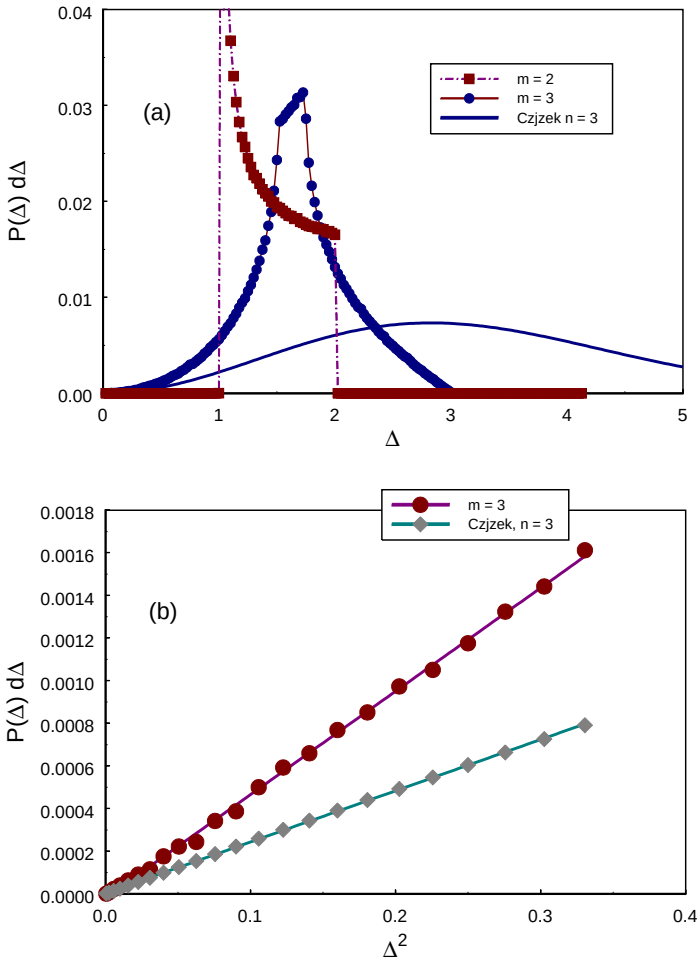

Figure 7. (a) $P(\Delta)\,\mathrm{d}\Delta$ calculated for $m = 2, 3$ number of point charges, as well as the Czjzek distribution for $n = 3$. (b) $P(\Delta)\,\mathrm{d}\Delta$ versus Δ^2 to show that both this for $m = 3$ and the GIM with $n = 3$ varies indeed as Δ^2 for small Δ although they are not equivalent.

The problem is rotationally invariant. Consider an infinite ensemble of groups of m point charges on the sphere: the distribution of the EFG tensor will not change if we rotate the frame of reference. From equations (10) and (44), we obtain $\langle\Delta^2\rangle = 4m$. Furthermore it is straightforward to show that:

$$\langle U_1^3\rangle = \frac{2m}{35} \tag{45}$$

$$\langle U_i^3\rangle = 0 \qquad i = 2, \ldots, 5 \tag{46}$$

$$\langle U_i^4\rangle = \frac{3m(7m-2)}{175} \qquad i = 1, \ldots, 5 \tag{47}$$

$$\langle U_1^6\rangle = \frac{53m}{1001} + \frac{15m(m-1)}{49} + \frac{3m(m-1)(m-2)}{25}. \tag{48}$$

More generally the coefficient of m^d (d is an integer) in U_1^{2d} comes from terms of the type:

$$\langle Z_{k_1}^2 Z_{k_2}^2 \cdots Z_{k_d}^2 \rangle$$

with $k_1 \neq k_2 \neq \cdots \neq k_d$. This yields for the average even powers:

$$\langle U_1^{2d} \rangle = m^d \frac{(2d)!}{10^d d!} + m^{d-1} \ldots . \tag{49}$$

Similarly for the odd powers, $\langle U_1^{2d+1} \rangle$ is also a polynomial in m^d because the largest power of m comes from averages like:

$$\langle Z_{k_1}^2 Z_{k_2}^2 \cdots Z_{k_{d-1}}^2 Z_{k_d}^3 \rangle$$

(note the difference from the case of the even powers) with $k_1 \neq k_2 \neq \cdots \neq k_d$. This is because the independence of the Z_k and the zero averages $\langle Z_k \rangle = 0$ prevent one from selecting factors $Z_{k_p}^s$ with $s < 2$ in the latter averages. The ratios $\langle U_1^{2d+1} \rangle / \langle U_1^2 \rangle^{d+1/2}$ go to zero when $m \to \infty$ since they vary as $1/\sqrt{m}$. It can be shown from equation (49) that:

$$\lim_{m \to \infty} \frac{\langle U_1^{2d} \rangle}{\langle U_1^2 \rangle^d} = \frac{(2d)!}{d! 2^d}.$$

The ratios on the right-hand side are the moments of the normal distribution $N(0, 1)$ centred on zero and of unit standard deviation. That proves that the distribution of U_1 tends to a normal distribution when $m \to \infty$, a result which may also be derived from the central limit theorem [50, 63] applied to equation (43). Similarly the central limit theorem applied to the random vector $\boldsymbol{U}$, the sum of m independent and identically distributed random vectors, would establish that the distribution of $\boldsymbol{U}$ tends to a multivariate Gaussian distribution when $m \to \infty$. This implies the validity of the GIM model for this rotationally invariant distribution. The third moments given by relations (45) and (46) are the first which emphasize the *asymmetric* character of the distribution of U_1 in contrast to the distributions of U_k for $k \neq 1$ as stressed in section 3.

Although the distributions of the U_k are not Gaussian in a strict sense when m is finite (equations (42), (43), (45)–(48)), they are well approximated by Gaussian distributions for large m. As a consequence of statistical isotropy, the U_k are uncorrelated but not mutually independent even if deviations from independence become smaller and smaller as m increases. It is only in the limit $m \to \infty$ that the U_k become truly mutually independent. Numerical simulations confirm indeed that in all cases, the covariance matrix is as expected (equation (12)):

$$\tilde{\Lambda} = \frac{m}{5} \mathcal{I}_5. \tag{50}$$

To discuss the problem of the degrees of freedom and the QS distributions, let us consider first the case of one charge: $m = 1$. There are two parameters, for example the polar angles (θ, ϕ). Therefore the EFG tensor cannot have more than two degrees of freedom. Since it is impossible with only two parameters to determine the orientation of the EFG principal axes (three parameters such as the Euler angles (α, β, γ) are needed), we can at most determine one axis. This is sufficient only in the case $\eta = 0$. As the system is rotationally invariant and as two parameters are needed to define the principal z axis, the value of V_{zz} (in the principal axis system) must be fixed. A direct calculation with one single charge in equation (5) immediately shows that the conditions required by rotational invariance are satisfied.

For the case of two charges, $m = 2$, four independent random variables are available, that is $4 - 3 = 1$ structural degree of freedom [1, 29]. Three parameters are needed for the

EFG principal axis system, and thus V_{zz} and η must both depend on only one parameter, as in fact was shown by Czjzek *et al* [1]. For $m = 2$, the distribution of U_1 is calculated to be:

$$P(U_1) = \begin{cases} 0 & U_1 < -1, \text{ or } U_1 > 2 \\ \dfrac{\pi}{6} & -1 \leqslant U_1 \leqslant 1/2 \\ \dfrac{1}{3}\sin^{-1}\left(\dfrac{2-U_1}{1+U_1}\right) & 1/2 \leqslant U_1 \leqslant 2 \end{cases} \tag{51}$$

in perfect agreement with figure 8. For $-1 \leqslant U_1 \leqslant 1/2$, an average value of $P(U_1) \cong 0.5235(2)$ is found from a computer simulation with 8×10^6 sets of two charges, while the exact value is $\pi/6 \cong 0.523\,598\ldots$. Figure 8 shows the distributions $P(U_i)$ for $m = 1$ to 4. As expected, $P(U_1)$ is dissymmetric but less and less so as m increases, while the $P(U_i)$ for $i > 1$ are identical, symmetric and already very well approximated by a normal distribution (figure 8) $P_G(U_i) = \exp(-U_i^2/(0.4m))/\sqrt{(}0.4m\pi)$ (using $\langle U_i^2\rangle = m/5$ from equations (10) and (44)).

For $m = 3$, $P(U_1)$ is strongly dissymmetric with an infinite slope at $U_1 = -1.5$ and a discontinuous and non-zero slope at $U_1 = 0$. The five $P(U_i)$ disagree with the assumption that the U_i would be linearly related to only three Gaussian random variables as would be required by the degenerate Gaussian model Cz(3). The latter assumption is further not valid if it is restricted to the vicinity of $\boldsymbol{U} = \mathbf{0}$ [29] as a linear combination of Gaussian random variables cannot account for the slope discontinuity of U_1. The behaviour of U_1 is the fundamental reason why $f(V_{zz}, \eta)$ varies as V_{zz}^2 for small values of V_{zz} [29]. The associated QS distribution strongly differs from $P_3(\Delta)$, given by equation (28) for $n = 3$, as is shown by a direct comparison of the simulated QS distribution (using $\langle\Delta^2\rangle = 4m = 12$) with $P_3(\Delta)$ for the same value of $\langle\Delta^2\rangle = n\sigma^2 = 3\sigma^2$, where $\sigma^2 = 4m/n = 4$ (figure 7). The definition and the direct determination of a number n of degrees of freedom from the QS distribution remain unsolved problems for $m = 3$.

We observe that there is a very fast convergence of $P(U_i)$ for $i = 2, \ldots, 5$ to the normal distribution with increasing m, but a much slower one for $P(U_1)$. In any case, U_1 will also become normally distributed in the limit $m \to \infty$ as discussed previously. In fact, all five $P(U_i)$ are already very well approximated by normal distributions for $m = 4$ charges.

The 'structural' degrees of freedom (section 4.4), in number n_s, are associated with the physically relevant independent random variables [1, 29] which must be considered to define the arrangement of atoms. In the degenerate Gaussian model, Czjzek [29] considered $n_s \leqslant 4$. However n_s is already 5 for $m = 4$. In any case, the question is: is it possible to derive n_s solely from the QS distribution? Equivalently, can we determine m from $P(\Delta)$? To simulate the situation which experimentalists are faced with in Mössbauer spectroscopy, we must define a way to determine the numbers n and m given only the QS distribution and ignoring in general the various contributions to the observed EFG. As it is not possible *a priori* to guess a functional form and even to define n for the latter distribution, we have to try to fit such distributions with model distributions such as $P_n(\Delta)$ (equation (28)), as done almost systematically in the literature. No fit of reasonable quality can be obtained with $P_n(\Delta)$ for $m \leqslant 3$ while n would be considered to be five whenever $m \geqslant 5$. For $m = 4$, the distribution deviates but not drastically from $P_5(\Delta)$. There is no simple way to define and thus to determine n and consequently m and n_s from general QS distributions and furthermore no one-to-one correspondence between n and m when a meaning can be given to n. To conclude, the consequences of statistical invariance by rotation are easily verified by computer simulations which further show that statistical degrees of freedom of

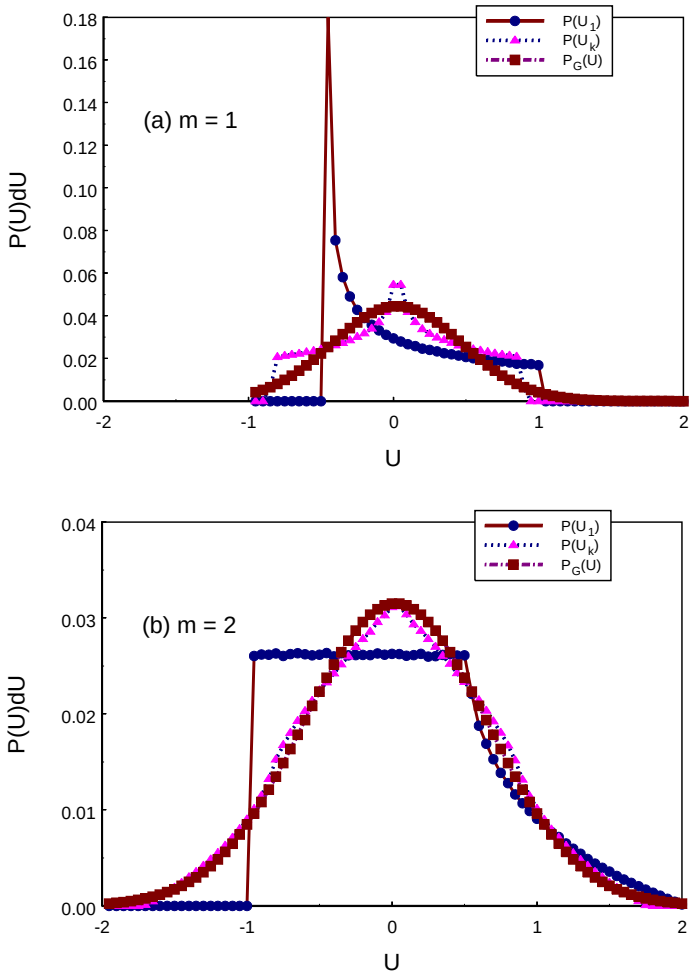

Figure 8. $P(U_i)\,\mathrm{d}U_i$ calculated for (a) $m = 1$, (b) $m = 2$, (c) $m = 3$, (d) $m = 4$ number of point charges, and different i as noted ($\mathrm{d}U_i = 0.05$) as compared to a Gaussian $P_G(U)$ (squares).

the QS distribution, when they can be defined, must not be confused with the number of degrees of freedom associated with the structure.

6. A simple extension of the GIM model

In 1985, we introduced [9] a different class of models which seems worth being further investigated. The following tensor, written here in a slightly different way than in [9], was considered:

$$\tilde{V}(x) = (1-x)\tilde{V}_0 + x\tilde{V}_{GI} \qquad 0 \leqslant x \leqslant 1. \tag{52}$$

The $\tilde{V}_0$ mimics the EFG contribution of a well defined neighbourhood of a given atomic species and is characterized by the parameters $V_{zz}(0)$ and $\eta(0)$. In the following, we will set $\eta(0) = 0$ so that the corresponding QS is $\Delta(0) = |V_{zz}|$. The $\tilde{V}_{GI}$ (called Gaussian

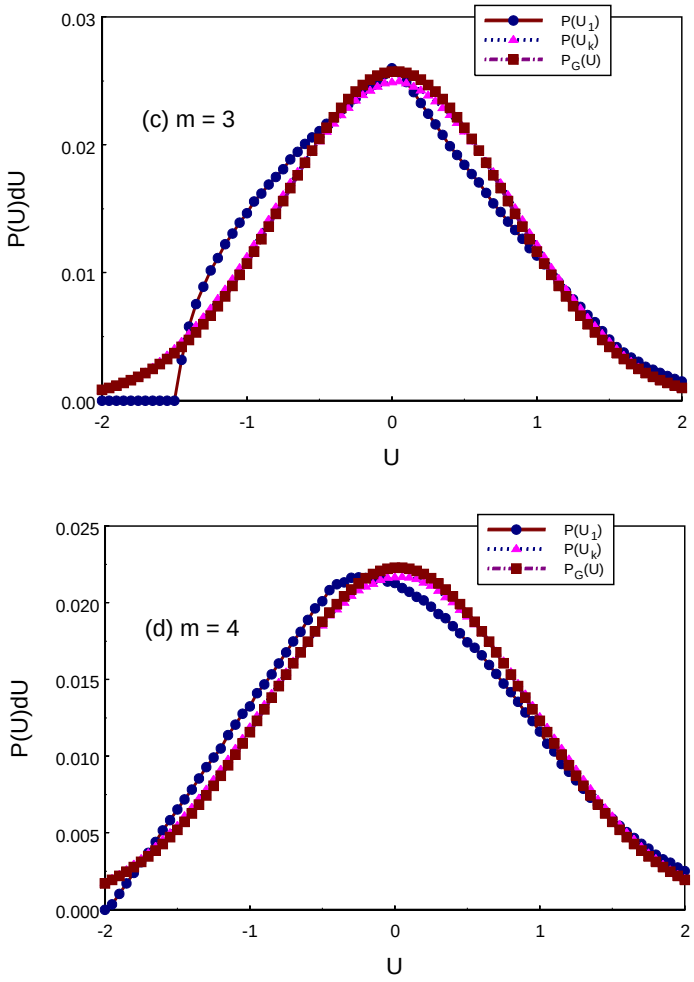

Figure 8. (Continued)

isotropic; see section 4) is related to disorder of more remote atomic shells and to random contributions to the total EFG. The QS $\Delta(0)$ for $x = 0$ is deduced from (see equation 6):

$$\Delta^2(0) = 4\sum_k U_k^2(0)$$

where the $U_k(0)$ are taken here as the components of the vector $\boldsymbol{U}(0)$ associated with the diagonal tensor $\tilde{V}_0$. The parameter x allows one to change the influence of the latter part. It is necessary to rotate $\tilde{V}_0$ in all directions using correct weights in order to obtain a rotationally invariant tensor $\tilde{V}(x)$. If $\eta(0) = 0$, the distribution of the EFG tensor $\tilde{V}_0^{(R)}$ obtained from $\tilde{V}_0$ by uniform random rotations is the same as the distribution of the EFG tensor of section 5 for a single charge but with a charge $U_1(0)$ instead of 1. ($m = 1$; see figure 8 for the shapes of the marginal distributions of the $U_k^{(R)}(0)$.) The latter result can be easily derived from equation (A1) in appendix A with all $U_k(0)$ equal to zero except $U_1 = U(0)$: the new $U_k^{(R)}(0)$ are indeed given by equation (4) with β and γ replacing θ and ϕ and with $q = U_1(0)$. The fact that $m = 1$ ensures that the QS distribution associated

with $\tilde{V}_0^{(R)}$ is given by $\delta(\Delta - \Delta(0))$ as expected from the relation:

$$4\sum_k (U_k^{(R)}(0))^2 = \Delta^2(0)$$

which is valid whatever the rotation $R(\alpha, \beta, \gamma)$. However, as solely the QS distribution associated with equation (52) was derived [58], the final result does not depend on whether $\tilde{V}_0$ is rotated or not (section 4.3). The speed at which the $\tilde{V}_{GI}$ contribution dominates the $\tilde{V}_0$ one was also investigated by varying x. An identical model was later numerically investigated [81]. This model is intended to describe an amorphous solid possessing a strong short-range order. This is the case in some amorphous solids, for instance in those which are formed in a reversible manner from single crystals under the influence of pressure [82]. An example is for instance berlinite-type $FePO_4$ [83]. Anisotropic effects may further be introduced if $\tilde{V}_0$ is now considered as a tensor which is not rotated uniformly in all directions (section 4.2). The latter case may model for instance single crystals in which disorder is due to alloying elements or to defects, etc.

To calculate the QS distribution or the bivariate distribution $f(V_{zz}, \eta)$ from computer simulations and numerical calculations as discussed below, the most convenient frame of reference to express the initial ensemble of EFG tensors is the principal axis system of the tensor $\tilde{V}(0)$. As shown by equation (52), the U_k are still normal and independent with means given by:

$$\begin{aligned} &\langle U_1(x)\rangle = (1-x)U_1(0) \\ &\langle U_k(x)\rangle = 0 \qquad k = 2, 3, 4 \\ &\langle U_5(x)\rangle = (1-x)U_5(0). \end{aligned} \tag{53}$$

The variances of the U_k are solely due to the random part of $\tilde{V}(x)$, that is:

$$\langle (U_k - \langle U_k\rangle)^2\rangle = \tfrac{1}{20}x^2\langle \Delta_g^2\rangle = \tfrac{1}{4}x^2\sigma^2 \qquad k = 1, \ldots, 5 \tag{54}$$

where σ is the sole parameter which enters the χ distribution equation (28), and $\langle \Delta_g^2\rangle = 5\sigma^2$ is the second moment of the latter distribution for $x = 1$. We notice that the covariance matrix of $\boldsymbol{U}$ is still the one required for statistical invariance $\tilde{\Lambda} = (1/20)x^2\langle \Delta_g^2\rangle \tilde{I}_5$ (equation (12)) but the latter invariance is not fulfilled as $\langle U_i\rangle \neq 0$ ($i = 1, \ldots, 5$). Nevertheless, the 'relevant' physics is contained here in the ensemble of configurations described by $\tilde{V}(x)$ (equation (52)) in the frame of reference of the fixed part of $\tilde{V}_0$. It is the rotational invariance and the 'averaged' nature, due to the central limit theorem, of configurations of atoms leading to the $\tilde{V}_{GI}$ term which justify the latter conclusions. The distribution $f(V_{zz}, \eta)$ derived here for an anisotropic solid holds also for a truly isotropic solid in the sense discussed in subsection 4.2.1 on the degenerate Gaussian models. There, atomic configurations are redistributed so as to produce only short-range structural correlations at a scale $\ll L$ and GIM configurations for more remote shells. This solid would differ from an isotropic solid obtained from an anisotropic one containing structural correlations at a scale of L by averaging over all correctly weighted rotations. Correlations at a scale $\ll L$ must indeed be considered for solids showing a significant contribution of the $\tilde{V}_{GI}$ term in equation (52). Only the anisotropic system is considered below to derive $f(V_{zz}, \eta)$. Although the distribution of $\boldsymbol{U}$ is multivariate normal (appendix C), such a useful characteristic of $P(\boldsymbol{U})$ would not be preserved for an isotropic solid as a consequence of the results shown in appendix B. From the multivariate normal distribution of $\boldsymbol{U}$, we therefore

obtain (equations (3) and (5)):

$$T^2 = \frac{\Delta^2}{x^2\sigma^2} = \frac{1}{x^2\sigma^2}\sum_{k=1}^{5} W_k^2$$
$$W_k = 2U_k \qquad k = 1, \ldots, 5. \tag{55}$$

T^2 is distributed according to a non-central χ^2 distribution [68] with five degrees of freedom, that is:

$$q_5(\Delta) = \sqrt{\frac{2}{\pi}}\left[\frac{x\sigma\Delta}{\omega^3}\right]\exp\left(-\frac{\omega^2+\Delta^2}{2(x\sigma)^2}\right)\left[\frac{\omega\Delta}{(x\sigma)^2}\cosh\left(\frac{\omega\Delta}{(x\sigma)^2}\right) - \sinh\left(\frac{\omega\Delta}{(x\sigma)^2}\right)\right]. \tag{56}$$

$\omega = (1-x)\Delta(0)$ is the noncentrality parameter whose square has been obtained from the sum of the squares of the means of the W_k. It is easy to check that equation (28) with $n = 5$ is recovered when $x \to 1$ since:

$$\lim_{y\to 0}(y\cosh(y) - \sinh(y)) \approx \tfrac{1}{3}y^3.$$

The average QS is calculated from:

$$\langle\Delta\rangle = (\sqrt{2/\pi})x\sigma(1+Z^{-2})\exp(-Z^2/2) + (\omega + 2x\sigma/Z - 4\omega/Z^4)\,\mathrm{erf}(Z/\sqrt{2})$$
$$Z = \omega/(x\sigma). \tag{57}$$

The error function:

$$\mathrm{erf}(x) \equiv \frac{2}{\sqrt{\pi}}\int_0^x \exp(-t^2)\,\mathrm{d}t$$

can be calculated with high precision from [84]:

$$\mathrm{erf}(x) \cong \begin{cases} \dfrac{2}{\pi}\displaystyle\sum_{j=0}^{12}\frac{2}{2j+1}\exp\left(-\frac{(2j+1)^2}{36}\right)\sin\left(\frac{x(2j+1)}{3}\right) & |x| \leqslant 4.7 \\ \mathrm{sign}(x) & |x| > 4.7. \end{cases} \tag{58}$$

In the limit $Z \to 0$, from equation (57), the average value of Δ becomes:

$$\langle\Delta\rangle = \frac{8x\sigma}{3}\sqrt{\frac{2}{\pi}}\left(1 + \frac{Z^2}{10} + \frac{13Z^4}{2240}\right). \tag{59}$$

The variance of the QS distribution is calculated from the following:

$$\sigma_\Delta^2 \equiv \langle\Delta^2\rangle - \langle\Delta\rangle^2 = 5x^2\sigma^2 + (1-x)^2\Delta^2(0) - \langle\Delta\rangle^2. \tag{60}$$

An equation similar to equation (55) could be used to deduce QS distributions of the non-central χ type with $n < 5$ as proposed for instance in [7, 8]. Such distributions raise however problems related to anisotropic effects or to their structural significance analogous to those raised by the 'degenerate Gaussian models' and the Coey model. It is also possible to express the bivariate distribution $f(V_{zz}, \eta)$ (see appendix C). With the simplifying assumption that $\eta(0) = 0$ and after dropping a constant factor, the bivariate distribution becomes:

$$f(V_{zz}, \eta) \propto \frac{V_{zz}^4\eta}{x^5\sigma^5}\left(1 - \frac{\eta^2}{9}\right)\exp\left(-\frac{\omega^2 + V_{zz}^2(1+\eta^2/3)}{2x^2\sigma^2}\right)$$
$$\times \int_0^1 I_0(z)\exp(\Omega(3t^2-1))\,\mathrm{d}t \tag{61}$$

where $I_0(z)$ is a modified Bessel function, $\omega = (1-x)|V_{zz}(0)|$ and z and Ω are given by:

$$z = \eta|\Omega|(1-t^2)$$
$$\Omega = \frac{(1-x)V_{zz}V_{zz}(0)}{2x^2\sigma^2}.$$

It is the exponential factor in the integral of equation (61) which is responsible for the asymmetry of the $f_e(V_{zz})$ distribution.

In order to present contour plots of the distribution given by equation (61), we choose a different polar representation (r, ϕ) than that used by Czjzek [55]. He used (in our notation: see equation (6)) $S^2 = (3/2)r^2 = (3/2)V_{zz}^2(1+\eta^2/3)$ and $D^3 = r^3\sin(3\phi)$. This projects the variation of V_{zz} and η into the range $\pm\pi/6$. (In addition, for both representations, η is only a function of ϕ, but V_{zz} is a function of both r and ϕ.) We choose the following transformation, where the full parameter space of (V_{zz}, η) is the upper half-plane (as here $eQ/2 = 1$):

$$r = \Delta = |V_{zz}|\sqrt{1+\eta^2/3}$$
$$\cos(\phi) = \frac{(1-\eta^2)\,\mathrm{sign}(V_{zz})}{(1+\eta^2/3)^{3/2}} \qquad 0 < \phi < \pi.$$

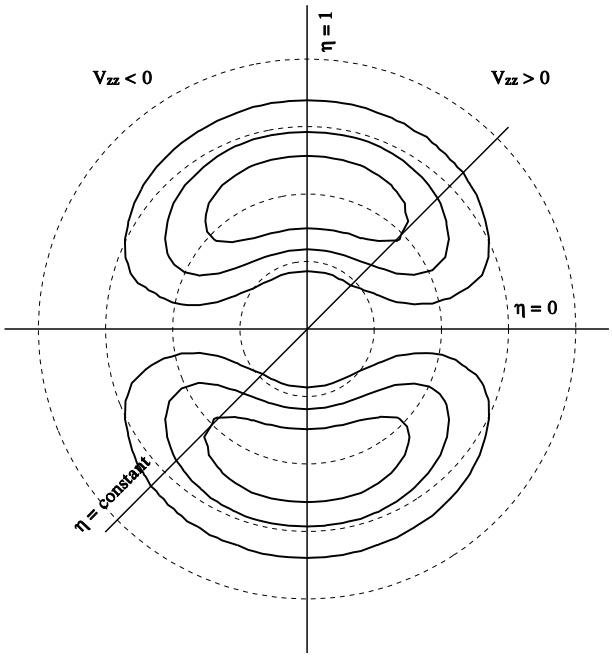

Figure 9. Contour plot of the Czjzek distribution function, equations (13) and (27), in the polar representation of section 6, table 2. The plot has been reflected into the lower half plane as well. $\eta = 0$ is the horizontal axis. The dashed lines are circles of constant Δ (in steps of 1). Radial lines are lines of constant η.

First we show in figure 9 the distribution given by Czjzek, and called here the Gaussian isotropic model, equation (13), using this different polar transformation of coordinates, and already presented in figure 2. An interesting property of this new plot is that $V_{zz} > 0$ is in the right, and $V_{zz} < 0$ in the left upper half-plane. The x-axis is the line of $\eta = 0$, while the

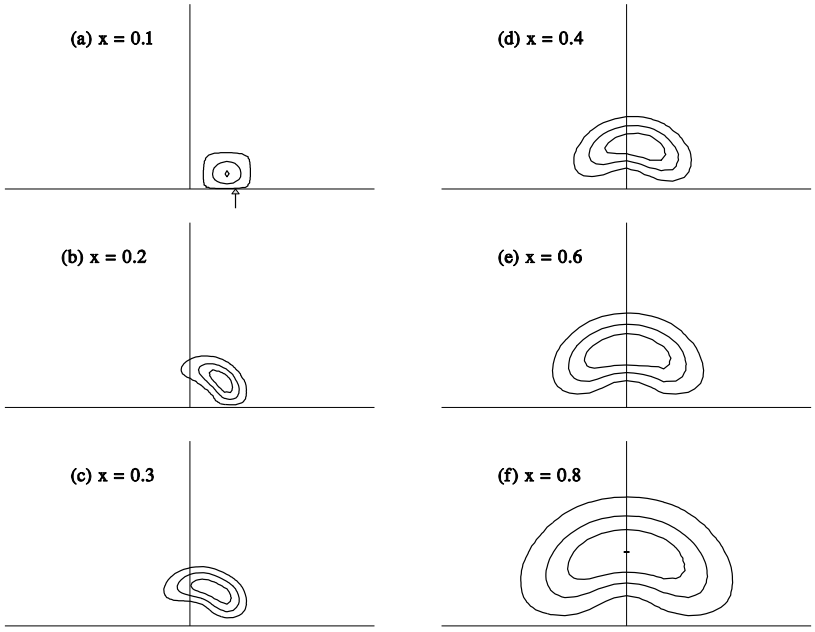

Figure 10. Contour plot of equation (61) in the polar representation of section 6, table 2. For these plots, $V_{zz}(0)/\sigma = 1$ and $\eta(0) = 0$ has been chosen, and V_{zz} normalized to σ. The mixing parameter x has been chosen from (a) 0.1 to (f) 0.8. $x = 0$ (not shown) corresponds to a delta function at $V_{zz}/\sigma = 1$, and $\eta = 0$ which is given by the arrow in (a).

Table 2. Transformation used for figures 9 and 10.

Variable	$0 < \phi \leqslant \pi/2$	$\pi/2 < \phi \leqslant \pi$
$V_{zz}(r, \phi)$	$r\cos(\phi/3)$	$-r\cos((\pi - \phi)/3)$
$\eta(r, \phi)$	$\sqrt{3}\tan(\phi/3)$	$\sqrt{3}\tan((\pi - \phi)/3)$

positive y-axis $\eta = 1$. Lines of constant η are radial, and lines of constant Δ are circles. These are shown as dashed lines on the figure, where V_{zz} has again been normalized to σ ($\sigma^2 = \langle\Delta^2\rangle/5$ since the number of degrees of freedom $n = 5$). The transformation from (r, ϕ) to (V_{zz}, η) is shown in table 2. A line at constant ϕ through the origin yields a cut at constant η for a given sign of V_{zz}. If the function in the upper half-plane is reflected into the lower half-plane, a line of constant ϕ determines the conditional distribution $f(V_{zz}|\eta)$.

We now show in figure 10 contour plots of the distribution given by function (60) for several values of the mixing parameter x for $V_{zz}(0) = 1$. In the case of $x = 0$, $f(V_{zz}, \eta)$ is a delta function. This broadens quickly for increasing x, mainly in the direction of increasing η. The negative V_{zz} half plane is reached by crossing the $\eta = 1$ axis.

The model given by equation (52) was also investigated by computer simulation as a function of x to study the influence of disorder on the distributions $f_a(\eta)$, $f_e(V_{zz})$ and of $q_5(\Delta)$. Random EFG tensors were generated with the help of a pseudo-random number generator and ensemble averages were performed to obtain the previous distributions. Numerical calculations of $f_e(V_{zz})$ and of $f_a(\eta)$ were also performed with the help of equation (61). Figures 11, 12 and 16 prove that the simulation results for $\langle\Delta\rangle$ as well

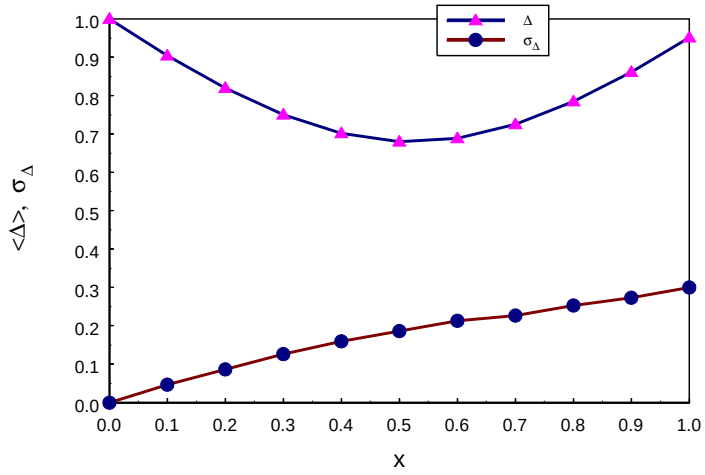

Figure 11. Average $\langle\Delta\rangle$ (full circles) and standard deviation σ_Δ (full triangles) as a function of x for $\Delta(0) = 1$, $\eta(0) = 0$ and $\sigma = 1/\sqrt{5}$ from equations (57) and (60).

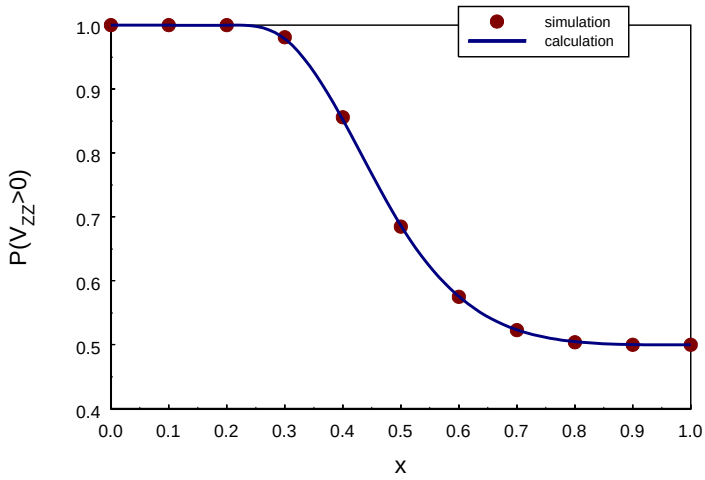

Figure 12. Percentage area of $V_{zz,+}$ as a function of x for $\Delta(0) = 1$, $\eta(0) = 0$ (solid line: theoretical values calculated from equation (61)).

as σ_Δ, p^+ and $f_a(\eta)$ are in excellent agreement with the theoretical values as calculated from equations (57) and (60). We have taken $\Delta(0) = 1$, $\sigma = 1/\sqrt{5}$ and $\eta(0) = 0$. From the relative area of the negative part of the $f_e(V_{zz})$ distribution, we conclude that three domains have to be distinguished (see figure 12).

- There is a 'crystalline' domain for $x \lesssim 0.3$ where the behaviour is dominated by the 'ordered' part $\tilde{V}_0$.
- There is a mixed domain for the range $\sim 0.3 < x \lesssim 0.7$, with intermediate characteristics and a fast decrease of $p_+ = \text{prob}(V_{zz} > 0)$.
- There is a 'random' domain for $x \gtrsim 0.7$ which is dominated by the GIM term with distributions almost identical with those of the GIM.

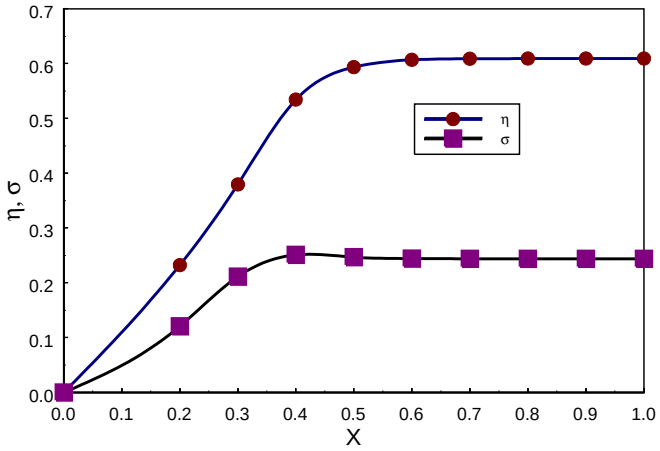

Figure 13. $\langle\eta\rangle$ and σ_η as a function of x for $\Delta(0) = 1$ and $\eta(0) = 0$.

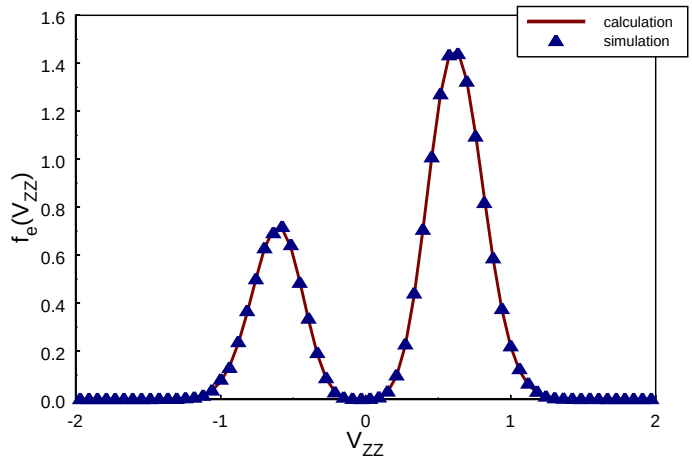

Figure 14. $f_e(V_{zz})$ as a function of V_{zz} for $\Delta(0) = 1$, $\eta(0) = 0$ and $x = 0.5$.

The 'crystalline' domain tends to shrink and the random domain tends to extend when $\eta(0)$ is larger than zero. Different conclusions are apparently drawn from the x-dependence of the average $\langle\eta\rangle$ and of σ_η (see figure 13). Both increase from 0 to values close to the GIM values (0.61 and 0.24 respectively; see section 3) when x increases from 0 to 0.5 and remain almost constant for larger values of x. Such results can be understood from the discussion of the 'universality' of the GIM distribution $r(\eta)$ given in section 3, equation (15). Figure 14 shows the asymmetric distribution $f_e(V_{zz})$ ($p_+ = 0.687$) for $\Delta(0) = 1$, $\sigma = 1/\sqrt{5}$, $\eta(0) = 0$ and $x = 0.5$. Figure 15 compares the positive parts of the distributions $f_e^+(V_{zz})$ (with $V_{zz} > 0$) with 'normalized' functions calculated for various values of x from the negative parts $f_e^-(V_{zz})$ (with $V_{zz} < 0$) according to:

$$g_e^-(V_{zz}) = \frac{p^+}{p^-} f_e^-(-V_{zz}) \qquad V_{zz} > 0 \tag{62}$$

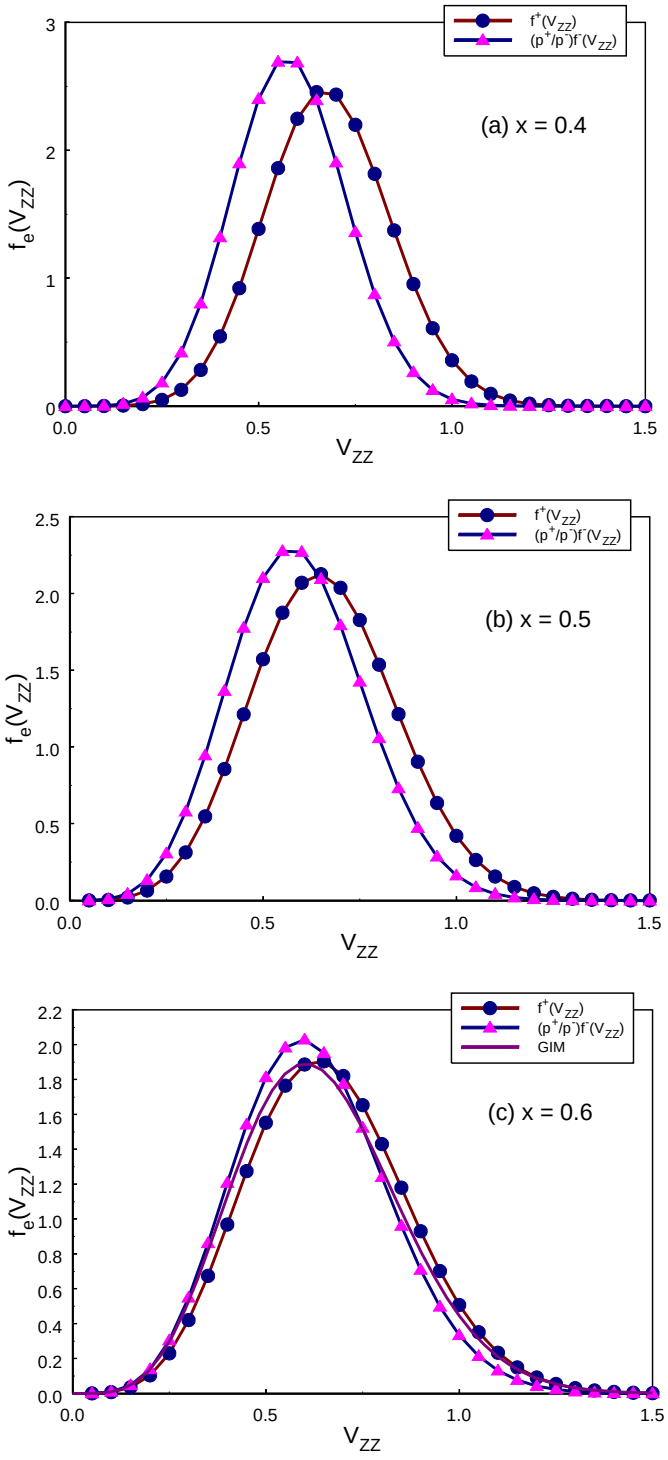

Figure 15. $f_e(V_{zz,+})$ and $(p_+/p_-)f_e(V_{zz-})$ as a function of $|V_{zz}|$ for $\Delta(0) = 1$, $\eta(0) = 0$ for: (a) $x = 0.4$; (b) $x = 0.5$; (c) $x = 0.6$. In (c), the curve for the GIM model, figure 1(c), is shown for comparison.

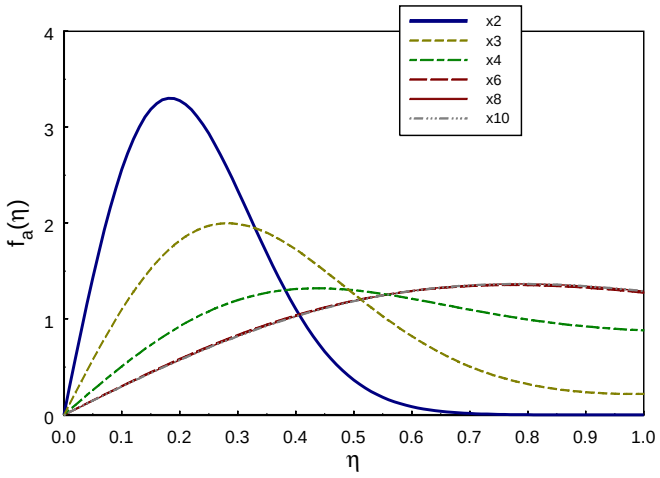

Figure 16. $f_a(\eta)$ as a function of η for $\Delta(0) = 1$, $\eta(0) = 0$ for x between 0.2 and 1.0.

with $p^- = 1 - p^+$. The marginal V_{zz} distributions $f_e^+(V_{zz})$ and $g_e^-(V_{zz})$ have very similar shapes for x larger than $\sim$0.5. For increasing x, the positive and negative V_{zz} parts converge, and for $x = 0.6$ (figure 15(c)) this is already very close to the marginal distribution $f_e(V_{zz})$, figure 1(c), which is shown in figure 15(c) as a solid line. In order to compare these two figures, an effective σ_{eff} has been used to scale V_{zz}/σ, where $\sigma_{eff}^2 = \langle\Delta^2\rangle/5$ and $\langle\Delta^2\rangle = 5x^2\sigma^2 + (1-x)^2\Delta^2(0)$ (see equation (60)). With $\sigma^2 = 1/5$ and $\Delta(0) = 1$, this yields $\sigma_{eff}^2 = (x^2+(1-x)^2)/5$. As expected from the discussion of section 3, the distribution of $f_a(\eta)$ deviates little from the GIM distribution $r(\eta)$ for $x \gtrsim 0.5$ (see equation (15) and figure 16). The conclusions drawn from the $f_a(\eta)$ distributions do not contradict therefore those drawn from $f_e(V_{zz})$ which are the relevant distributions which must be used to account properly for the overall behaviour of the model given in equation (52) as a function of x.

7. Applications to Mössbauer spectroscopy

7.1. Some remarks

(a) Turek [88] has recently used a superoperator formalism to calculate Mössbauer profiles in the presence of the Czjzek distribution for $n = 5$ [1] and a hyperfine magnetic field.

(b) With ^{57}Fe Mössbauer spectroscopy, it is in fact difficult to establish experimentally detailed properties of the investigated EFG distributions. Some distributions of asymmetry parameters have been reported, although ^{57}Fe Mössbauer spectra are insensitive to the distribution of η and mainly sensitive to its average value. We demonstrate this with a series of simulations. Figure 17(a) and (b) shows spectra simulated with the full Hamiltonian for (a) $V_{zz} = 0.4$ mm s^{-1} and for (b) $V_{zz} = 1$ mm s^{-1} in a field $B = 5$ T perpendicular to the γ-rays. Many spectra have been calculated for various different model distributions of η. We have in particular tried the following (cases (1), (2) and (3) are given in 17(c) as histograms):

(1) A δ-function at $\eta = 0.5$: $\sigma_\eta = 0$.

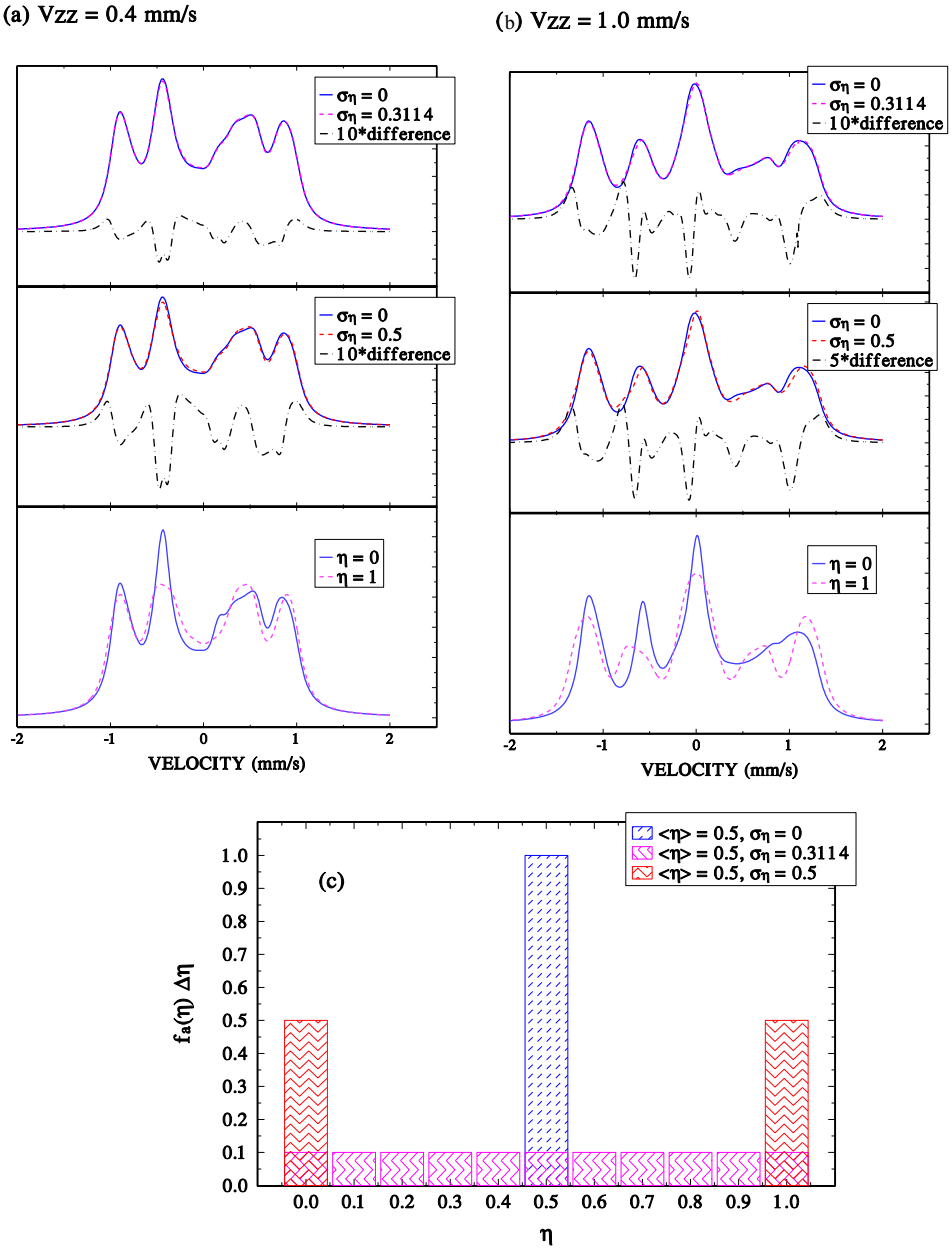

Figure 17. Simulated ^{57}Fe Mössbauer spectra with $B_{hf} = 5$ T, perpendicular to the γ-ray beam for two different values of V_{zz}: (a) 0.4 mm s^{-1}; (b) 1.0 mm s^{-1}. The η distributions used in the above are shown in (c) (see text, section 7.1).

(2) A uniform discrete distribution between 0 and 1 (calculated with $\eta = k/10$, $k = 0, \ldots, 10$): $\sigma_\eta = 0.3114$.

(3) The sum of a spectrum with $\eta = 0$ and one with $\eta = 1$: $\sigma_\eta = 0.5$.

(4) Not shown here are: a uniform distribution between $0.5 - \eta_0$ and $0.5 + \eta_0$ with

$0 < \eta_0 < 0.5$ and further a triangular distribution.

All distributions had the same mean $\langle\eta\rangle = 0.5$ but different widths (standard deviations) σ_η, which were varied from 0 to 0.5 (obtained for case (3) above). Only spectra showing the largest differences are shown in figure 17. Figures 17(a) and (b) show at the top the spectra for cases (1) and (2) including the difference (enlarged for clarity). Shown in the middle are the spectra for cases (1) and (3) including again the differences. At the bottom, the two spectra for $\eta = 0$ and $\eta = 1$ are shown.

Figure 17 proves that spectra are almost identical whatever the value of σ_η. In the presence of further distributions of IS's and of V_{zz}, it seems hopeless to extract more that the average $\langle\eta\rangle$ from an ^{57}Fe Mössbauer experiment. (This is of course not the case for certain other Mössbauer isotopes, or for NMR or PAC experiments.)

7.2. Ambiguity problem: QS distributions in classical ^{57}Fe and ^{119}Sn Mössbauer spectroscopy

In order to reliably compare experimental and theoretical results we must consider the sources of possible distortions to distributions obtained from classical ^{57}Fe and ^{119}Sn Mössbauer spectra. Two main problems may be distinguished. The first is of extrinsic nature and is due to the fact that the extraction of distributions from Mössbauer (or other) spectra belongs to the class of ill-posed 'inverse' problems. Small changes in the spectra may lead to large changes in the calculated distributions. Regularization methods are consequently required, and various methods are now available, to extract trustworthy pieces of information from experimental results. However, in addition, hyperfine parameter distributions in disordered or complex crystalline solids are *a priori* multivariate.

Some well known 'non-uniqueness' problems have been qualitatively discussed by Rancourt [92]. They are for example the determination of V_{zz} and η from a knowledge only of Δ, or that of η and the direction of the hyperfine field $\boldsymbol{B}_{hf}(\theta, \phi)$ in the principal axis system of the EFG tensor from a knowledge only of ϵ, the quadrupole lineshift in first-order perturbation theory. The ambiguity problem which we quantitatively discuss here cannot be reduced by a further change of variables. For these two examples, the physically meaningful and unambiguous parameters are Δ and ϵ. As mentioned by Rancourt, there exist different levels of ambiguity. Only the deepest irreducible level is discussed here. It is related to the intrinsic one-dimensional character of a Mössbauer spectrum in which only the photon energy (Doppler velocity) is varied. This partial one-dimensional information, from which one is trying to reconstruct a multi-dimensional distribution, produces an ambiguity in the derived distribution. As will be discussed below, identical Mössbauer spectra are obtained from different distributions. In systems which show a distribution of IS δ and of the quadrupole splitting Δ, the distribution which we must seek to obtain from the data is actually $f(\delta, \Delta)$. (The quantity $f(\delta, \Delta)\,\mathrm{d}\delta\,\mathrm{d}\Delta$ is the relative area associated with $\delta \leqslant \mathrm{IS} \leqslant \delta + \mathrm{d}\delta$ and $\Delta \leqslant \mathrm{QS} \leqslant \Delta + \mathrm{d}\Delta$ but not necessarily with the fraction of iron atoms with $\mathrm{IS} = \delta$ and $\mathrm{QS} = \Delta$ since the Lamb–Mössbauer factors are not *a priori* the same for all iron atoms.)

In the case of Mössbauer spectroscopy on isotopes with a $\frac{1}{2} \leftrightarrow \frac{3}{2}$ transition, such as ^{57}Fe and ^{119}Sn, severe ambiguity problems occur in the determination of $f(\delta, \Delta)$, at least from spectra taken in zero external magnetic field. This means that different distributions, say $f(\delta, \Delta)$ and $g(\delta, \Delta)$, produce identical spectra if they fulfil an as yet unreported relation established below. Only some of the $g(\delta, \Delta)$ distributions can be excluded as being physically implausible. Moreover, the ambiguity problem yields irreducible solutions $g(\delta, \Delta)$, that is solutions which cannot be related to $f(\delta, \Delta)$ by simple operations (for

instance symmetrization, etc). An example can be presented which shows that this is indeed the case. For this purpose, we consider a distribution $f(\delta, \Delta) = \delta(\delta - \delta_0)p(\Delta)$, which yields a spectrum symmetric with respect to the fixed IS δ_0. It can be shown that the very same spectrum results from a distribution $g(\delta, \Delta) = q(\delta)\delta(\Delta)$ of the IS with zero quadrupole splitting. The relation between q and p is:

$$q(\delta) = \begin{cases} p(2(\delta_0 - \delta)) & \delta \leqslant \delta_0 \\ p(2(\delta - \delta_0)) & \delta \geqslant \delta_0. \end{cases} \tag{63}$$

More generally, any non-magnetic spectrum may be considered as resulting from a distribution of IS's with zero quadrupole splitting: $g(\delta, \Delta) = q(\delta)\delta(\Delta)$ where $q(\delta)$ is no longer given by equation (63). It is immediately possible to object that the distribution $q(\delta)$ has no physical meaning in most cases. However, the latter distribution will be seen below to be of practical interest. The calculation of $q(\delta)$ may equivalently be looked at as a way to remove the Lorentzian broadening from the spectrum. In any case, the 'mathematical' ambiguity associated with $q(\delta)$ raises the problem of a possible physical ambiguity. The following question is thus raised: What conditions must two different distributions fulfil to give rise to identical Mössbauer spectra? That is, if $C_{exp}(v)$ represents the experimental spectrum at Doppler velocity v, C_∞ the background non-resonant counting rate and A a constant:

$$C_{exp}(v)/C_\infty \equiv 1 - Ac_{exp}(v) = 1 - Ac_f(v) = 1 - Ac_g(v). \tag{64}$$

We will use the thin absorber approximation for simplicity. Then:

$$c_h(v) = \frac{1}{2}\int_{-\infty}^{+\infty} \mathrm{d}\delta \int_0^{+\infty} \mathrm{d}\Delta\, h(\delta, \Delta)\left[\frac{1}{1 + (4(v - \delta + \Delta/2)^2/\Gamma^2)} + \frac{1}{1 + (4(v - \delta - \Delta/2)^2/\Gamma^2)}\right] \tag{65}$$

where $h = f, g$. A similar relation may also be obtained when this approximation is not valid by first using the method of For instance Dibar Ure and Flinn [94] for finite thickness (blackness removal). The characteristic function ϕ of the distribution $h(\delta, \Delta)$ is defined as [95]:

$$\phi_h(t_1, t_2) \equiv \langle \exp(\mathrm{i}t_1\delta + \mathrm{i}t_2\Delta)\rangle_h = \int_{-\infty}^{+\infty} \mathrm{d}\delta \int_0^{+\infty} \mathrm{d}\Delta\, h(\delta, \Delta)\exp(\mathrm{i}t_1\delta + \mathrm{i}t_2\Delta). \tag{66}$$

Averages with respect to a distribution h will be denoted hereafter as $\langle \ldots \rangle_h$. The notation $\langle \ldots \rangle_q$ (i.e. $h = q$) will denote averages taken over the pure IS distribution $q(\delta)\delta(\Delta)$ discussed previously. We wish to establish conditions on f and g such that (equation (64)):

$$c_{exp}(v) \equiv c_f(v) \equiv c_g(v). \tag{67}$$

Let us take the Fourier transforms of the terms of equation (67) in order to introduce the characteristic functions defined above. We note that Fourier transforms have been used in the past to analyse Mössbauer spectra. For instance Dibar Ure and Flinn [94] have used this for the removal of thickness effects. More recently, Vincze [96] has used the Fourier transform method in order to extract the even part of the distribution of the dominant part of the hyperfine interaction distribution from broadened Mössbauer spectra. Equation (67) becomes:

$$\int_{-\infty}^{+\infty} \exp(\mathrm{i}tv)c_f(v)\,\mathrm{d}v = \int_{-\infty}^{+\infty} \exp(\mathrm{i}tv)c_g(v)\,\mathrm{d}v. \tag{68}$$

Assuming that all the Lorentzian lines have the same full width at half-maximum (FWHM) Γ (equation (65)), we obtain (deleting common factors):

$$\int_{-\infty}^{+\infty} \mathrm{d}\delta \int_{0}^{+\infty} \mathrm{d}\Delta\, f(\delta, \Delta)[\exp(\mathrm{i}t\delta + \mathrm{i}t\Delta/2) + \exp(\mathrm{i}t\delta - \mathrm{i}t\Delta/2)]$$
$$= \int_{-\infty}^{+\infty} \mathrm{d}\delta \int_{0}^{+\infty} \mathrm{d}\Delta\, g(\delta, \Delta)[\exp(\mathrm{i}t\delta + \mathrm{i}t\Delta/2) + \exp(\mathrm{i}t\delta - \mathrm{i}t\Delta/2)]. \qquad (69)$$

In other words, the 'ambiguity' equation given by:

$$\phi_f(t, +t/2) + \phi_f(t, -t/2) = \phi_g(t, +t/2) + \phi_g(t, -t/2) = 2\phi_q(t) \qquad (70)$$

is the sought-after relation between the characteristic functions of f and g. The two terms with index f or g in equation (70) are the characteristic functions of the random variables $\delta + \Delta/2$ and $\delta - \Delta/2$, respectively. This ambiguity equation (equation (70)) emphasizes the basic reason for the existence of such a problem in Mössbauer spectroscopy: one is trying to reconstruct a two-dimensional characteristic function from the sum of two symmetric one-dimensional cuts. If two distinct distributions $g_1(\delta, \Delta)$ and $g_2(\delta, \Delta)$ are solutions of equation (70), any linear combination $g(\delta, \Delta) = \alpha g_1(\delta, \Delta) + (1-\alpha) g_2(\delta, \Delta)$ with $0 \leqslant \alpha \leqslant 1$ is also a solution of it.

As a check of equation (70), we notice that the characteristic function of the distribution $q(\delta)$ given by equation (63) is:

$$\phi_q(t) = \langle \exp(\mathrm{i}t\delta) \rangle_q = \tfrac{1}{2} \exp(\mathrm{i}t\delta_0)[\phi_p(+t/2) + \phi_p(-t/2)]. \qquad (71)$$

From $f(\delta, \Delta) = \delta(\delta - \delta_0)p(\Delta)$, we derive $\phi_f(t_1, t_2) = \exp(\mathrm{i}t_1\delta_0)\phi_p(t_2)$, while $g(\delta, \Delta) = q(\delta)\delta(\Delta)$ and $\phi_g(t_1, t_2) = \phi_q(t_1)$. Equation (70) thus yields $\phi_q(t)$ for these particular distributions.

We assume that the moments of the distributions $h(\delta, \Delta)$ exist up to some order n (with $n \geqslant 3$). If we take the derivatives of all terms of equation (70), k times with respect to t and set $t = 0$, we obtain (see equation (66)):

$$\langle (\delta + \Delta/2)^j + (\delta - \Delta/2)^j \rangle_h = \text{constant} \qquad (72)$$

with $j = 1, \ldots, k$ (with $k \leqslant n$) whatever the distribution h which yields $c_h(v) = c_{exp}(v)$ from equation (65). As surprising as it may look, equation (72) means that a distribution, even devoid of physical meaning, which yields a spectrum identical with the experimental one nevertheless must contain exact quantitative information about its shape. Equation (72) yields:

$$\langle \delta \rangle_h = \langle \delta \rangle_q = \text{constant} = \delta_0 \qquad (73)$$

$$\sigma^2_{\delta,h} + \langle \Delta^2/4 \rangle_h = \sigma^2_{\delta,q} = \text{constant}' \qquad (74)$$

$$\langle (\delta - \delta_0)^3 \rangle_h + \tfrac{3}{4}\{\langle \delta\Delta^2 \rangle_h - \delta_0 \langle \Delta^2 \rangle_h\} = \langle (\delta - \delta_0)^3 \rangle_q = \text{constant}'' = m^3_{\delta,q} \qquad (75)$$

for $j = 1, 2, 3$ respectively. For $j = 2$ and $j = 3$, the moments obtained for low-order moments have been combined in equations (74) and (75). In equations (73)–(75), $\sigma^2_{\delta s} = \langle (\delta - \delta_0)^2 \rangle_s$ (where $s = h$ or q). Equation (73) expresses the fact that the centre of gravity of the experimental spectrum is the same for all distributions which fit $c_{exp}(v)$ using Lorentzian lines with identical linewidths (FWHM) and according to the usual criterion of quality of fit. It is clear that a similar relationship $\langle \Delta \rangle_h = \text{constant}$ cannot be expected because $\langle \Delta \rangle_q$ by definition is equal to zero. Equations (73)–(75) suggest a convenient method to obtain useful and practical relationships between fitted parameters. This is given by the points below.

(1) Consider that the experimental spectrum $c_{exp}(v)$ results from a pure IS distribution, and extract the associated distribution $q(\delta)$. From a practical point of view, this is the simplest fit of $c_{exp}(v)$ with a distribution of hyperfine parameters. It provides a 'thinned' spectrum (removal of a Lorentzian linewidth of FWHM Γ) and some constants which may be convenient for many purposes.

(2) Calculate the moments of $q(\delta)$: $\langle\delta\rangle_q$, $\sigma_{\delta,q}$ and $m_{\delta,q}$ as given by equations (73)–(75).

The last term in the bracket on the left-hand side of equation (75) is the numerator of the correlation coefficient ρ_h between δ and Δ^2. If a fit to $c_{exp}(v)$ is possible using a distribution $g(\delta, \Delta)$ with δ and Δ distributed independently (that is, $g(\delta, \Delta) = u(\delta)v(\Delta)$), then equation (75) reduces to $\langle(\delta - \delta_0)^3\rangle_g = \langle(\delta - \delta_0)^3\rangle_q$. The model-independent histogram methods [89, 90] frequently used to extract hyperfine parameter distributions from experimental spectra are particularly convenient to deal with the ambiguity problem (some recent reviews of this method are given in [91]).

The thinning effect is illustrated by the following example of a spectrum consisting of n Lorentzian lines of FWHM Γ at velocities v_j $(j = 1, \ldots, n)$ with $\sum_{j=1}^{n} a_j = 1$:

$$C_{\exp}(v)/C_\infty = 1 - A\sum_{j-1}^{n} \frac{a_j}{1 + (4(v - v_j)^2/\Gamma^2)}.$$

The latter spectrum is equivalently calculated from equations (64) and (65) with:

$$h(\delta, \Delta) = q(\delta)\delta(\Delta)$$

$$q(\delta) = \sum_{j=1}^{n} a_j \delta(\delta - v_j).$$

A 'thinned' spectrum is thus obtained from a fit of the experimental spectrum with a 'pure' IS distribution.

We note that equation (70) may immediately be extended to the case of trivariate distributions of the type $f(B_{hf}, \delta, \epsilon)$ and $g(B_{hf}, \delta, \epsilon)$ where B_{hf} is the hyperfine magnetic field, and ϵ the first-order quadrupolar shift for $\frac{1}{2} \leftrightarrow \frac{3}{2}$ Mössbauer transitions (yielding a sextuplet of lines). Within this approximation, the magnetic ambiguity equation is:

$$\sum_{j=1}^{6} I_j \phi_h(\alpha_j t, t, \beta_j t) = \phi_q(t) \tag{76}$$

where $h = f, g, \ldots$, and I_j is the relative intensity of line j in the elementary sextet (with $\sum_{j=1}^{6} I_j = 1$; for instance $I_1 = I_6 = 3/12$, $I_2 = I_5 = 2/12$, $I_3 = I_4 = 1/12$). All lines are assumed to be Lorentzian with an FWHM of Γ. The right-hand side of equation (76) is associated with the previous 'isomer shift' distribution. As mentioned previously, the latter is equivalent to the removal of a Lorentzian linewidth of Γ. $\alpha_j B_{hf}$ describe the lineshifts due to the nuclear Zeeman effect for lines of the sextet ($j = 1, \ldots, 6$) and β_j indexes the sign of the quadrupole lineshift ($\beta_j = 1$ for $j = 1, 6$, else it equals -1). In cases where the distribution h would be perfectly known, another level of ambiguity is associated with the fact, mentioned by Rancourt [92], that ϵ is itself a product of several factors. As mentioned previously, this level is ignored in the present calculation. Invariants similar to those derived for bivariate distributions $h(\delta, \Delta)$ may be associated with equation (76). All trivariate distributions $h(B_{hf}, \delta, \epsilon)$ which fit $c_{exp}(v)$ (using Lorentzian lines with equal linewidths) satisfy:

$$\sum_{j=1}^{6} I_j \langle(\alpha_j B_{hf} + \delta + \beta_j \epsilon)^k\rangle_h = \text{constant} = \langle\delta^k\rangle_q.$$

In addition, assuming now $I_{7-k} = I_k$, $k = 1, 2, 3$ we obtain:

$$\langle\delta\rangle_h + (4I_1 - 1)\langle\epsilon\rangle_h = \langle\delta\rangle_q$$

as well as:

$$\langle B_{hf}^2\rangle\left(\sum_{j=1}^{6} I_j\alpha_j^2\right) + \langle\delta^2\rangle_h + \langle\epsilon^2\rangle_h + (8I_1 - 2)\langle\delta\epsilon\rangle_h = \text{constant}' = \langle\delta^2\rangle_q.$$

When equation (76) is applied to an assumed trivariate normal distribution, the ambiguity will in general be less than in the bivariate quadrupole case discussed below as soon as the Zeeman line shift $|\alpha_j B_{hf}|$ is significantly larger than either σ_δ or σ_Δ. If these two latter widths are both much smaller than the typical maximum width $|\alpha_1 B_{hf}|$, the distribution becomes *de facto* approximately one dimensional and is much less sensitive to the detailed (but physically reasonable) assumptions on the δ and Δ distributions.

As bivariate normal distributions have recently been used to analyse Mössbauer spectra [26, 27] of for instance diamagnetic oxide glasses [26], it is worth looking into the ambiguity resulting from equation (70) in the case of such distributions $f(\delta, \Delta)$. Moreover they provide a good illustration of the aforementioned problems.

7.2.1. The example of a bivariate normal distribution $f(\delta, \Delta)$. The distribution $f(\delta, \Delta)$ and its characteristic function $\phi_f(t_1, t_2)$ are (see section 4, equations (23) and (24) and [64]):

$$f(\delta, \Delta) = \frac{1}{2\pi}\frac{1}{\sigma_{\delta,f}\sigma_{\Delta,f}\sqrt{1-\rho_f^2}}\exp\left\{\frac{-1}{2(1-\rho_f^2)}\left[\left(\frac{\delta-\delta_0}{\sigma_{\delta,f}}\right)^2 - 2\rho_f\left(\frac{\delta-\delta_0}{\sigma_{\delta,f}}\right)\left(\frac{\Delta-\Delta_0}{\sigma_{\Delta,f}}\right) + \left(\frac{\Delta-\Delta_0}{\sigma_{\Delta,f}}\right)^2\right]\right\} \tag{77}$$

$$\phi_f(t_1, t_2) = \exp\left\{\mathrm{i}(t_1\delta_0 + t_2\Delta_0) - \left(\frac{1}{2}\sigma_{\delta,f}^2 t_1^2 + \rho\sigma_{\delta,f}\sigma_{\Delta,f}t_1t_2 + \frac{1}{2}\sigma_{\Delta,f}^2 t_2^2\right)\right\}$$

where the set of parameters $(\delta_0, \sigma_{\delta,f}, \Delta_0, \sigma_{\Delta,f}, \rho_f)$ is such that:

$$\begin{aligned}
&\beta_0 \equiv \langle\beta\rangle_f \\
&\sigma_{\beta,f} \equiv \langle(\beta-\beta_0)^2\rangle_f^{1/2} \\
&\rho_f \equiv \frac{\langle(\delta-\delta_0)(\Delta-\Delta_0)\rangle_f}{\sigma_{\delta,f}\sigma_{\Delta,f}}
\end{aligned} \tag{78}$$

where $\beta = \delta$ or Δ. ρ_f is the usual correlation coefficient with $-1 \leqslant \rho_f \leqslant +1$. The left-hand side of equation (70) can be written as:

$$\sum_{\epsilon=\pm1}\exp\left\{\mathrm{i}t(\delta_0 + \epsilon\Delta_0/2) - \frac{t^2}{2}\left[\sigma_{\delta,f}^2 + \epsilon\rho_f\sigma_{\delta,f}\sigma_{\Delta,f} + \frac{1}{4}\sigma_{\Delta,f}^2\right]\right\}. \tag{79}$$

To prove that solutions exist for a $g(\delta, \Delta)$ different from $f(\delta, \Delta)$ which fulfil equation (70), we will first discuss the case where $g(\delta, \Delta)$ is bivariate normal such as $f(\delta, \Delta)$, and then the case where $g(\delta, \Delta)$ is different. Let us define:

$$\begin{aligned}
&x = 2\sigma_{\delta,f}/\sigma_{\Delta,f} \qquad x \geqslant 0 \\
&a = x^2 + x^{-2} - 2
\end{aligned} \tag{80}$$

where a is seen to be positive whenever $x \neq 1$ and zero for $x = 1$. We further require:

$$\begin{aligned}\sigma_{\delta,g}^2 &= \alpha\sigma_{\delta,f}^2 + (1-\alpha)\sigma_{\Delta,f}^2/4 = \sigma_{\delta,f}^2(\alpha + (1-\alpha)/x^2)\\ \sigma_{\Delta,g}^2 &= 4(1-\alpha)\sigma_{\delta,f}^2 + \alpha\sigma_{\Delta,f}^2 = \sigma_{\Delta,f}^2(\alpha + (1-\alpha)x^2)\end{aligned} \tag{81}$$

with $0 \leqslant \alpha \leqslant 1$. The correlation coefficient ρ_g must satisfy:

$$\rho_g\sigma_{\delta,g}\sigma_{\Delta,g} = \rho_f\sigma_{\delta,f}\sigma_{\Delta,f} \tag{82}$$

that is, the condition:

$$\frac{\rho_g}{\rho_f} = \frac{1}{\sqrt{1 + a\alpha - a\alpha^2}}. \tag{83}$$

The bivariate normal distribution $g(\delta, \Delta)$ with a set of parameters (δ_0, $\sigma_{\delta,g}$, Δ_0, $\sigma_{\Delta,g}$, ρ_g) is by construction such that (with $\epsilon = \pm 1$):

$$\sigma_{\delta,g}^2 + \epsilon\rho_g\sigma_{\delta,g}\sigma_{\Delta,g} + \tfrac{1}{4}\sigma_{\Delta,g}^2 = \sigma_{\delta,f}^2 + \epsilon\rho_f\sigma_{\delta,f}\sigma_{\Delta,f} + \tfrac{1}{4}\sigma_{\Delta,f}^2. \tag{84}$$

The two distributions $f(\delta, \Delta)$ and $g(\delta, \Delta)$ thus verify the ambiguity equation (70), as shown by an inspection of equation (79).

The ratio ρ_g/ρ_f is equal to unity for $\alpha = 0$ and for $\alpha = 1$. It decreases to a minimum of $1/\sqrt{(1 + a/4)}$ for $\alpha = 1/2$. The ratio is monotonic decreasing over $\alpha \in \{0, 1/2\}$ and monotonic increasing over $\alpha \in \{1/2, 1\}$. We note that our solution (equations (80)–(83)) shows no ambiguity for the case of $x = 1$, that is, for $a = 0$. In contrast, large changes in $\sigma_{\delta,g}$, $\sigma_{\Delta,g}$ and ρ_g are allowed when x is either small or large compared to unity. For $\alpha = 0$, as expected $\sigma_{\delta,g} = \sigma_{\Delta,f}/2$ and $\sigma_{\Delta,g} = 2\sigma_{\delta,f}$ as this corresponds to an interchange of the corresponding variances $\sigma_{\delta,f}^2$ and $\sigma_{\Delta,f}^2$ in equation (79).

Distributions $g(\delta, \Delta)$ constructed from degenerate normal distributions also yield spectra identical to those obtained from the bivariate normal distribution $f(\delta, \Delta)$. A first example is the unphysical distribution of solely the isomer shift:

$$q(\delta)\delta(\Delta) = \frac{1}{2}\delta(\Delta)\left[\frac{1}{\sigma_+\sqrt{2\pi}}\exp\left\{-\frac{(\delta-\delta_+)^2}{2\sigma_+^2}\right\} + \frac{1}{\sigma_-\sqrt{2\pi}}\exp\left\{-\frac{(\delta-\delta_-)^2}{2\sigma_-^2}\right\}\right] \tag{85}$$

with:

$$\begin{aligned}\delta_\pm &= \delta_0 \pm \tfrac{1}{2}\Delta_0\\ \sigma_\pm^2 &= \sigma_{\delta,f}^2 \pm \rho_f\sigma_{\delta,f}\sigma_{\Delta,f} + \tfrac{1}{4}\sigma_{\Delta,f}^2.\end{aligned} \tag{86}$$

As the assumption of a linear dependence between δ and Δ is commonly found in the literature, the second example is more relevant to experimental situations. We assume that:

$$g(\delta, \Delta) = \delta(\delta - \delta_l - \beta\Delta)\frac{1}{\sigma_l\sqrt{2\pi}}\exp\left\{-\frac{(\Delta-\Delta_l)^2}{2\sigma_l^2}\right\}. \tag{87}$$

As $\Delta \geqslant 0$, a normal (Gaussian) distribution of Δ is *a priori* expected to properly describe an actual distribution of Δ only if the weight of the $\Delta < 0$ part is small or negligible compared to unity, typically $\langle\Delta\rangle_l \gtrsim 2\sigma_l$. However, equation (65) shows that a spectrum can actually be calculated from a distribution $h(\delta, \Delta)$ with any weight for the part $\Delta < 0$ (changing the lower limit of integration to $-\infty$ in equation (65)). For ^{57}Fe and ^{119}Sn, the spectrum only depends on $|\Delta|$. The associated distribution $g_a(\delta, \Delta)$ when restricted to $\Delta \geqslant 0$ is obtained by folding $\Delta \leqslant 0$ onto $\Delta \geqslant 0$. Thus:

$$\begin{aligned}g_a(\delta, \Delta) = \frac{1}{\sigma_l\sqrt{2\pi}}&[\exp\{-(\Delta-\Delta_l)^2/(2\sigma_l^2)\}\delta(\delta-\delta_l-\beta\Delta)\\ &+ \exp\{-(\Delta+\Delta_l)^2/(2\sigma_l^2)\}\delta(\delta-\delta_l+\beta\Delta)].\end{aligned} \tag{88}$$

The distribution of Δ is thus that of the absolute value of a Gaussian variable, namely:

$$p_a(\Delta) = \frac{1}{\sigma_l\sqrt{2\pi}}[\exp\{-(\Delta - \Delta_l)^2/(2\sigma_l^2)\} + \exp\{-(\Delta + \Delta_l)^2/(2\sigma_l^2)\}] \quad (89)$$

with $\Delta \geqslant 0$. We see that $g_a(\delta, \Delta)$ and $g(\delta, \Delta)$ yield identical spectra. Thus in equation (87), we allow negative Δ values. A similar conclusion also holds for equation (77). In practice, the second doublet matters only in the range where the second exponential in equation (89) is significant. Under such conditions, equation (87) is also a legitimate form. The ambiguity equation remains unchanged with the extension of Δ to negative values (done for theoretical simplicity). If $\Delta_l/\sigma_l \gg 1$, then $p_a(\Delta)$ can be considered Gaussian (Figure 18(c)). The characteristic function of $g(\delta, \Delta)$ is given by:

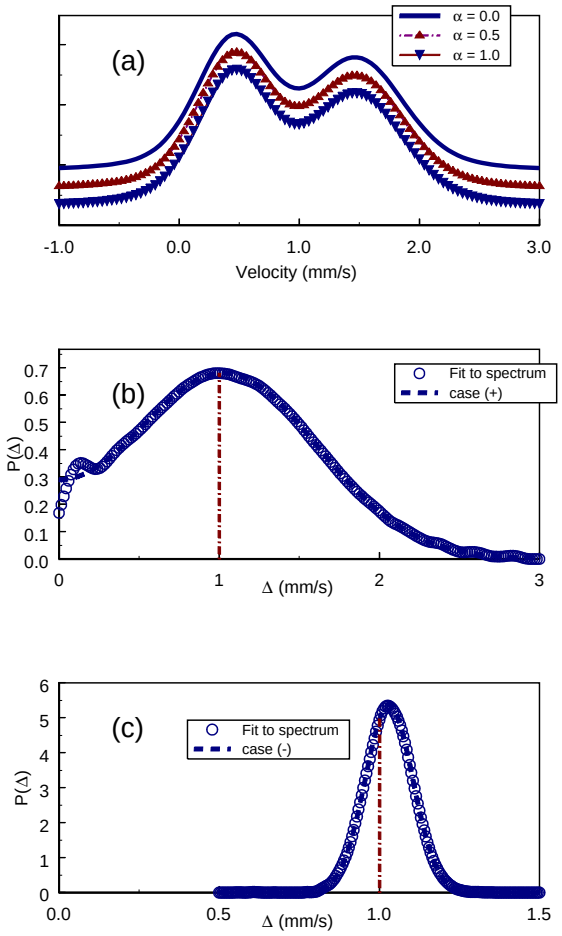

Figure 18. (a) Shown are three spectra calculated for bivariate normal distributions using the values given in table 3, and for $\alpha = 0$ compared to $\alpha = 1/2$ and 1. The spectra are shifted for clarity and are otherwise indistinguishable. QS distributions deduced from a fit of the spectrum $\alpha = 1$ of (a) using a model-independent fitting method [90]: (b) $\delta = 0.9069$ mm s$^{-1} + 6.3238 \times 10^{-2}\Delta$ and (c) $\delta = -3.0999$ mm s$^{-1} + 3.9533\Delta$. In both (b) and (c), dashed lines represent the theoretical distributions $p_{\pm}(\Delta)$ calculated for the corresponding parameters.

$$\phi_g(t_1, t_2) = \exp\{\mathrm{i}t_1\delta_l + \mathrm{i}(\beta t_1 + t_2)\Delta_l - \tfrac{1}{2}(\beta t_1 + t_2)^2\sigma_l^2\}.$$

The associated term of the ambiguity equation (70) is:

$$\sum_{\epsilon=\pm 1/2} \exp\left\{\mathrm{i}t(\delta_l + (\beta+\epsilon)\Delta_l) - \frac{1}{2}t^2(\beta+\epsilon)^2\sigma_l^2\right\}$$

which when identified with equation (79) yields:

$$\begin{aligned} &\Delta_l = \Delta_0 \\ &\delta_l = \delta_0 - \beta\Delta_0 \\ &\beta\sigma_l^2 = \rho_f\sigma_{\delta,f}\sigma_{\Delta,f} \\ &\sigma_l^2(4\beta^2+1) = 4\sigma_{\delta,f}^2 + \sigma_{\Delta,f}^2 \end{aligned} \tag{90}$$

showing that β has the same sign as ρ_f (assuming here that $\rho_f \neq 0$). Defining z as:

$$z = \frac{4\rho_f\sigma_{\delta,f}\sigma_{\Delta,f}}{4\sigma_{\delta,f}^2 + \sigma_{\Delta,f}^2} \tag{91}$$

it follows that $0 < |z| \leqslant 1$ and that z is unique for a given bivariate normal distribution as both $\rho_h\sigma_{\delta,h}\sigma_{\Delta,h}$ and $4\sigma_{\delta,h}^2 + \sigma_{\Delta,h}^2$ are constant for all ambiguity solutions given by equations (80)–(83). Therefore, two solutions of the sign of ρ_h are obtained for β and consequently for σ_l^2 and δ_l:

$$\begin{aligned} &\beta_\pm = \frac{z}{2[1 \pm \sqrt{1-z^2}]} \begin{cases} 0 < |\beta_+| \leqslant 1/2 \\ 1/2 \leqslant |\beta_-| \end{cases} \\ &\sigma_{l,\pm}^2 = \frac{1}{2}(4\sigma_{\delta,f}^2 + \sigma_{\Delta,f}^2)[1 \pm \sqrt{1-z^2}] \\ &\delta_{l,\pm} = \delta_0 - \beta_\pm\Delta_0. \end{aligned}$$

In most cases, only the β_+ solution would be considered as physically plausible. The condition $\Delta_l \geqslant 2\sigma_l$ will not necessarily be obeyed for the β_+ solution as shown by figure 18(b). The latter point is discussed below where it will be seen not to have serious consequences.

Calculations using $f(\delta, \Delta)$, $q(\delta)\delta(\Delta)$ and $g(\delta, \Delta)$ (taken from equations (77), (85) and (87)) show that the expressions given in equations (73)–(75) are valid in all cases. For instance, equations (85) and (87) yield:

$$\begin{aligned} &\langle\delta\rangle_q = \tfrac{1}{2}[\delta_+ + \delta_-] = \delta_0 = \langle\delta\rangle_f = \langle\delta\rangle_g \\ &\langle\delta^2\rangle_q = \tfrac{1}{2}[\sigma_+^2 + \delta_+^2 + \sigma_-^2 + \delta_-^2] = \sigma_{\delta,f}^2 + \delta_0^2 + \langle\tfrac{1}{4}\Delta^2\rangle_f \end{aligned}$$

that is:

$$\sigma_{\delta,q}^2 = \sigma_{\delta,f}^2 + \langle\tfrac{1}{4}\Delta^2\rangle_f \tag{92}$$

as expected from equation (74). Furthermore from equation (87) we obtain:

$$\sigma_{\delta,g}^2 = \beta^2\sigma_l^2.$$

Therefore, using equations (90) we obtain:

$$\begin{aligned} \sigma_{\delta,g}^2 + \langle\tfrac{1}{4}\Delta^2\rangle_g &= \tfrac{1}{4}\sigma_l^2(4\beta^2+1) + \tfrac{1}{4}\Delta_0^2 = \sigma_{\delta,f}^2 + \tfrac{1}{4}\sigma_{\Delta,f}^2 + \tfrac{1}{4}\Delta_0^2 \\ &= \sigma_{\delta,f}^2 + \langle\tfrac{1}{4}\Delta^2\rangle_f = \sigma_{\delta,q}^2. \end{aligned}$$

Although we have not proven it, the possible solutions to the ambiguity problem in the case of the bivariate normal distribution are likely to be constituted of these three solutions

together with all possible linear combinations of them with positive normalized weights. This is based on the fact that a characteristic function $\phi_q(t)$ which is given by the sum of two exponentials of second-degree polynomials, which are themselves proportional to characteristic functions, can only be obtained as the sum of similar exponential terms as the exponential of a polynomial of degree greater than 2 cannot be a characteristic function [93].

Finally, the bivariate normal distribution (equation (77)), the 'isomer shift' distribution (equation (85)) and the distribution with a linear dependence of δ on Δ (equation (87)) are certainly different distributions. One cannot be transformed into another by any simple operation.

To convince the reader of the need to take such an ambiguity problem into account, we have calculated ^{57}Fe Mössbauer spectra using bivariate normal distributions $f(\delta, \Delta)$ in equation (65). The necessary input parameters have been taken from the fits of such spectra from CaO–SiO_2–FeO glasses using this distribution [26]. In particular we have considered among others the parameters reported by Alberto *et al* [26], in their table 1 for Fe^{2+}(IV), sample A (see table 3, $\alpha = 1$). Table 3 reports the values of the parameters used for the calculations of the simulated spectra shown in figure 18. An examination of these spectra shows clearly that they are identical despite large changes in the standard deviations $\sigma_{\delta,h}$ and $\sigma_{\Delta,h}$. The isomer shift δ of Fe^{2+} is known to range between $\sim$0.6 and $\sim$1.6 mm s^{-1} [97]. Thus a physically reasonable value of $\sigma_{\delta,h}$ should be less than about 0.25 mm s^{-1}. The standard deviations $\sigma_{\delta,h}$ reported in table 3 over a wide range of α are thus *a priori* consistent with this estimation. Selecting a particular value of $\sigma_{\delta,h}$, and as a consequence $\sigma_{\Delta,h}$, may thus involve a certain degree of arbitrariness. Furthermore we note that we have assumed the bivariate distribution $f(\delta, \Delta)$ to be Gaussian, and the Mössbauer spectrum to be exactly known. This is however not necessarily the case experimentally, which further adds to the arbitrariness.

Table 3. Parameters used to calculate the spectra of figure 18 with bivariate normal distributions of δ and $\Delta(h(\delta, \Delta) = f(\delta, \Delta)$ for $\alpha = 1$). Here, $x = 0.2809$, and $a = 10.7514$. The symbols are defined in the text.

α	δ_0 (mm s^{-1})	Δ_0 (mm s^{-1})	$\sigma_{\delta,h}$ (mm s^{-1})	$\sigma_{\Delta,h}$ (mm s^{-1})	ρ_h
0	0.972	1.03	0.2844	0.1597	0.4780
1/2	0.972	1.03	0.2089	0.4177	0.2489
1	0.972	1.03	0.0799	0.5687	0.4780

Linear variations (equation (87)) Δ either $\geqslant 0$ or $\leqslant 0$	
(+)	$\sigma_{l,+} = 0.5861$
	$\delta_+ = 0.9069 + 6.3238 \times 10^{-2}\Delta$
(−)	$\sigma_{l,-} = 0.0741$
	$\delta_- = -3.0999 + 3.9533\Delta$

The theoretical spectra calculated for the linear dependencies, $\delta = \delta_{l,\pm} + \beta_\pm \Delta$, with the parameters of table 3 and if necessary with $\Delta < 0$ (see discussion below equation (87)) are also identical to those in figure 18(a) for various bivariate normal distributions, confirming the validity of our analysis. Table 3 yields $\Delta_0/\sigma_{l,-} \simeq 13.9$ and $\Delta_0/\sigma_{l,+} \simeq 1.76$. Thus negative values of Δ have to be considered for the (+) term only. To check the validity of equations (87), (90) and (91), we have fitted a spectrum calculated from a bivariate normal distribution with $\alpha = 1$ (table 3) with a model-independent method [90]. We have assumed

either + or − in $\delta = \delta_{l,\pm} + \beta_\pm \Delta$ (with $\Delta \geqslant 0$) with the values of $\delta_{l,\pm}$ and $\beta_\pm$ given in table 3. The fitted spectra cannot be distinguished from the simulated ones and so are not shown in figure 18(a). Figure 18(b) compares the distribution obtained from the fit with the theoretical distribution $p_a(\Delta)$ calculated for $\Delta_l = \Delta_0 = 1.03$ mm s^{-1} and $\sigma_l = 0.5861$ mm s^{-1} (table 3, case (+)). For the fit, a single isomer shift $\delta = \delta_{l,+} + \beta_+ \Delta$ for each Δ was used. This is similar to typical situations in practice. From the preceding discussion, the theoretical spectrum (with negative Δ) is equivalent to a situation with two isomer shifts for small Δ (and $\Delta \geqslant 0$). This explains the small distortions seen in figure 18(b) for small Δ. However the overall agreement is very good. Figure 18(c) shows an excellent agreement between the fitted distribution and the normal one calculated for $\langle\Delta\rangle = 1.03$ mm s^{-1} and a standard deviation $\sigma = 0.0741$ mm s^{-1} (table 3). As $\Delta_l/\sigma_{l,-} \gg 1$, the assumption of a single-valued δ for every Δ (i.e. $\delta = \delta_{l,-} + \beta_- \Delta$) is now perfectly valid. The average QS and the standard deviation ($\langle\Delta\rangle$, σ_Δ) obtained from the fitted distributions are (1.05, 0.557) mm s^{-1} for the (+) case, and (1.03, 0.0767) mm s^{-1} for the (−) case. $\langle\Delta\rangle_+$ and $\sigma_{\Delta+}$ from the distribution $p_a(\Delta)$ are given by:

$$\langle\Delta\rangle_+ = \sqrt{\frac{2}{\pi}}\sigma_{l,+} \exp\{-\Delta_0^2/(2\sigma_{l,+}^2)\} + \Delta_0 \operatorname{erf}(\Delta_0/(\sqrt{2}\sigma_{l,+}))$$

$$\sigma_{\Delta+}^2 = \sigma_{l,+}^2 + \Delta_0^2 - \langle\Delta\rangle_+^2.$$

The theoretical values are $\langle\Delta\rangle_+ = 1.0486$ mm s^{-1} and $\sigma_{\Delta+} = 0.5521$ mm s^{-1} for $\Delta_0 = 1.03$ mm s^{-1} and $\sigma_{l,+} = 0.5861$ mm s^{-1} (table 3, (+)). Similarly, $\langle\Delta\rangle_- = 1.03$ mm s^{-1} and $\sigma_{\Delta-} = 0.0741$ mm s^{-1}. In both cases, a very good agreement is found between the theoretical values and those found for the fit. Both figures 18(b) and (c) confirm further that a spectrum calculated from a *bivariate* normal distribution can as well be accounted for by a distribution of Δ including linear dependencies of δ on Δ.

The spectrum given in figure 18(a) ($\alpha = 0$) has also been fitted with a distribution of IS's assuming zero QS: $g(\delta, \Delta) = q(\delta)\delta(\Delta)$. The values found (equations (73)–(75)) are $\delta_0 = 0.972$ mm s^{-1}, $\sigma_{\delta,q}^2 = 0.356$ (mm s^{-1})^2 and $m_{\delta,q}^3 = 0.343 \times 10^{-1}$ (mm s^{-1})^3. The theoretical values calculated from $g(\delta, \Delta)$, equation (87) for the (−), case in table 3 are 0.972, 0.352 and 0.335×10^{-1} in the same units, respectively. The usefulness of fitting with an IS distribution $q(\delta)$ is thus confirmed (see discussion below equation (75)). In addition, using this method it is possible to use 'thin' spectra (removal of the linewidth Γ) and to calculate invariants, which may help to fit and interpret them.

Our calculations demonstrate that significant errors may result from the assumptions generally done to calculate QS distributions from for instance ^{57}Fe Mössbauer spectra. Most often in the literature, one of the following assumptions is made:

- δ is fixed so that $f(\delta, \Delta)$ reduces to $\delta(\delta - \delta_0)p(\Delta)$.
- δ is a function of the QS: $\delta = F(\Delta)$. Usually a linear relation is assumed: $\delta = \delta_l + \beta\Delta$.
- δ and Δ are distributed according to a bivariate normal distribution including a correlation coefficient.

Our results (for instance those shown in table 3) prove that an ambiguity may remain which cannot be easily removed by physical guidance but point out the interest of using quantitative information about shapes of spectra. The latter ambiguity may be termed *physical ambiguity* to distinguish it from the *mathematical ambiguity*. Mathematical ambiguity is associated with solutions of the ambiguity equation which can be rejected with certainty without the need of performing supplementary experiments. However it is not possible to completely remove the uncertainty which results from the previous physical ambiguity although physical considerations may reduce it to an acceptable level in many circumstances (using the

relations given in equations (73)–(75)). This explains the many difficulties in the literature about QS distributions especially for the ^{57}Fe isotope. Thus care must be taken when discussing details of QS distributions. More generally, our discussion raises the problem of the definition of a method for constructing all solutions for the ambiguity problem for a given $\phi_q(t)$, that is $f(\delta, \Delta)$ such that $\phi_f(t, t/2)+\phi_f(t, -t/2) = 2\phi_q(t)$. The present section finally leads us to emphasize that the quality of fit, although necessary, cannot be a sufficient criterion for judging the validity of the associated QS distribution. An important problem is further to develop experimental techniques to overcome partially or totally the fundamental ambiguity due to the partial information provided by classical Mössbauer spectra.

The considerations of this section are by no means restricted to QS distributions in the case of ^{57}Fe and ^{119}Sn Mössbauer spectroscopy. We have discussed this case in detail because it is experimentally the most important and also the most acute. Both σ_δ and σ_Δ broaden the resonant lines in a similar fashion, and so are most difficult to separate. Supplementary experiments such as in this case spectra in an external magnetic field should be exploited to at least reduce these ambiguities, both mathematical and physical. A similar analysis could be made for other hyperfine methods which are used to determine QS distributions. In the case of NMR spectroscopy for instance, there is a difficulty in separating QS from Knight shift distributions in disordered solids.

8. Conclusions

We have presented some considerations on the consequences of statistical isotropy of the EFG tensor which help to clarify the nature of the assumptions often made in the literature on disordered solids from Mössbauer experiments or more generally from hyperfine methods. The η distribution which is found for the reference model [1], called here the Gaussian isotropic model (GIM), is seen to be at least approximately valid for a class of disordered solids much broader than the sole GIM class. The latter distribution is thus the most *a priori* reasonable distribution for a disordered solid. The GIM yields also a universal distribution $f(V_{zz}, \eta)$ which results from the universality of the central limit theorem in statistics. This model distribution is made possible in some solids by the peculiar characteristics of the physical contributions to the EFG. The sole free parameter in this model, denoted here as σ, determines the actual physical scale and yields for instance the width of the distribution. If the GIM model is valid, no precise conclusion can be drawn about the structure from EFG measurements alone. By contrast, no universal distribution $f(V_{zz}, \eta)$ is able to account for the various situations encountered in disordered solids with so widely different electronic structures and short- as well as medium-range orders. The generalized χ-type QS distributions:

$$P_n(\Delta) \propto \Delta^{n-1} \exp\left(-\frac{\Delta^2}{2\sigma^2}\right) \qquad n \leqslant 4$$

are good mathematical approximations which lead to satisfying fits of many ^{57}Fe Mössbauer spectra but are of no help to obtain the number of structural degrees of freedom of the local environments of the probe atoms. The name 'shell model' which is still widely used to designate such QS fits is confusing and cannot be justified by a single argument. We propose to replace this by the names 'generalized χ models' when only QS distributions are considered and fitted with the latter mathematical models and by the names 'degenerate Gaussian models' when explicit assumptions *à la* Czjzek [29] are made about the distribution of the EFG tensor. The consequences of the assumptions made in the 'degenerate Gaussian models' Cz(n) have never been checked experimentally. Simulations have been performed

and presented here to obtain some general features of the marginal distributions of V_{zz} and of η for Cz(n) models ($1 \leqslant n \leqslant 4$). The η distribution which is found for the GIM is also a good approximation of the η distributions of the Cz(3) and Cz(4) models. The former approximations of QS distributions have not yet received strong physical support from an experimental point of view due to various difficulties (an ambiguity problem which occurs when trying to extract QS distributions from $\frac{1}{2} \leftrightarrow \frac{3}{2}$ Mössbauer spectra has also been considered in subsection 7.2). This is also the case from the point of view of simulations with structural models (due to an insufficient number of atoms used in such simulations).

Structural models with built-in medium-range order are now beginning to receive strong experimental support. One cannot exclude that such studies would show EFG and QS distributions consistent with Czjzek's extensions or modifications of them for $n < 5$ if amorphous solids are scrutinized at the appropriate scale both experimentally (typically at the scale of DCEMS for instance) and with structural models. New models of EFG distributions in disordered solids are worth being investigated. The methods used in this paper can be applied to any physical property which is related to a second rank tensor (such as atomic level stresses, dipolar tensors etc). Some of them have already been applied to atomic level stresses in [8]. They are now being applied to analyse the EFG distributions found in ^{27}Al and ^{65}Cu NMR spectra of AlCuFe quasicrystals and their approximants [98]. For these isotopes, NMR spectroscopy is very sensitive to fine details of the EFG distribution. The EFG distribution of the quasicrystals has been found to follow a GIM model to high accuracy. It has also been possible to follow the appearance of new crystalline sites in the approximant phases, with distinctive EFG values superimposed on the GIM distribution. This effect would have gone unnoticed without the help of the GIM model distribution to analyse the results.

Acknowledgments

Part of this work was started during the visit of one of the authors (RAB) at the Ecole des Mines, Nancy, supported by the CNRS. GLC thanks R Delannay for a useful discussion.

Appendix A

The rotations from the x, y, z to the x', y', z' system defined by the Euler angles (α, β, γ) are shown in figure A1. The rotation α (where $0 \leqslant \alpha < 2\pi$) is around the z-axis; the rotation β (where $0 \leqslant \beta < \pi$) is around the y_1-axis; the rotation γ (where $0 \leqslant \gamma < 2\pi$) is around the z_2-axis.

After a rotation of the frame of reference defined by the Euler angles (α, β, γ), the new tensor elements expressed here by the five components of $\boldsymbol{U}'$ are linearly related to the old components of $\boldsymbol{U}$ by:

$$U'_i = \sum_{j=1}^{5} a_{ij} U_j \qquad i = 1, \ldots, 5 \tag{A1}$$

or equivalently:

$$\boldsymbol{U}' = \mathcal{O}(\alpha, \beta, \gamma)\boldsymbol{U}$$

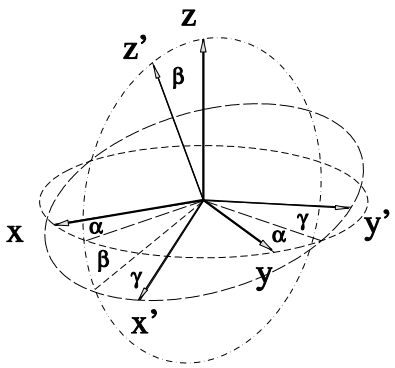

Figure A1. The rotations from the x, y, z to the x', y', z' system defined by the Euler angles (α, β, γ). A circle on the x, y-plane is shown as a short-dashed line. The rotation α is around the z-axis producing the x_1, y_1, z_1 system (shown as dashed lines). The rotation β is around the y_1-axis producing the x_2, y_2, z_2 system. A circle on the x_1, z_1-plane is shown as a dot–dashed line. The rotation γ is around the z_2-axis producing the x', y', z' system. A circle on the x', y'-plane is shown as a long-dashed line.

where $\mathcal{O}(\alpha, \beta, \gamma)$ is an orthogonal 5×5 matrix:

$$O_{ij}(\alpha, \beta, \gamma) = a_{ij}$$
$$\sum_{j=1}^{5} a_{ij}^2 = 1. \tag{A2}$$

Explicit expressions for the different coefficients are given below:

- For $i = 1$:

$$a_{11} = \frac{1}{2}[3\cos^2(\beta) - 1]$$
$$a_{12} = \frac{\sqrt{3}}{2}\sin(2\beta)\cos(\alpha)$$
$$a_{13} = \frac{\sqrt{3}}{2}\sin(2\beta)\sin(\alpha)$$
$$a_{14} = \frac{\sqrt{3}}{2}\sin^2(\beta)\sin(2\alpha)$$
$$a_{15} = \frac{\sqrt{3}}{2}\sin^2(\beta)\cos(2\alpha).$$

- For $i = 2$:

$$a_{21} = -\frac{\sqrt{3}}{2}\sin(2\beta)\cos(\gamma)$$
$$a_{22} = \cos(\alpha)\cos(2\beta)\cos(\gamma) - \sin(\alpha)\cos(\beta)\sin(\gamma)$$
$$a_{23} = \sin(\alpha)\cos(2\beta)\cos(\gamma) + \cos(\alpha)\cos(\beta)\sin(\gamma)$$
$$a_{24} = [\sin(2\alpha)\cos(\beta)\cos(\gamma) + \cos(2\alpha)\sin(\gamma)]\sin(\beta)$$
$$a_{25} = [\cos(2\alpha)\cos(\beta)\cos(\gamma) - \sin(2\alpha)\sin(\gamma)]\sin(\beta).$$

- For $i = 3$:

$$\begin{aligned}
a_{31} &= \frac{\sqrt{3}}{2}\sin(2\beta)\sin(\gamma)\\
a_{32} &= -\cos(\alpha)\cos(2\beta)\sin(\gamma) - \sin(\alpha)\cos(\beta)\cos(\gamma)\\
a_{33} &= \cos(\alpha)\cos(\beta)\cos(\gamma) - \sin(\alpha)\cos(2\beta)\sin(\gamma)\\
a_{34} &= \sin(\beta)[\cos(2\alpha)\cos(\gamma) - \sin(2\alpha)\cos(\beta)\sin(\gamma)]\\
a_{35} &= -\sin(\beta)[\cos(2\alpha)\cos(\beta)\sin(\gamma) + \sin(2\alpha)\cos(\gamma)].
\end{aligned}$$

- For $i = 4$:

$$\begin{aligned}
a_{41} &= -\frac{\sqrt{3}}{2}\sin^2(\beta)\sin(2\gamma)\\
a_{42} &= \sin(\beta)[\sin(\alpha)\cos(2\gamma) + \cos(\alpha)\cos(\beta)\sin(2\gamma)]\\
a_{43} &= \sin(\beta)[\sin(\alpha)\cos(\beta)\sin(2\gamma) - \cos(\alpha)\cos(2\gamma)]\\
a_{44} &= \cos(2\alpha)\cos(\beta)\cos(2\gamma) - \tfrac{1}{2}\sin(2\alpha)[1+\cos^2(\beta)]\sin(2\gamma)\\
a_{45} &= -\sin(2\alpha)\cos(\beta)\cos(2\gamma) - \tfrac{1}{2}\cos(2\alpha)[1+\cos^2(\beta)]\sin(2\gamma).
\end{aligned}$$

- For $i = 5$:

$$\begin{aligned}
a_{51} &= \frac{\sqrt{3}}{2}\sin^2(\beta)\cos(2\gamma)\\
a_{52} &= \sin(\beta)[\sin(\alpha)\sin(2\gamma) - \cos(\alpha)\cos(\beta)\cos(2\gamma)]\\
a_{53} &= -\sin(\beta)[\sin(\alpha)\cos(\beta)\cos(2\gamma) + \cos(\alpha)\sin(2\gamma)]\\
a_{54} &= \cos(2\alpha)\cos(\beta)\sin(2\gamma) + \tfrac{1}{2}\sin(2\alpha)[1+\cos^2(\beta)]\cos(2\gamma)\\
a_{55} &= \tfrac{1}{2}\cos(2\alpha)[1+\cos^2(\beta)]\cos(2\gamma) - \sin(2\alpha)\cos(\beta)\sin(2\gamma).
\end{aligned}$$

Appendix B

If the EFG tensor is statistically isotropic, the distributions of the tensor elements remains unchanged after a rotation of the frame of reference defined by the Euler angles (α, β, γ) (appendix A). The random vectors $\boldsymbol{U}'$ and $\boldsymbol{U}$ are identically distributed:

$$\boldsymbol{U}' \stackrel{\mathrm{d}}{=} \boldsymbol{U}. \tag{B1}$$

Their characteristic functions (equation (22) and below, [50, 52, 95]) are identical. If we choose:

$$\begin{aligned}
&\alpha = 0\\
&\beta = \cos^{-1}\left(\frac{1}{\sqrt{3}}\right) \approx 54.7356^\circ\\
&\gamma = 90^\circ
\end{aligned} \tag{B2}$$

we deduce (appendix A and equation (B1)):

$$\begin{aligned}
U_1' &\stackrel{\mathrm{d}}{=} \sqrt{\tfrac{2}{3}}U_2 + \sqrt{\tfrac{1}{3}}U_5\\
U_2' &\stackrel{\mathrm{d}}{=} \sqrt{\tfrac{1}{3}}U_3 + \sqrt{\tfrac{2}{3}}U_4.
\end{aligned} \tag{B3}$$

We further assume that the U_k are independent random variables and we define their characteristic functions:

$$\begin{aligned} &\phi_1(t) = \langle \exp(\mathrm{i}tU_1)\rangle \\ &\phi_k(t) = \phi(t) = \langle \exp(\mathrm{i}tU_k)\rangle \qquad k = 2,\ldots,5. \end{aligned} \tag{B4}$$

The U_k for $k = 2,\ldots,5$ are identically distributed in the statistically isotropic case (section 3), so they have the same characteristic function $\phi(t)$. Moreover, as the U_k for $k = 2,\ldots,5$ have symmetric distributions, $\phi(t)$ is a real function. Rotational invariance and relations (B3) prove that:

$$\phi_1(t) = \phi(\sqrt{\tfrac{2}{3}}t)\phi(\sqrt{\tfrac{1}{3}}t) = \phi(t) \tag{B5}$$

where the last equality comes from the second relation (B3). Relations (B4) and (B5) prove that the five U_k are identically distributed. If we now set:

$$\begin{aligned} &\alpha = 45^\circ \\ &\beta = \cos^{-1}\left(\frac{1}{\sqrt{3}}\right) \approx 54.7356^\circ \\ &\gamma = 0^\circ \end{aligned} \tag{B6}$$

we deduce:

$$U_1' \stackrel{\mathrm{d}}{=} \sqrt{\tfrac{1}{3}}(U_2 + U_3 + U_4) \tag{B7}$$

that is:

$$\phi(t) = \phi^3(\sqrt{\tfrac{1}{3}}t) \tag{B8}$$

and more generally:

$$\phi(t) = \prod_{j=1}^{5} \phi(a_{ij}t) \qquad i = 1,\ldots,5 \tag{B9}$$

from equations (A1) and (B1) and with condition (A2). The functional equations (B8) or (B9) have a unique solution:

$$\phi(t) = \exp\left(-\frac{s^2t^2}{2}\right) \tag{B10}$$

that is the characteristic function of a normal distribution with zero mean and variance s^2 [50, 63, 64, 95]. The U_k for $k = 1,\ldots,5$ are therefore independent and identically distributed Gaussian random variables with a covariance matrix given by:

$$\tilde{\Lambda} = s^2\tilde{I}_5.$$

Finally from equation (5), we obtain:

$$s^2 = \frac{\langle\Delta^2\rangle}{20}. \tag{B11}$$

In summary, if the distribution of the EFG tensor is assumed to be invariant by rotation and if the components of $\boldsymbol{U}$ are assumed to be independent, then the distribution of $\boldsymbol{U}$ is multivariate normal with a zero mean vector and a covariance matrix $\tilde{\Lambda} = \langle\Delta^2\rangle\tilde{I}_5/20$ (equation (12)).

Appendix C

The distribution of the random vector $\boldsymbol{U}$ associated with the EFG tensor (equation (52)) can be more simply calculated in the frame of reference of $\tilde{V}_0$ as the U_k are normal and independent with means given by:

$$\langle U_1 \rangle = (1-x)U_1(0)$$
$$\langle U_k \rangle = 0 \qquad k = 2, 3, 4$$
$$\langle U_k \rangle = (1-x)U_5(0)$$

(equation (53)) and a common variance given by:

$$\langle (U_k - \langle U_k \rangle)^2 \rangle = \frac{x^2\sigma^2}{4} \qquad k = 1, \ldots, 5$$

(equation (54)). This distribution is:

$$P(\boldsymbol{U}) \propto \left(\frac{1}{(x\sigma)^5}\right) \exp\left(\frac{4(1-x)\boldsymbol{U}\cdot\boldsymbol{U}(0)}{(x\sigma)^2}\right) \times \exp\left(-\frac{(1-x)^2 V_{zz}^2(0)(1+\eta^2(0)/3) + V_{zz}^2(1+\eta^2/3)}{2(x\sigma)^2}\right). \tag{C1}$$

The constants $V_{zz}(0)$, $\eta(0)$ and $\boldsymbol{U}(0)$ are associated with $\tilde{V}(0)$, the 'ordered' contribution to the total EFG tensor, and where only the x and σ contributions to the constant normalization factor have been retained. To calculate the bivariate distribution $f(V_{zz}, \eta)$, it is necessary to diagonalize $\tilde{V}$, that is to change the set of variables from $\boldsymbol{U} = (U_1, \ldots, U_5)$ to $(V_{zz}, \eta, \alpha, \beta, \gamma)$. This will introduce a factor $V_{zz}^4\eta(1-\eta^2/9)$ which comes from the Jacobian of the transformation $2\sin(\beta)V_{zz}^4\eta(1-\eta^2/9)$ as shown by equation (5) of Czjzek *et al* [1] (see also section 3). It is the $\sin(\beta)$ term which allows us to transform the integral over β described below into an integral over $t = \cos(\beta)$.

It solely remains to express the scalar product $\boldsymbol{U}\cdot\boldsymbol{U}(0)$ in equation (C1) in terms of the new variables. In the principal axis system of the total EFG tensor, the latter scalar product is $\boldsymbol{U}'\cdot\boldsymbol{U}'(0)$ and the sole non-zero components of $\boldsymbol{U}'$ are $U_1' = V_{zz}/2$ and $U_5' = (V_{xx} - V_{yy})/(2\sqrt{3})$ (see equation (4)). With the simplifying assumption $\eta(0) = 0$, the only non-zero component of $\boldsymbol{U}(0)$ is $U_1(0) = V_{zz}(0)/2$. From the relations given in appendix A, it is deduced that:

$$U_1'(0) = \tfrac{1}{4}V_{zz}(0)(3\cos^3(\beta) - 1)$$
$$U_5'(0) = \frac{\sqrt{3}}{4}V_{zz}(0)\sin^2(\beta)\cos(2\gamma).$$

That is, the scalar product in equation (C1) can be written as:

$$\boldsymbol{U}\cdot\boldsymbol{U}(0) = \boldsymbol{U}'\cdot\boldsymbol{U}'(0) = \tfrac{1}{8}V_{zz}V_{zz}(0)(3\cos^2(\beta) - 1 + \eta\sin^2(\beta)\cos(2\gamma)). \tag{C2}$$

Integrating the transformed equation (C1) over $t = \cos(\beta)$ from 0 to 1 and over $\phi = 2\gamma$ with $0 \leqslant \phi \leqslant \pi$ and defining $\Omega \equiv (1-x)V_{zz}V_{zz}(0)/(2x^2\sigma^2)$, we obtain finally equation (61) which can be calculated numerically. Equations (C1) and (C2) also yield the distribution $P(\alpha, \beta, \gamma)$ after integration over V_{zz} and η. As expected, $P(\alpha, \beta, \gamma)$ does not reduce to the uniform distribution (proportional to $\sin(\beta)$) which would be obtained for a statistically isotropic distribution of the EFG tensor.

A similar calculation might be performed to obtain the bivariate distribution $f(V_{zz}, \eta)$ for $\eta(0)$ different from zero which would be expressed in the form of a slightly more involved integral than the one of equation (61).

Appendix D

A Gram–Schmidt method was used to construct random 5×5 orthogonal matrices for the computer simulations of the Cz(n) models [78] (see subsection 4.2.2). Five vectors $\boldsymbol{p}_i$ (with $i = 1, \ldots, 5$) with independent Gaussian components identically distributed and with zero mean and unit variance are first generated by the classical Box–Müller method [78]. The vector $\boldsymbol{q}_1 = \boldsymbol{p}_1/\|\boldsymbol{p}_1\|$ is first calculated. The sets of vectors:

$$\boldsymbol{r}_i = \boldsymbol{p}_i - \sum_{j=1}^{i-1} (\boldsymbol{p}_i \cdot \boldsymbol{q}_j)\boldsymbol{q}_j$$

and:

$$\boldsymbol{q}_i = \boldsymbol{r}_i/\|\boldsymbol{r}_i\|$$

with $i = 2, \ldots, 5$ allow us finally to construct the orthogonal matrix sought after whose columns are the five vectors $\boldsymbol{q}_i$:

$$\tilde{H} = (\boldsymbol{q}_1, \ldots, \boldsymbol{q}_5)$$

as in equation (33).

References

[1] Czjzek G, Fink J, Götz F, Schmidt H, Coey J M D, Rebouillat J P and Lienard A 1981 *Phys. Rev.* B **23** 2513
[2] Stöckmann H J 1981 *J. Magn. Res.* **44** 145
[3] Cohen M H and Reif F 1957 *Solid State Physics* vol 5 (New York: Academic) p 321
[4] Kanert O and Mehring M 1971 *NMR, Basic Principles and Progress* vol 3, ed P Diehl, E Fluck and R Kosfeld (Heidelberg: Springer) p 3
[5] Seeger A, Ehmann J and Fähnle M 1996 *Z. Naturf.* a **51** 489
[6] Grenèche J M and Varret F 1993 *Mössbauer Spectroscopy Applied to Magnetism and Materials Science* vol 1, ed G J Long and F Grandjean (New York: Plenum) ch 5, pp 161–203
[7] Le Caër G, Cadogan J M, Brand R A, Dubois J M and Güntherodt H J 1984 *J. Phys. F: Met. Phys.* **14** L73
[8] Le Caër G, Dubois J M and Brand R A 1984 *Amorphous Metals and Non-equilibrium Processing* ed M von Allmen (Les Ulis: Editions de Physique) p 249
[9] Le Caër G, Brand R A and Dehghan K 1985 *J. Physique Coll.* **46** C8 169
[10] Brand R A, Ghafari M, Keune W, Güntherodt H and Gronert H 1988 *Z. Phys. Chem., NF* **157** 121
[11] Ghafari M, Brand R A and Keune W 1988 *Hyperfine Interact.* **42** 931
[12] Swartzendruber L J, Shechtman D, Benderski L and Cahn J W 1985 *Phys. Rev.* B **32** 1383
Eibschütz M, Chen H S and Hauser J J 1986 *Phys. Rev. Lett.* **56** 169
[13] Le Caër G, Brand R A and Dubois J M 1987 *Phil. Mag. Lett.* **56** 143
[14] Brand R A, Le Caër G and Dubois J M 1988 *Proc. JIMIS-5: Non-Equlibrium Solid Phases of Metals and Alloys, Trans. JIM Suppl.* **29** 471
[15] Le Caër G, Brand R A and Dubois J M 1988 *Hyperfine Interact.* **42** 943
[16] Brand R A, Le Caër G and Dubois J M 1990 *J. Phys.: Condens. Matter* **2** 6413
[17] Ping J Y, Rancourt D G and Stadnik Z M 1992 *Hyperfine Interact.* **69** 493
[18] Dunlap R A and Lawther D W 1993 *Mater. Sci. Eng. Rep.* **10** 141
[19] Brand R A, Pelloth J, Hippert F and Calvayrac Y 1994 *Hyperfine Interact.* **94** 2249
[20] Hippert F, Brand R A, Pelloth J and Calvayrac Y 1994 *J. Phys.: Condens. Matter* **6** 11 189
[21] Stadnik Z M 1996 *Mössbauer Spectroscopy Applied to Magnetism and Materials Science* vol 2, ed G J Long and F Grandjean (New York: Plenum) ch 6, p 125
[22] Quivy A, Quiquandon M, Calvayrac Y, Faudot F, Gratias D, Berger C, Brand R A, Simonet V and Hippert F 1996 *J. Phys.: Condens. Matter* **8** 4223
[23] Nakai Y 1992 *J. Phys. Soc. Japan* **61** 4583
[24] Ping J Y and Rancourt D G 1994 *Hyperfine Interact.* **92** 1203
[25] Dou Lixin, Hodgson R J W and Rancourt D G 1995 *Nucl. Instrum. Methods* B **100** 511
[26] Alberto H V, Pinto da Cunha J L, Mysen B O, Gil J M and Ayres de Campos N 1996 *J. Non-Cryst. Solids* **194** 48
[27] Lagarec K and Rancourt D G 1997 *Nucl. Instrum. Methods* B **129** 266

[28] Le Caër G and Dubois J M 1987 *Key Eng. Mater.* **13–15** 555
[29] Czjzek G 1982 *Phys. Rev.* B **25** 4908
[30] Varret F and Henry M 1980 *Rev. Phys. Appl.* **15** 1057
[31] Heubes P, Korn D, Schatz G and Zibold G 1979 *Phys. Lett.* **74A** 267
[32] Damonte L C, Mendoza-Zélis L and López-García A R 1989 *Phys. Rev.* B **39** 12 492
[33] Shastri A, Borsa F, Torgeson D R, Shield J E and Goldman A I 1994 *Phys. Rev.* B **50** 15 651
[34] Hippert F, Brand R A and Calvayrac Y 1999 to be published
[35] Shastri A, Borsa F, Torgeson D R, Shield J E and Goldman A I 1994 *Phys. Rev.* B **50** 4224
[36] Rabbani S R, Caticha N, dos Santos J G and Pusiol D J 1995 *Phys. Rev.* B **51** 8848
[37] Yahiaoui E M, Berger R, Servent Y, Kliava J, Cugunov L and Mednis A 1994 *J. Phys.: Condens. Matter* **6** 9415
[38] Legein C 1994 *Thèse* (Université du Maine, Le Mans) unpublished
[39] Jäger C, Kunath G, Losso P and Schelen G 1993 *Solid State Nucl. Magn. Reson.* **2** 73
[40] Kendall M G and Stuart A 1969 *The Advanced Theory of Statistics* 3rd edn, vol 1 (London: Griffin) p 268
[41] Blaha P, Schwarz K and Dederichs P H 1988 *Phys. Rev.* B **37** 2792
[42] Dufek P, Blaha P and Schwarz K 1995 *Phys. Rev. Lett.* **75** 3545
[43] Averbuch P 1961 *C. R. Acad. Sci., Paris* **253** 2674
[44] Mallows C L 1961 *Biometrika* **48** 133
[45] Ullah N and Porter C E 1963 *Phys. Lett.* **6** 301
[46] Ullah N 1964 *Nucl. Phys.* **58** 65
[47] Olson W H and Rao Uppuluri V R 1970 *Sankhya* A **32** 325
[48] Averbuch P 1982 *Solid State Commun.* **42** 113
[49] Averbuch P 1993 *J. Physique* I **3** 559
[50] Cramer H 1971 *Mathematical Methods of Statistics* 12th edn (Princeton, NJ: Princeton University Press)
[51] Porter C E and Rosenzweig N 1960 *Ann. Acad. Sci. Fenn.* A **6** 5
[52] Mehta M L 1991 *Random Matrices* 2nd edn (New York: Academic)
[53] Beenakker C W J 1997 *Rev. Mod. Phys.* **69** 731
[54] Gühr T, Müller-Groeling A and Weidenmüller H A 1998 *Phys. Rep.* **299** 189
[55] Czjzek G 1983 *Hyperfine Interact.* **14** 189
[56] Levy Yeyati A, Weissmann M and Lopez-Garcia A 1988 *Phys. Rev.* B **37** 10 608
[57] Grenèche J M, Varret F and Teillet J 1988 *J. Physique* **49** 243
[58] Bonnenefant A, Friedt J M, Maurer M and Sanchez J P 1982 *J. Physique* **43** 1475
[59] McGreevy R L 1993 *J. Non-Cryst. Solids* **156–158** 949
[60] Hausleitner C and Hafner J 1993 *Phys. Rev.* B **47** 5689
[61] Maret M, Lançon F and Billard L 1993 *J. Physique* I **3** 5689
[62] Legein C, Buzarè J Y, Emery J and Jacoboni C 1995 *J. Phys.: Condens. Matter* **7** 3853
[63] Feller W 1957 *An Introduction to Probability Theory and Its Applications* vol 2 (New York: Wiley)
[64] Bryc W 1995 *The Normal Distribution Characterizations with Applications (Lecture Notes in Statistics 100)* (New York: Springer)
[65] Barra J R 1981 *Mathematical Basis of Statistics* (New York: Academic) ch 7
[66] Petrilli H M and Frota-Pessôa S 1990 *J. Phys.: Condens. Matter* **2** 135
[67] Zou J and Carlsson A E 1994 *Phys. Rev.* B **50** 99
[68] Evans M, Hastings N and Peacock B 1993 *Statistical Distributions* 2nd edn (New York: Wiley) p 80
[69] Gaskell P H and Wallis D J 1996 *Phys. Rev. Lett.* **76** 66
[70] Uhlherr A and Elliott S R 1994 *J. Phys.: Condens. Matter* **6** L99
Fayos R, Bermejo F J, Dawidowski J, Fischer H E and González M A 1996 *Phys. Rev. Lett.* **77** 3823
Wilson M and Madden P A 1998 *Phys. Rev. Lett.* **80** 532
[71] Steinhardt P J, Nelson D R and Ronchetti M 1983 *Phys. Rev.* B **28** 784
[72] Alben R, Cargill G S III and Wenzel J 1976 *Phys. Rev.* B **13** 835
[73] Yan X, Hirscher M, Egami T and Marinero E E 1991 *Phys. Rev.* B **43** 9300
[74] Tomida T and Egami T 1993 *Phys. Rev.* B **48** 3048
[75] Tomida T and Egami T 1995 *Phys. Rev.* B **52** 3290
[76] Lines M E and Eibschütz M 1983 *Phys. Rev.* B **27** 5308
[77] Mathai A M and Provost S B 1992 *Quadratic Forms in Random Variables, Theory and Applications* (New York: Dekker) ch 5
[78] Sloane N J A 1983 *Lecture Notes in Computer Science* ed T Beth (Berlin: Springer) p 71
[79] Kendall M G and Buckland W R 1960 *A Dictionary of Statistical Terms* 2nd edn (Edinburgh: Oliver and Boyd) p 79
[80] Le Caër G and Brand R A 1992 *Hyperfine Interact.* **71** 1507
[81] Maurer M 1986 *Phys. Rev.* B **34** 8996

[82] Kruger M B and Jeanloz R 1990 *Science* **249** 647
[83] Pasternak M P, Rosenberg G Kh and Milner A P 1997 *Phys. Rev. Lett.* **79** 4409
[84] Moran P A P 1980 *Biometrika* **67** 675
[85] Heuberg P, Korn D, Schatz G and Zibold G 1979 *Phys. Lett.* **74A** 267
[86] Bererhi A, Bosio L and Cortès R 1979 *J. Non-Cryst. Solids* **30** 253
[87] Tsay S F 1993 *Phys. Rev.* B **48** 5945
[88] Turek I 1990 *Nucl. Instrum. Methods* B **52** 187
[89] Varret F, Gérard A and Imbert P 1971 *Phys. Status Solidi* b **43** 723
Hesse J and Rübartsch A 1974 *J. Phys. E: Sci. Instrum.* **7** 526
Brand R A, Lauer J and Herlach D 1983 *J. Phys. F: Met. Phys.* **13** 675
[90] Le Caër G and Dubois J M 1979 *J. Phys. E: Sci. Instrum.* **12** 1083
Le Caër G, Dubois J M, Wagner H G, Fisher H and Gonser U 1984 *Nucl. Instrum. Methods* B **233** 25
[91] Longworth G 1988 *Mössbauer Spectroscopy Applied to Inorganic Chemistry* vol 2, ed G Long (New York: Plenum)
Nagy D L and Röhlich U 1991 *Hyperfine Interact.* **66** 105
Campbell S J and Aubertin F 1988 *Mössbauer Spectroscopy Applied to Inorganic Chemistry* vol 3, ed G Long (New York: Plenum)
[92] Rancourt D G 1996 *Mössbauer Spectroscopy Applied to Magnetism and Materials Science* vol 5, ed G Long and F Grandjean (New York: Plenum) ch 5, p 105
[93] Marcinkiewicz J 1938 *Math. Z.* **44** 612
[94] Ure M C D and Flinn P A 1971 *Mössbauer Methodology* vol 7, ed I J Gruverman (New York: Plenum) p 245
[95] Lukacs E 1970 *Characteristic Functions* 2nd edn (London: Griffin)
[96] Vincze I 1982 *Nucl. Instrum. Methods* **199** 247
[97] Menil F 1985 *J. Phys. Chem. Solids* **46** 763
[98] Brand R A, Hippert F and Calvayrac Y 1998 to be published